
Report No. K-TRAN: KU-02-8
FINAL REPORT

EVALUATION OF NEXRAD OPERATIONAL PRECIPITATION ESTIMATES IN KANSAS

C. Bryan Young, Ph.D., P.E.
Tanya M. Brown
Nathaniel A. Brunsell, Ph.D.
The University of Kansas
Lawrence, Kansas

May 2008

KANSAS DEPARTMENT OF TRANSPORTATION

**Division of Operations
Bureau of Materials and Research**

The logo for the Kansas Department of Transportation is displayed within a dark blue rectangular box. It features a stylized yellow swoosh that starts under the letter 'K' and ends with a five-pointed star above the letter 'S'. Below this graphic, the word "KANSAS" is written in large, bold, white, sans-serif capital letters. Underneath "KANSAS", the words "DEPARTMENT OF TRANSPORTATION" are written in a smaller, bold, white, sans-serif font, also in all capital letters.

KANSAS
DEPARTMENT OF TRANSPORTATION

1 Report No. K-TRAN: KU-02-8	2 Government Accession No.	3 Recipient Catalog No.	
4 Title and Subtitle Evaluation of NEXRAD Operational Precipitation Estimates in Kansas		5 Report Date May 2008	
		6 Performing Organization Code	
7 Author(s) C. Bryan Young, Ph.D., P.E., Tanya M. Brown, Nathaniel A. Brunsell, Ph.D.		8 Performing Organization Report No.	
9 Performing Organization Name and Address The University of Kansas Department of Civil, Environmental and Architectural Engineering 2150 Learned Hall 1530 W. 15th Street Lawrence, Kansas 66045-7609		10 Work Unit No. (TRAIS)	
		11 Contract or Grant No. C1280	
12 Sponsoring Agency Name and Address Kansas Department of Transportation Bureau of Materials and Research 700 SW Harrison Street Topeka, Kansas 66603-3745		13 Type of Report and Period Covered Final Report June 2001 - Spring 2008	
		14 Sponsoring Agency Code RE-0291-01	
15 Supplementary Notes For more information write to address in block 9.			
16 Abstract <p>This report presents two separate evaluations of NEXRAD operational precipitation estimates for Kansas. The first evaluation uses daily gauge data from the National Weather Service (NWS) cooperative network. This gauge network is independent of data used to develop the NEXRAD operational products, and thus provides a realistic assessment of NEXRAD error characteristics. Many studies of NEXRAD error characteristics compare NEXRAD estimates against hourly rain gauge data that were used to produce the multisensory estimates. Results for such studies should be treated with caution, as they likely underestimate the true error characteristics of the NEXRAD product. NEXRAD bias, correlation, and percent detection are mapped across northern Kansas to demonstrate the spatial distribution of NEXRAD errors as compared with daily rain gauge data.</p> <p>The second evaluation compares NEXRAD estimates of intense precipitation with data from the high-density ALERT network in Johnson County, Kansas. A small number of the ALERT gauges are used at times by the National Weather Service for the production of NEXRAD estimates. As such, the ALERT gauge network is not a completely independent data source. Thirty-four storms over the period 1998 through 2004 were evaluated using this gauge dataset. The ALERT data were spatially interpolated using Kriging techniques prior to comparison with the NEXRAD data.</p> <p>This report presents NEXRAD error characteristics relative to gauge observations for northern Kansas. Errors in NEXRAD estimates appear to be quite large; however, it must be considered that the errors presented in this report are relative to gauge observations – not true rainfall totals. As such, the error terms combine NEXRAD uncertainty, gauge observation errors, and the spatial sampling error inherent in the gauge/NEXRAD mismatch. As a remotely sensed product, NEXRAD estimates should be used to augment – not replace – gauge measurements of precipitation. In areas where no gauge data are available, NEXRAD provides a good source of information on the spatial distribution and relative intensity of rainfall.</p>			
17 Key Words NEXRAD Radar, precipitation, ALERT gauge		18 Distribution Statement No restrictions. This document is available to the public through the National Technical Information Service, Springfield, Virginia 22161	
19 Security Classification (of this report) Unclassified	20 Security Classification (of this page) Unclassified	21 No. of pages 115	22 Price

EVALUATION OF NEXRAD OPERATIONAL PRECIPITATION ESTIMATES IN KANSAS

Final Report

Prepared by

C. Bryan Young, Ph.D., P.E.
Tanya M. Brown
Nathaniel A. Brunsell, Ph.D.

The University of Kansas
Lawrence, Kansas

A Report on Research Sponsored By

THE KANSAS DEPARTMENT OF TRANSPORTATION
TOPEKA, KANSAS

THE UNIVERSITY OF KANSAS
LAWRENCE, KANSAS

May 2008

© Copyright 2008, **Kansas Department of Transportation**

PREFACE

The Kansas Department of Transportation's (KDOT) Kansas Transportation Research and New-Developments (K-TRAN) Research Program funded this research project. It is an ongoing, cooperative and comprehensive research program addressing transportation needs of the state of Kansas utilizing academic and research resources from KDOT, Kansas State University and the University of Kansas. Transportation professionals in KDOT and the universities jointly develop the projects included in the research program.

NOTICE

The authors and the state of Kansas do not endorse products or manufacturers. Trade and manufacturers' names appear herein solely because they are considered essential to the object of this report.

This information is available in alternative accessible formats. To obtain an alternative format, contact the Office of Transportation Information, Kansas Department of Transportation, 700 SW Harrison, Topeka, Kansas 66603-3745 or phone (785) 296-3585 (Voice) (TDD).

DISCLAIMER

The contents of this report reflect the views of the authors who are responsible for the facts and accuracy of the data presented herein. The contents do not necessarily reflect the views or the policies of the state of Kansas. This report does not constitute a standard, specification or regulation.

ABSTRACT

This report presents two separate evaluations of NEXRAD operational precipitation estimates for Kansas. The first evaluation uses daily gauge data from the National Weather Service (NWS) cooperative network. This gauge network is independent of data used to develop the NEXRAD operational products, and thus provides a realistic assessment of NEXRAD error characteristics. Many studies of NEXRAD error characteristics compare NEXRAD estimates against hourly rain gauge data that were used to produce the multisensory estimates. Results for such studies should be treated with caution, as they likely underestimate the true error characteristics of the NEXRAD product. In Chapter 3, NEXRAD bias, correlation, and percent detection are mapped across northern Kansas to demonstrate the spatial distribution of NEXRAD errors as compared with daily rain gauge data.

The second evaluation compares NEXRAD estimates of intense precipitation with data from the high-density ALERT network in Johnson County, Kansas. A small number of the ALERT gauges are used at times by the National Weather Service for the production of NEXRAD estimates. As such, the ALERT gauge network is not a completely independent data source. Thirty-four storms over the period 1998 through 2004 were evaluated using this gauge dataset. The ALERT data were spatially interpolated using Kriging techniques prior to comparison with the NEXRAD data.

In general terms, the NEXRAD estimates exhibit better agreement with NWS rain gauges in the eastern portion of the state than they do in the central and western areas. Over the long term, NEXRAD tends to underestimate rainfall across Kansas when compared to NWS rain gauge observations. However, during storms with intense

rainfall, NEXRAD often overestimates storm total accumulations when compared to gauge data. The results of this study show marked improvement in NEXRAD estimates of warm season precipitation over the eight-year study period.

This report presents NEXRAD error characteristics relative to gauge observations for northern Kansas. Errors in NEXRAD estimates appear to be quite large; however, it must be considered that the errors presented in this report are relative to gauge observations – not true rainfall totals. As such, the error terms combine NEXRAD uncertainty, gauge observation errors, and the spatial sampling error inherent in the gauge/NEXRAD mismatch (in Chapter 3). As a remotely sensed product, NEXRAD estimates should be used to augment – not replace – gauge measurements of precipitation. In areas where no gauge data are available, NEXRAD provides a good source of information on the spatial distribution and relative intensity of rainfall.

ACKNOWLEDGMENT

This project was supported by the Kansas Department of Transportation through the K-TRAN Cooperative Transportation Research Program. The authors sincerely appreciate this support. Mr. Robert Reynolds, P.E., of KDOT deserves special thanks for his contribution as project monitor.

TABLE OF CONTENTS

Abstract.....	iii
Acknowledgment.....	v
Table of Contents.....	vi
List of Figures.....	viii
List of Tables.....	x
Chapter 1 - Introduction.....	1
1.1 Background.....	1
1.2 NEXRAD Primer.....	2
1.2.1 Level II (Volume Scan).....	4
1.2.2 Stage I.....	4
1.2.3 Stage II.....	6
1.2.4 Stage III / P1 / MPE.....	7
1.2.5 Stage IV.....	9
1.3 Study Motivation and Objectives.....	9
Chapter 2 - Literature Review.....	11
2.1 Background.....	11
2.2 Studies in the ABRFC.....	11
2.3 Other Studies of Interest.....	14
Chapter 3 - Evaluation of NEXRAD Estimates using Daily Gauge Data.....	17
3.1 Introduction.....	17
3.2 Study Area and Data.....	17
3.3 Methodology.....	19
3.4 Results.....	21
3.5 Discussion and Conclusions.....	25
Chapter 4 - Evaluation of NEXRAD Estimates using ALERT Rain gauges.....	43
4.1 Introduction.....	43
4.2 Study Area.....	43
4.3 Data Preparation and Storm Selection.....	44
4.4 Methods.....	47

4.5	Results	54
4.6	Conclusions.....	56
	Chapter 5 - Summary and Conclusions.....	61
5.1	Summary	61
5.2	Conclusions and Recommendations	62
	References.....	64
	Appendix A - Scatter Plots for Hourly Accumulations.....	66
	Appendix B - Scatter Plots for Storm Total Accumulations.....	84

LIST OF FIGURES

Figure 1.1: NWS Hourly Rain gauges in Kansas.....	2
Figure 1.2: WSR-88D Radar Sites in and near Kansas.....	3
Figure 3.1: Locations of NEXRAD Radar Units and Daily Rain gauges	18
Figure 3.2: NEXRAD-Gauge Joint Distributions for Daily and Seasonal Totals over the Warm and Cold Seasons	22
Figure 3.3: NEXRAD-Gauge Bias and Correlation for Accumulations 1998-2004	23
Figure 3.4: NEXRAD Percent Detection for Daily Rainfall 1998-2004.....	24
Figure 3.5: 1998 Warm Season	29
Figure 3.6: 1999 Warm Season	30
Figure 3.7: 2000 Warm Season	31
Figure 3.8: 2001 Warm Season	32
Figure 3.9: 2002 Warm Season	33
Figure 3.10: 2003 Warm Season	34
Figure 3.11: 2004 Warm Season	35
Figure 3.12: 1998 Cold Season.....	36
Figure 3.13: 1999 Cold Season.....	37
Figure 3.14: 2000 Cold Season.....	38
Figure 3.15: 2001 Cold Season.....	39
Figure 3.16: 2002 Cold Season.....	40
Figure 3.17: 2003 Cold Season.....	41
Figure 3.18: 2004 Cold Season.....	42
Figure 4.1: ALERT Network Rain gauges used in the Study.....	44
Figure 4.2: Example of Close-up Radar Image	46
Figure 4.3: Example of Regional Radar Image	46
Figure 4.4: Linear Model for the Semivariogram	50
Figure 4.5: Spherical Model for the Semivariogram	50
Figure 4.6: Exponential Model for the Semivariogram.....	50
Figure 4.7: Gaussian Model for the Semivariogram	51
Figure 4.8: Gaussian Model with a Nugget Effect	51

Figure 4.9: Screen Shot of the Semivariogram Fitting Procedure 52
Figure 4.10: Comparison of Storm Total Spatial Averages 58

LIST OF TABLES

Table 3.1: Missing Hours for NEXRAD Product	18
Table 3.2: Warm Season Bias.....	27
Table 3.3: Warm Season Correlation	27
Table 3.4: Warm Season Percent Detection:	27
Table 3.5: Cold Season Bias.....	28
Table 3.6: Cold Season Correlation	28
Table 3.7: Cold Season Percent Detection	28
Table 4.1: Summary of Statistics for Hourly Accumulations.....	57
Table 4.2: Summary of Statistics for Storm Totals	57
Table 4.3: Statistics for Hourly Totals for all 34 Events	59
Table 4.4: Statistics for Storm Totals for all 34 Events	60

CHAPTER 1 - INTRODUCTION

1.1 Background

The Next Generation Weather Radar (NEXRAD) system produces estimates of hourly precipitation across the entire country. NEXRAD estimates are produced in near real-time by merging radar and rain gauge observations on a 4 x 4 km² grid. Although the primary purpose for these estimates is flood forecasting by the National Weather Service, they serve as an archive of high spatial and temporal resolution rainfall data that can be used to augment available rain gauge data for the analysis of historical storms.

In many parts of Kansas, rain gauge data can be hard to come by. The NWS currently collects data for 131 hourly recording gauges and 344 daily non-recording gauges in Kansas. As such, the average distance to the nearest hourly rain gauge in Kansas is nearly 14 miles and the average distance to the nearest daily rain gauge is about 7.4 miles – assuming that the record for the nearest available gauge is complete. Figure 1.1 shows the locations of hourly gauges in Kansas. In some locations, the nearest gauge is over 40 miles away.

Given the types of storms encountered in the Midwest, this separation distance may mean the difference between heavy rainfall and no rainfall. NEXRAD estimates can help fill this data gap, but it is first important to understand the error characteristics inherent in this remotely-sensed product.

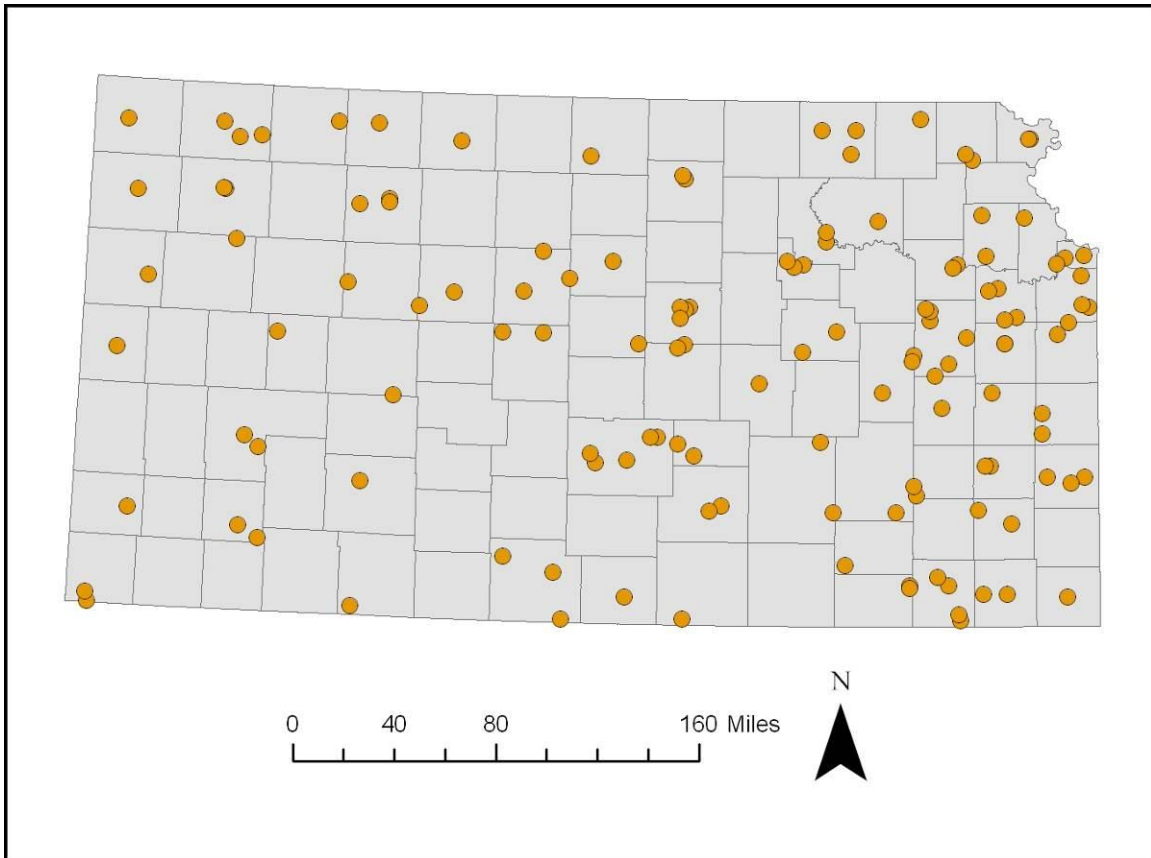


Figure 1.1: NWS Hourly Rain gauges in Kansas

1.2 NEXRAD Primer

The NEXRAD system is complicated and dynamic. There are multiple operational products that vary greatly, and these products have changed over time. This section provides a brief primer; more details on the NEXRAD system are available in Fulton et al. (1998) and Seo and Breidenbach (2002).

The NEXRAD system consists of 141 Weather Surveillance Radar, 1998 Doppler (WSR-88D) units across the 48 contiguous United States. Figure 1.2 shows radar installations in and near Kansas. Each radar has a nominal range of 230 km, although this can be affected by topography and atmospheric conditions. Development of rainfall

estimates from these radars involves several stages of data collection and processing.

These phases generate various products along the way, including:

- Level II (Volume Scan)
- Stage I
- Stage II
- Stage III / P1 / MPE
- Stage IV

This section briefly discusses the development of each product.

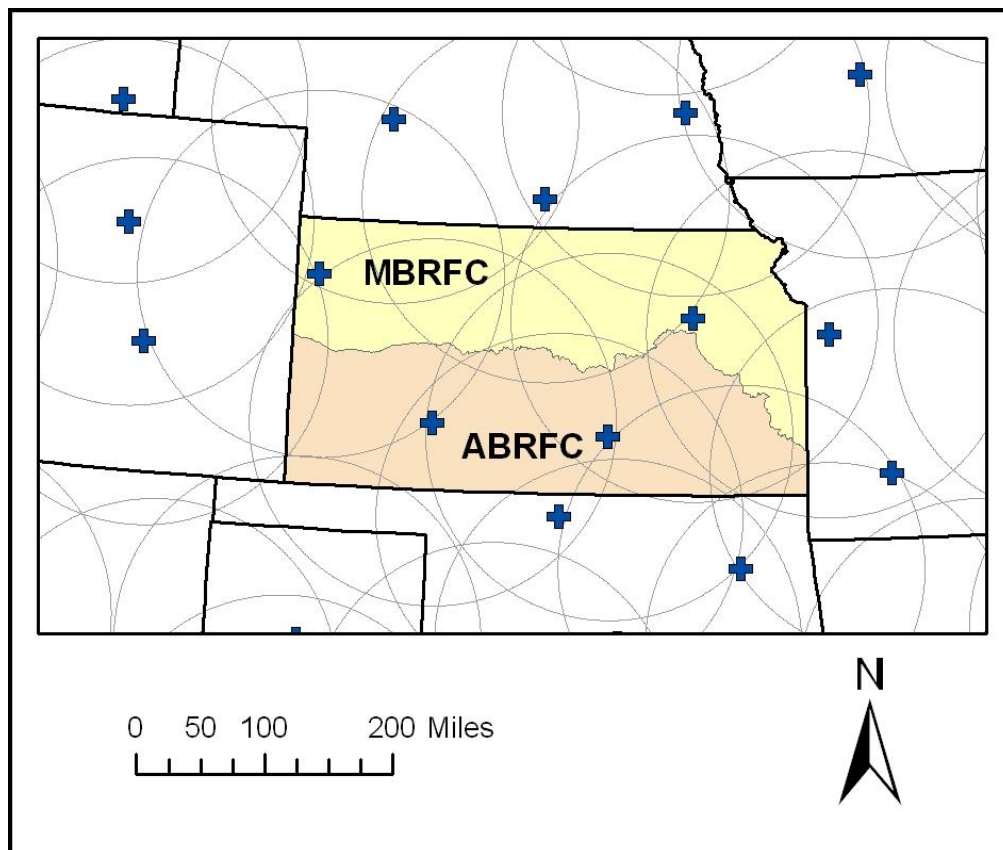


Figure 1.2: WSR-88D Radar Sites in and near Kansas. NOTE: The MBRFC is the area of coverage for the Missouri Basin River Forecast Center. The ABRFC is the area of coverage for the Arkansas-Red Basin River Forecast Center.

1.2.1 Level II (Volume Scan)

Initially, the radar collects information about the reflectivity of the atmosphere at multiple ranges and elevations surrounding the WSR-88D installation. This is accomplished using what is called the volume scan: a 360-degree scan around the radar that covers 14 different tilts (generally from 0.5 degrees above horizontal up to 20 degrees above horizontal). This volume scan is repeated every six minutes during rain events.

To obtain the reflectivity along one trajectory, the radar emits a pulse of electromagnetic energy and then measures the backscatter versus time. The time it takes for energy to be reflected back to the radar antenna is easily converted to distance, and the magnitude of the backscatter is an indirect measure of the water droplet distribution in the atmosphere. The radar rotates, emitting a pulse and measuring response at one-degree increments in a full 360-degree sweep. As such, the resolution of these reflectivity measurements is one degree by one kilometer every six minutes, and the results are stored in polar coordinates for the 14 different tilts. The resulting files are known as the level II, or volume scan, data.

1.2.2 Stage I

The level II files do not contain estimates of precipitation, just reflectivity. The objective of Stage I processing is to generate precipitation estimates from the reflectivity data. Unfortunately, the relationship between the measured reflectivity and the rainfall rate is not unique: a given reflectivity measurement may indicate the presence of a few, large water droplets or many, many small ones. In addition, the radar is unable to assess the downward velocity of the droplets: the 'Doppler' in WSR-88D refers the unit's

ability to measure wind speeds. Although the backscatter, or reflectivity, is not a perfect predictor of water droplet size, it can serve as a surrogate measure of rainfall rate. Rain rates are related to reflectivity using what is known as the Z-R relationship, which assumes the power law form of:

$$Z = aR^b \quad \text{Equation 1.1}$$

Where Z is the reflectivity factor in mm^6/m^3 , R is the rain rate in mm/h, and a and b are coefficients. The coefficients of the Z-R relationship can be altered depending on the location of the radar and on the type of rainfall that is occurring.

In Stage I processing, the raw reflectivity data are evaluated for quality control prior to application of the Z-R relationship. Quality control at this stage is automated, and involves detecting and removing radar artifacts such as anomalous propagation (AP), bright band, ground clutter, hail, and others. Details of these quality control mechanisms are presented in Fulton et al. (1998).

After quality control, the reflectivity data are converted to rainfall rates via the Z-R relationship and are adjusted for mean-field bias using available rain gauge data. The resulting rainfall amounts are aggregated to the hourly time step and re-mapped from polar coordinates to a Cartesian grid. The Cartesian grid used by the NWS is known as the Hydrologic Rainfall Analysis Project (HRAP) grid. This grid is a regular (square) grid when viewed in a polar stereographic map projection. The polar stereographic projection used for the HRAP grid does not preserve area or distance across the grid. As such, the cell size used (4.625 km) is true only on the central latitude of the projection, 60 degrees north. The grid size in Kansas ranges from 4.08 km in the south to 4.14 km in the north.

Stage I estimates have been archived by the NWS and are available online as part of the national archive of NEXRAD data. Although the Stage I hourly precipitation product is bias-adjusted using rain gauge data, this bias adjustment is very limited due to the number of gauges available during Stage I processing. The bias adjustment is also done as a mean-field correction and does not allow for spatially variable bias. As such, the Stage I product is commonly considered a radar-only estimate of rainfall.

1.2.3 Stage II

Stage II processing is carried out at each of the thirteen NWS River Forecast Centers (RFCs). Kansas is covered by two different RFCs: the Arkansas-Red Basin River Forecast Center (ABRFC) and the Missouri Basin River Forecast Center (MBRFC). Figure 1.2 shows the two RFC coverage areas in Kansas.

Stage II involves merging the Stage I product with recorded rain gauge data. The primary source of rain gauge data is the NWS network of recording rain gauges, but other data sources are used where available. For example, the ABRFC is able to integrate data from the Oklahoma Mesonet gauge network, and the MBRFC uses a few of the ALERT rain gauges in the Kansas City metropolitan area.

The Stage II process adjusts the radar estimates using both mean field bias correction and merging of radar and gauge fields on a pixel-by-pixel basis. The mean field bias correction is straightforward: the goal is to adjust the average rainfall over the Stage I area so that it equals the gauge-observed average. The merging of radar and gauge data is more complex, but involves an approach that assigns weights to the gauge and Stage I data depending on distance from the nearest gauges. This weighting system assigns more weight to the gauge-estimated field when rain gauges are in or

near the HRAP pixel, and less weight if the nearest gauge is far away. The weights are computed such that the expected error variance of the combined product is minimized.

1.2.4 Stage III / P1 / MPE

This is where things get a bit more confusing. Over the past decade, the NWS has worked to improve the quality of NEXRAD precipitation estimates. As such, NEXRAD hardware and software algorithms have been changed along the way. The most significant of these changes have affected this phase of the process: the development of gridded precipitation estimates across the RFC regions. There are three major algorithms that have been used over the period of record: Stage III, P1, and MPE.

The Stage III product produces a mosaic of Stage II estimates across the RFC region. The objective of this product is a seamless precipitation map that can be used to drive the NWS river forecast models. The mosaic is produced using the average Stage II rainfall value from all available radar units for each HRAP cell. The Stage III phase permits manual intervention by the on-duty forecaster. The forecaster is able to switch between using the Stage III or a gauge-only field, and is also able to delineate areas of snow or ice.

The objective of the P1 product is the same as that of Stage III, although it uses a different method for merging the radar-only and gauge-only precipitation estimates. In brief, the P1 algorithm produces a mosaic of Stage I estimates and then applies a bias adjustment using rain gauge data. The bias adjustment is computed by interpolating the ratio of gauge-to-radar measurements at each available rain gauge. As such, the P1 process assigns a much higher weight to gauge data and tends to produce a more spatially continuous rainfall field than Stage III.

Recently, the NWS implemented a new approach to developing RFC-wide precipitation estimates. This approach is known as the Multisensor Precipitation Estimate (MPE) process. The main difference between the MPE and the Stage III product is that the MPE mosaics a radar-only field before applying gauge corrections. In addition, the mosaic is produced using data from the radar that provides information closest to ground level. Gauge and radar estimates are merged in a manner similar to the Stage II process, but this is done after the mosaic of Stage I data has been developed (Seo and Breidenbach 2002).

The ABRFC has served as a testbed for new algorithm introduction. As such, the timeline of implementation of Stage III, P1, and the MPE product is different for the ABRFC and the MBRFC. For the ABRFC, Stage III was used from May 1993 through December of 1996, P1 was used primarily from January 1997 through May 2003, and the MPE algorithm was implemented in June 2003. For the MBRFC, Stage III was used from November 1994 through December 2002, and the MPE algorithm has been used since January 2003.

The current NEXRAD MPE estimates are generally available in near-real time. Users can request data files from the NWS National Precipitation Verification Unit (NPVU) for specified dates.

1.2.5 Stage IV

The Stage IV product is simply a nationwide mosaic of Stage III precipitation estimates. It is not evaluated in this report, although the application of this data set would be attractive for storms that span the MBRFC/ABRFC watershed boundary.

1.3 Study Motivation and Objectives

NEXRAD rainfall estimates are a potential boon for hydrologists working on flood forecasting or on the analysis of historical storms. They are high resolution in both time (hourly) and space (approximately 4 x 4 km²), and provide continuous coverage across the state of Kansas. Before the use of NEXRAD data can become widespread; however, it is important to understand how accurate these estimates are. Due to the nature of the NEXRAD product, this accuracy may vary both in time and space. NEXRAD errors may vary significantly in space for several reasons, including but not limited to: range from the nearest radar, beam elevation, beam blockage, and precipitation climatology. To complicate factors, the accuracy may also vary in time due to seasonal effects, storm characteristics, and occasional changes to the NEXRAD hardware and processing algorithms.

The objective of this study is to provide information to KDOT on the accuracy of NEXRAD precipitation estimates in Kansas. This is accomplished through a review of the extant literature (Chapter 2) and two separate NEXRAD-gauge comparisons. The first comparison (Chapter 3) uses daily rain gauge observations from the NWS cooperative observer network to evaluate spatial and temporal changes in NEXRAD accuracy across Kansas. The second comparison (Chapter 4) uses the high-density

ALERT network in the Kansas City metropolitan area to evaluate NEXRAD estimates of high-intensity precipitation.

CHAPTER 2 - LITERATURE REVIEW

2.1 Background

Numerous prior studies have compared NEXRAD estimates with rain gauge observations. Many of these papers have focused on NEXRAD estimates from the Arkansas-Red Basin River Forecast Center (ABRFC), due to the early availability of those data and due to the fact that the ABRFC has served as a testbed for new hardware and software algorithms. The next section provides a summary of the literature relating to the ABRFC. A number of other studies are presented in Section 2.3 to illustrate the variability of NEXRAD performance from location to location.

Many of the existing studies of NEXRAD estimates rely on data from hourly rain gauges. Understandably, many of the hourly gauge networks across the country are included in the NEXRAD Stage III, P1, or Multisensor Precipitation Estimates (MPE). As such, many existing NEXRAD evaluations do not validate the product with an independent data set. This is a very important point: if the gauge data used to evaluate the product are the same as those merged with radar to produce the product, then the comparison will of course show lower errors than are actually occurring.

2.2 Studies in the ABRFC

An early study by Smith et al. (1996) compared gauge observations with NEXRAD Stage I estimates of rainfall for two radar sites (Twin Lakes, Oklahoma and Amarillo, Texas). Smith et al (1996) found that the Stage I product, which is considered a radar-only estimate of rainfall, significantly underestimates precipitation relative to gauge observation (14% to 100% depending on season and range from the radar). Smith et al. (1996) also showed that the Stage I radar-based estimates of rainfall were

highly dependent on range. In general, the radar detection of rainfall decreased with range, particularly from 150 km to 230 km, and the radar-predicted rainfall rates were highest in the 50-100 km range. The radar often overestimates rainfall in the 50-100 km range due to a phenomenon known as bright band. Bright band occurs when the radar beam intersects the freezing level of the atmosphere, where precipitation is partially frozen and produces a much higher backscatter effect.

Johnson et al. (1999) demonstrated long-term underestimation (5% to 10%) in the NEXRAD Stage III product by evaluating it with gauge estimates of mean areal precipitation over eight basins in Oklahoma, Arkansas, and Missouri. Their analysis also showed that Stage III tended to observe fewer hours of rainfall during storm events, but that the estimated precipitation in those hours was more intense than the gauge-only estimates. Johnson et al. (1999) recognized that hydrologic models using NEXRAD Stage III data as the precipitation input should be appropriately calibrated.

Young et al. (2000) compared the performance of Stage III for the period January 1994 – January 1996 with estimates produced using the P1 algorithm (January 1997 – June 1998). They found that the switch from Stage III to P1 reduced the overall bias (from -20.5% to +5.2%) and root mean square difference (RMSD) (from 2.66 mm to 1.56 mm) while improving percent detection (from 41% to 86%). Their study also showed that the range-dependent errors in NEXRAD Stage I estimates are mostly removed in Stage II and Stage III processing.

In addition to comparing gauge and NEXRAD data directly, Young et al. (2000) applied the error separation method (ESM) of Ciach and Krajewski (1999) to determine what percentage of the RMSD between NEXRAD and gauge estimates may be

attributable to the spatial variability of rainfall over the HRAP pixel. This is a common problem in NEXRAD-gauge comparisons: the gauge observes rainfall over a very small area (essentially a point estimate) and NEXRAD produces estimates over a large area (4 x 4 km²). Due to data limitations, Young et al. (2000) were not able to definitively apply the ESM. However, initial results showed that the spatial variability of rainfall could easily explain 5% to 20% of the NEXRAD-gauge RMSD.

Grassotti et al. (2003) compared NEXRAD operational estimates produced using the P1 algorithm with those from Weather Services International Corporation (WSI). In that study, the unbiased RMSD for the P1 product ranged from 5 to 15 mm/day. The P1 product estimated a high number of very light rainfall rates, probably due to the way that the gauge and radar estimates are combined in the P1 process.

Another evaluation of NEXRAD estimates in the ABRFC area (Young 2000) used hydrologic model calibration as a basis for comparing gauge and NEXRAD estimates of rainfall. That study used the Hydrologic Simulation Program – FORTRAN (HSPF) model, coupled with automated calibration software, to determine whether a model calibrated using NEXRAD data could produce better results than one using only gauge data. The basic finding was that if a gauge was available in or near the watershed (within 15-20 miles), then the gauge-driven model outperformed the NEXRAD-driven model. However, if nearest gauge was more than 15-20 miles away from the watershed, then the NEXRAD-driven model produced better estimates of streamflow. These comparisons used long-term measures of the accuracy of peak flow and base flow prediction. The differences between NEXRAD and gauge-driven models may be more dramatic for event-based models that simulate only storm flow.

2.3 Other Studies of Interest

NEXRAD evaluations have also been performed in other regions of the United States. Although the results of these studies may not be directly applicable to Kansas, it is good to review the general performance of NEXRAD products in other locations.

Young et al. (1999) demonstrated the difficulties associated with radar-based estimation of precipitation in the Appalachian Mountains of the northeastern United States. NEXRAD performance in mountainous areas is affected by ground clutter and beam blockage. In some cases, the radar beam reflects off of surrounding mountains and causes erroneous high rainfall rates. The mountains also block the radar beam, causing underestimation of rainfall further along the same beam path.

Bedient et al. (2000) compared NEXRAD and gauge-based HEC-1 simulations for three storms in Houston, Texas. The NEXRAD-derived rainfall was developed from the level II reflectivity data for this study and was bias corrected using the available rain gauge network. For all three storms, the NEXRAD-derived rainfall led to streamflow forecasts that were as good or better than the gauge-only simulations.

Neary et al. (2004) compared hydrologic predictions of streamflow for two subbasins in the Cumberland River Basin in Middle Tennessee using NEXRAD Stage III and gauge-derived estimates. Their analysis found that the NEXRAD-derived rainfall led to underestimation of storm runoff volume, but prediction of peak flow was comparable to the gauge-driven model.

Nelson et al. (2005) present an evaluation of an archival precipitation data set derived from WSR-88D reflectivity measurements for the Mississippi River basin. This study is unique, in that it evaluates a NEXRAD-derived precipitation product that was

not produced in real time. The data set evaluated by Nelson et al. (2005) was developed using 're-analysis' of the level II data, combined with information from rain gauges. Because the estimates are not produced in real-time, the algorithms can be more thorough in integrating gauge data. The archival precipitation data set compared well with gauge observations. The re-analysis product tends to overestimate rainfall by 1-20% at the hourly time step with correlation ranging from 0.57 to 0.69. RMSD was high for hourly estimates of precipitation, but long-term RMSD (at the yearly time step) ranged from 10% to 26% of the gauge-estimated rainfall.

CHAPTER 3 - EVALUATION OF NEXRAD ESTIMATES USING DAILY GAUGE DATA

3.1 Introduction

This chapter presents an evaluation of NEXRAD rainfall estimates from the Missouri Basin River Forecast Center (MBRFC) using non-recording, daily rain gauge observations collected as part of the National Weather Service (NWS) cooperative observer network. Although daily gauges cannot evaluate the product at the hourly time step, the independence and the relative high density of daily gauges make them suitable for this study. This chapter presents maps of the spatial patterns in these error characteristics across northern Kansas and tracks improvement in NEXRAD estimates over time.

3.2 Study Area and Data

The study area for this research is the portion of Kansas that is in the Missouri River Basin. Figure 3.1 displays the Missouri River Basin boundary along with the locations of NEXRAD WSR-88D units and the daily rain gauges used in this study.

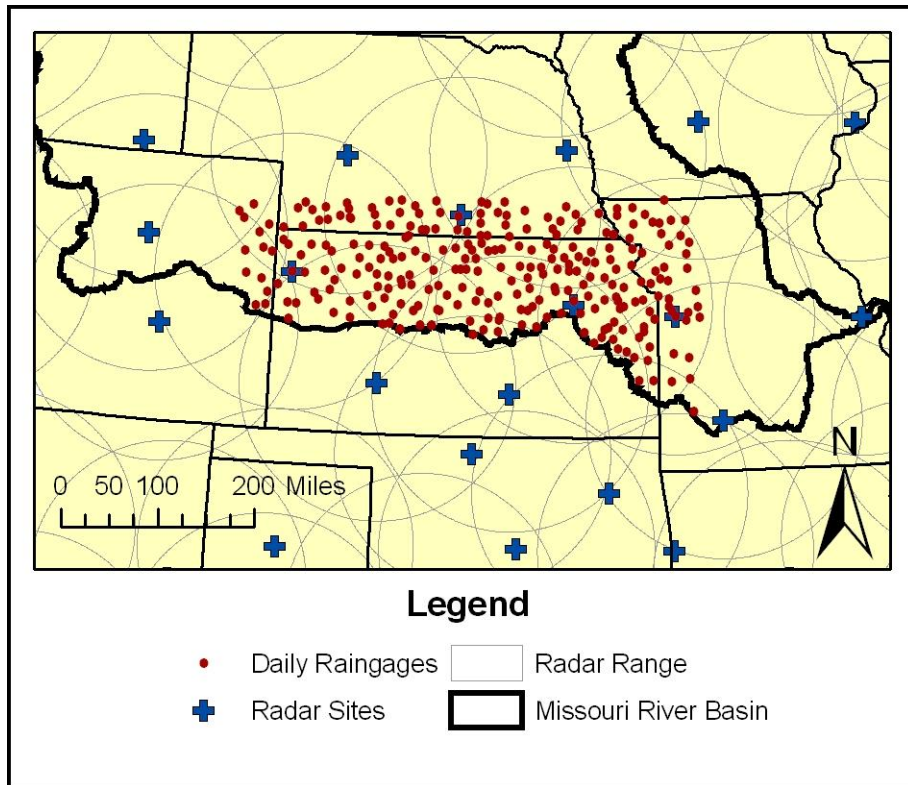


Figure 3.1: Locations of NEXRAD Radar Units and Daily Rain gauges

The NEXRAD database of hourly precipitation estimates compiled for this study is 98.1% complete for the period of record 1998-2004. This database was compiled from the NOAA Hydrologic Data Systems Group national archive of NEXRAD rainfall estimates and supplemented with files transferred to the University of Kansas from the MBRFC on a daily basis. Table 3.1 lists the largest gaps in this record; these gaps account for 92% of all missing hours. NEXRAD data for 1998 through 2002 were generated using the Stage III algorithm described in part by Fulton et al. (1998). Estimates in 2003 and 2004 were generated using the multisensor precipitation estimate (MPE) process, as discussed in Chapter 1.

Table 3.1: Missing Hours for NEXRAD Product

Period	Hours Missing
May 1999	222
Dec. 2000	493
Jan. 2001	104
Jul. 2001	70
Jan. 2003	216

The rain gauge data used for this comparison are from the NWS cooperative observer network, also referred to as the NWS Summary of the Day dataset. Figure 3.1 shows the 272 daily gauges used for this study. These gauges are typically 8 in. non-recording gauges. The time of observation varies from gauge to gauge, although 65% of the gauges are recorded at 7:00 or 8:00 am local time.

3.3 Methodology

The primary logistical challenge in this data comparison was matching the correct 24-hour NEXRAD accumulation to the hour of observation of the corresponding gauge. NEXRAD hourly files were accumulated to daily totals using a moving window sum, and these daily totals were extracted at the correct hour for corresponding gauge locations. Once the NEXRAD estimates of daily rainfall were extracted, summary statistics were computed for each gauge-pixel pair. The summary statistics used in this comparison include long-term NEXRAD bias (Equation 3.1), gauge-NEXRAD correlation (Equation 3.2), and NEXRAD detection conditioned on gauge observations exceeding a given threshold (Equation 3.3).

$$\text{Bias} = \frac{\sum P_R - \sum P_G}{\sum P_G} \cdot 100\% \quad \text{Equation 3.1}$$

$$\text{Correlation} = \frac{\sum P_G - \bar{P}_G \quad P_R - \bar{P}_R}{\sqrt{\sum P_G - \bar{P}_G^2 \quad P_R - \bar{P}_R^2}} \quad \text{Equation 3.2}$$

$$\text{Detection} = \frac{n_{P_R > 0, P_G > \text{thresh.}}}{n_{P_G > \text{thresh.}}} \cdot 100\% \quad \text{Equation 3.3}$$

where P_R and P_G are the 24-hour precipitation observed by NEXRAD and gauge, respectively, \bar{P}_R and \bar{P}_G are the average daily precipitation amounts for NEXRAD and

gauge, $n_{P_R>0, P_G>\text{thresh}}$ is the number of days that the NEXRAD pixel records precipitation and the corresponding gauge observation exceeds the specified threshold, and $n_{P_G>\text{thresh}}$ is the number of days the gauge value exceeds the specified threshold.

The gauge-pixel summary statistics were evaluated for multiple time spans, including the entire period of analysis (1998 through 2004), individual calendar years, and over the warm season (April through September) and cold season (October through March) for each calendar year. The summary statistics were imported to a geographic information system (GIS) and were interpolated across the Missouri River Basin to produce maps that display the spatial variation of gauge-pixel statistics. Each summary statistic was averaged in space over the portion of Kansas in the Missouri River Basin. This spatial averaging avoids results biased by the slight irregular density of NWS COOP gauges across the study area, as seen in Figure 3.1. Averaging gauge-pixel statistics over all gauge-pixel pairs could bias the results towards those exhibited in the eastern portion of the study area, where gauge density is higher.

It is important to recognize that there is a spatial mismatch in the precipitation estimates compared in this study (approximately $4 \times 4 \text{ km}^2$ for the NEXRAD estimates and 8 in diameter for the gauge observations). This spatial mismatch will contribute to differences in observed rainfall. It is also important to recognize that the gauge observations are not error free. Wind-induced undercatch, misrepresentation of rainfall due to poor gauge site conditions, difficulty measuring frozen precipitation, and human error are likely sources of error in the gauge records. Despite the possible sources of error, rain gauge observations are widely considered ground truth in evaluations of radar and satellite-based estimates of precipitation.

3.4 Results

Many gauge-radar comparisons present scatterplots of NEXRAD versus gauge observations of precipitation. Although scatterplots give an idea of the variability of observations, the number of data points often makes these graphs difficult to interpret. Figure 3.2 displays the joint distributions of NEXRAD and gauge observations over the warm and cold seasons for both daily and seasonal precipitation. In these graphs, the number of observation pairs in each bin are counted and expressed as a fraction of all recorded pairs. Ten percent of all observed gauge-NEXRAD pairs fall in each color band. The graph legend displays the cumulative percentage of observation pairs contained in that band and all darker color bands. Figure 3.2 demonstrates a high degree of scatter between the gauge and NEXRAD observations, especially for daily data. The season totals graphed in Figure 3.2(c) and 3.2(d) exhibit a definite linear relationship, but reveal bias and scatter in the long-term NEXRAD estimates as well.

Although Figure 3.2 characterizes the differences between NEXRAD and gauge observations, it does not tell the whole story. The quality of the NEXRAD estimate varies greatly across Kansas, in part affected by the density of radar sites, the number of gauges available for use in the NEXRAD product, and perhaps climatology as well. Figure 3.3 maps out NEXRAD bias and correlation for the entire period of analysis. There is noticeable variability in bias and correlation across the study area. NEXRAD bias is lowest in the eastern third of the study area. Bias on the western edge of Kansas tends towards -40%. NEXRAD-gauge correlation follows the same general pattern: relatively high values in the eastern portion of the study area, and low values along the western edge (near 0.6).

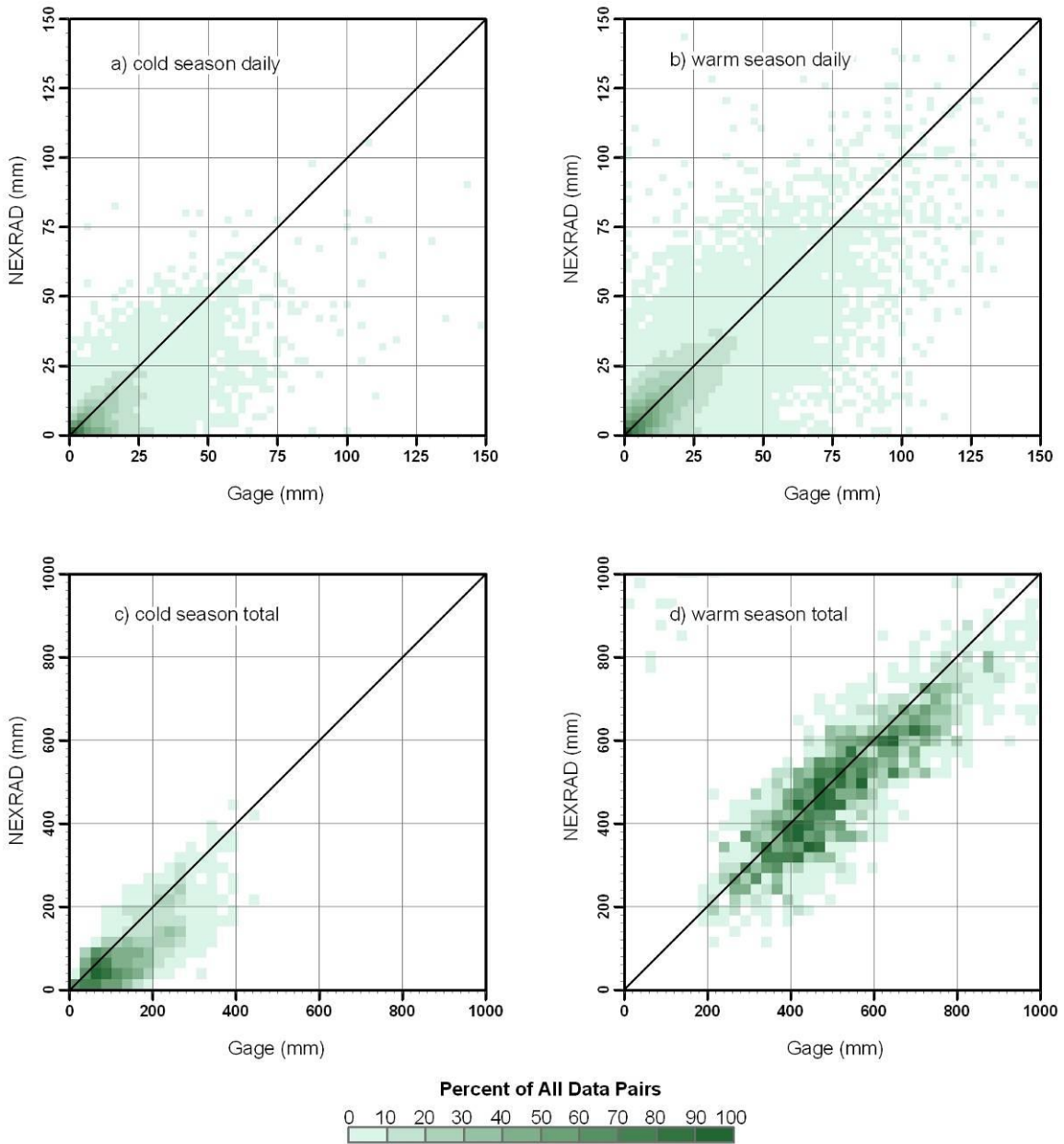


Figure 3.2: NEXRAD-Gauge Joint Distributions for Daily and Seasonal Totals over the Warm and Cold Seasons

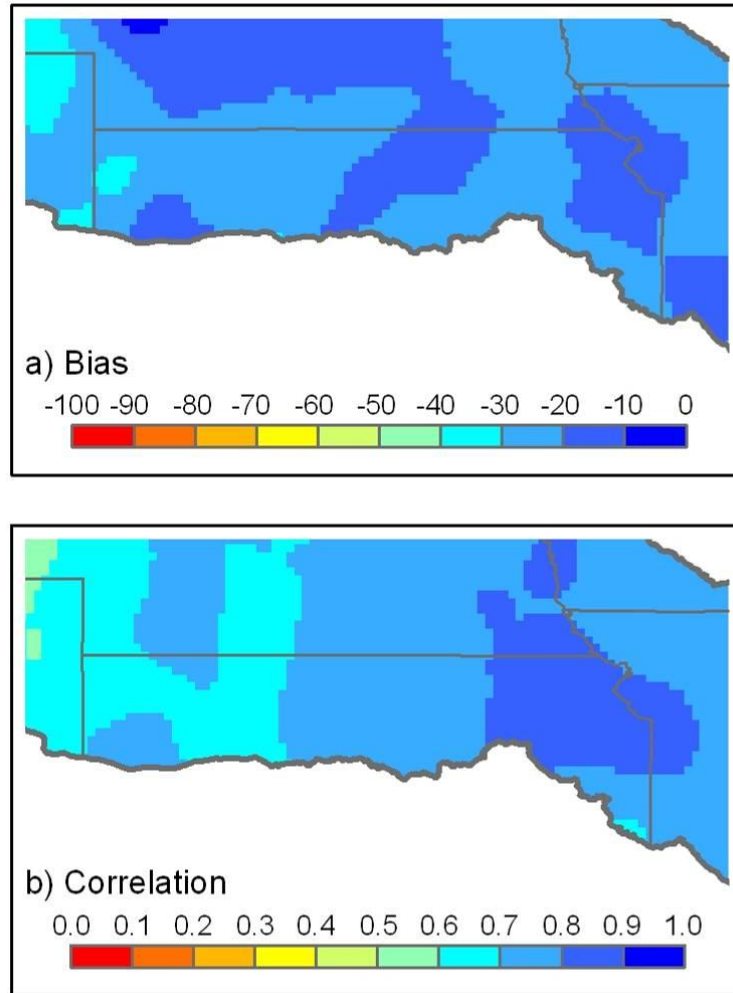


Figure 3.3: NEXRAD-Gauge Bias and Correlation for Daily Accumulations 1998-2004

In order to understand the source of the bias in Figure 3.3, the percent NEXRAD detection is evaluated in Figure 3.4. Figure 3.4 shows the percent of the time that the NEXRAD rainfall estimate exceeds zero when the gauge observation exceeds thresholds ranging from 0.0 to 0.5 inches. Mean detection improves across this range of gauge thresholds. In general, the eastern half of the study area has higher detection rates than the western portion. Percent detection is in large part responsible for problems observed in NEXRAD bias and correlation. Obviously, if the NEXRAD product does not detect precipitation, both bias and correlation suffer. Consistent bias can be

accounted for, for example in the calibration of a hydrologic model, while lack of detection is more problematic.

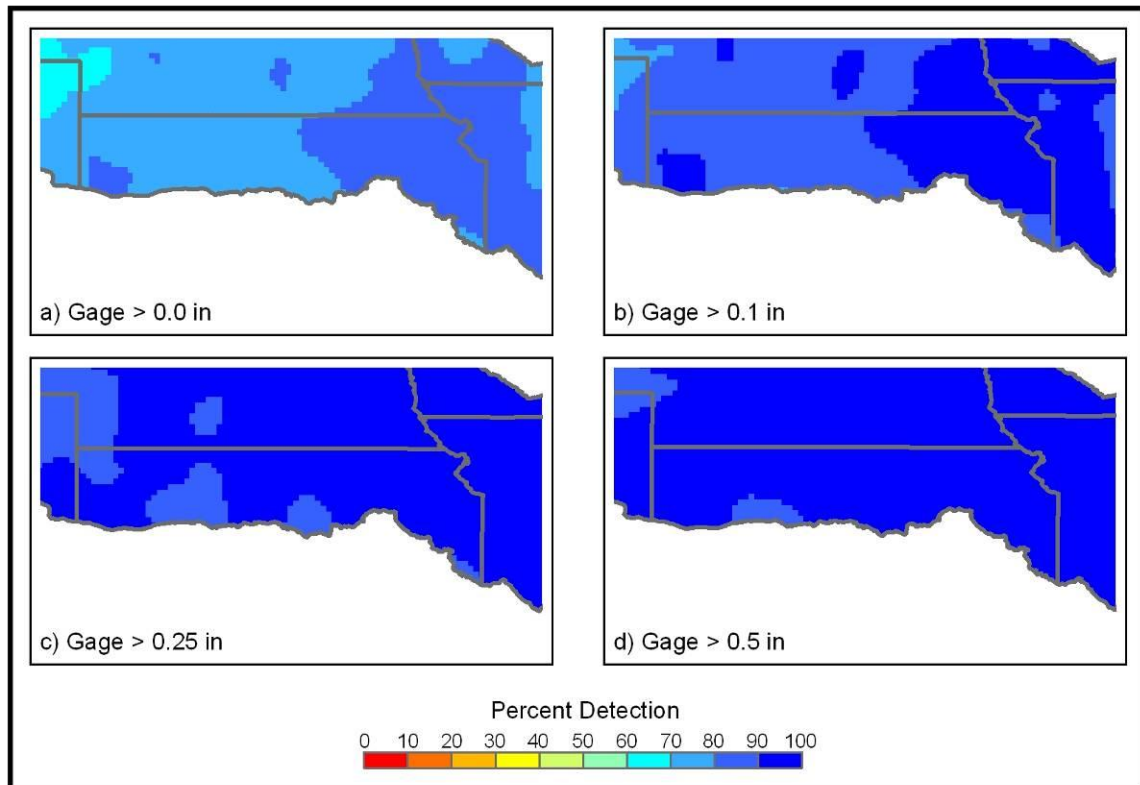


Figure 3.4: NEXRAD Percent Detection for Daily Rainfall 1998-2004

Understanding the spatial distribution of NEXRAD-gauge differences is important for those wanting to apply NEXRAD for modeling or analysis. It is also important to evaluate the NEXRAD-gauge differences over time. The NEXRAD operational product undergoes continual refinement of both hardware and algorithms. Over the period of record, the MBRFC has shifted from using the Stage III process (1998 through 2002) to the MPE algorithm (2003 and 2004).

Tables 3.2 through 3.7 investigate whether operational changes have improved NEXRAD estimates over time. Tables 3.2 through 3.4 show the average and range of the bias, correlation, and percent detection for warm season estimates of precipitation.

Tables 3.5 through 3.7 show the same statistics for cold season estimates. From these tables, it is clear that NEXRAD estimates of warm season precipitation have improved over the period evaluated in this study. In fact, mean warm season bias over the study area has decreased from -24.2% to -10.9%, while correlation has improved from 0.73 to 0.79 at the daily time step. This improvement is likely due to the implementation of the MPE algorithm. Table 3.5 through 3.7 show no apparent improvement in cold season estimates with the MPE product. This is no surprise given the difficulties associated with the remote sensing of frozen precipitation.

Figures 3.5 through 3.14 (at the end of this chapter) show the spatial variability in bias, correlation, and percent detection for each season in this study. These maps can be used to aid in the application and interpretation of NEXRAD precipitation estimates in Kansas.

3.5 Discussion and Conclusions

The NEXRAD-gauge comparisons in this paper are in general comparable to those reported in several other studies. The mean seasonal bias across the study area has ranged from -24.2% to -2.8%. This is worse than the -5% to -10% reported by Johnson et al. (1999) or +5% reported for the P1 product by Young et al. (2000). The average percent detection for a given season ranges from 80% to 90% in this study, which compares quite favorably to 41% for the Stage III product and 86% for the P1 product as reported by Young et al. (2000). The average correlation between 24-hour NEXRAD and gauge observations ranges from 0.72 to 0.79, which is in the upper portion of the 0.6 to 0.8 range reported by Grassoti et al. (2003) for daily observations in the ABRFC.

It must be noted that this study uses a gauge dataset that is independent of the NEXRAD operational product. The studies cited above all compare the NEXRAD estimates to gauge data that were available for inclusion in the NEXRAD estimates. As such, those papers may underestimate the true error characteristics of the NEXRAD product (at ungauged locations).

The summary statistics presented here treat the gauge measurements as ground truth. In reality, gauge error and the sampling uncertainty due to natural spatial variability of rainfall affect the reported results. As such, the correlation between NEXRAD and the true rainfall may be somewhat higher or lower than reported. However, the bias between NEXRAD and true rainfall is likely higher than NEXRAD-gauge bias, due to rain gauge undercatch. Studies have shown that average gauge underestimation due to wind undercatch may be on the order of 4-5% (Duchon and Essenberg 2001).

Non-operational applications of radar-based precipitation estimates may benefit significantly from re-analysis of the WSR-88D data. For example, the archival precipitation data set developed by Nelson et al. (2003) may be more accurate than the operational product. Nelson et al. (2005) showed bias in their archival data set to be less than 10%. In general, the re-analysis product overestimates rainfall compared to gauge estimates.

Maps presented in this report show the spatial variation in NEXRAD bias, correlation, and percent detection across northern Kansas. These maps should be helpful to those using NEXRAD for analysis or modeling efforts. This study also demonstrates that NEXRAD estimates of warm season precipitation for northern

Kansas have improved over the period 1998-2004. Average warm season bias has improved over the period of analysis from -24.2% to -10.9%, correlation has improved from 0.73 to 0.79, and NEXRAD detection from 80.9% to 88.5%. Cold season estimates of precipitation have not improved at all over the period of record, due to the distinct challenges of radar observation of frozen precipitation.

Table 3.2: Warm Season Bias

Year	Bias (%)		
	Minimum	Mean	Maximum
1998	-50.1	-24.2	-5.7
1999	-67.7	-23.3	2.2
2000	-46.5	-21.1	1.6
2001	-42.7	-18.9	2.4
2002	-38.0	-10.3	13.8
2003	-34.8	-2.8	28.9
2004	-34.6	-10.9	18.5

Table 3.3: Warm Season Correlation

Year	Correlation		
	Minimum	Mean	Maximum
1998	0.39	0.73	0.95
1999	0.46	0.72	0.88
2000	0.45	0.72	0.92
2001	0.45	0.78	0.94
2002	0.50	0.76	0.90
2003	0.49	0.79	0.95
2004	0.55	0.79	0.91

Table 3.4: Warm Season Percent Detection:

Year	Detection (%)		
	Minimum	Mean	Maximum
1998	60.9	80.9	92.5
1999	66.1	84.1	93.1
2000	70.8	85.1	94.1
2001	73.5	85.7	95.1
2002	69.9	84.1	100.0
2003	70.6	88.2	97.4
2004	78.0	88.5	96.0

Table 3.5: Cold Season Bias

Year	Bias (%)		
	Minimum	Mean	Maximum
1998	-38.7	-21.4	-4.3
1999	-37.2	-21.3	-4.5
2000	-39.9	-21.8	-4.1
2001	-40.9	-22.1	-3.8
2002	-42.0	-22.8	-5.0
2003	-43.8	-23.8	-5.5
2004	-39.5	-23.5	-7.6

Table 3.6: Cold Season Correlation

Year	Correlation		
	Minimum	Mean	Maximum
1998	0.56	0.75	0.88
1999	0.53	0.75	0.89
2000	0.53	0.75	0.89
2001	0.52	0.74	0.88
2002	0.54	0.75	0.89
2003	0.53	0.74	0.88
2004	0.50	0.74	0.91

Table 3.7: Cold Season Percent Detection

Year	Detection (%)		
	Minimum	Mean	Maximum
1998	69.6	80.5	90.5
1999	68.8	80.2	90.4
2000	67.7	80.1	90.2
2001	67.6	80.0	89.9
2002	68.2	80.1	89.8
2003	67.1	79.7	89.8
2004	66.5	79.0	89.8

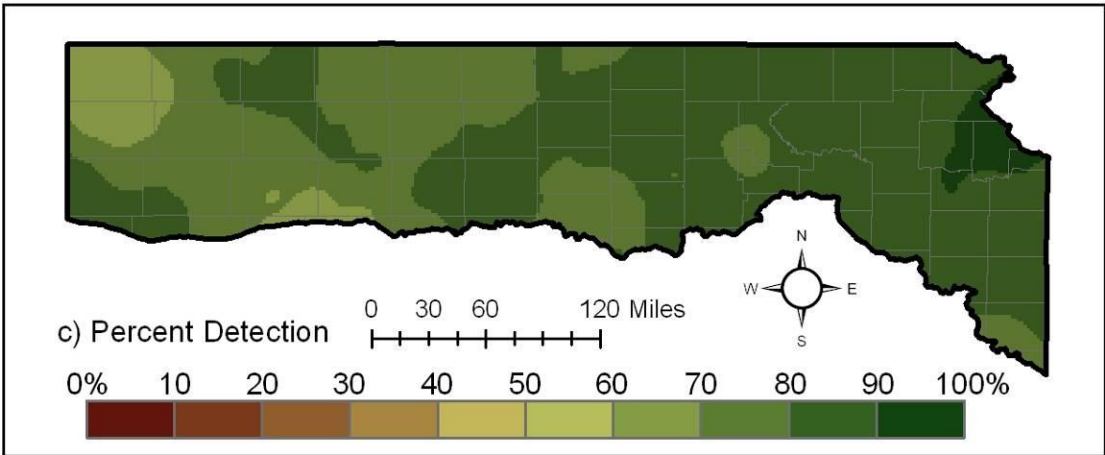
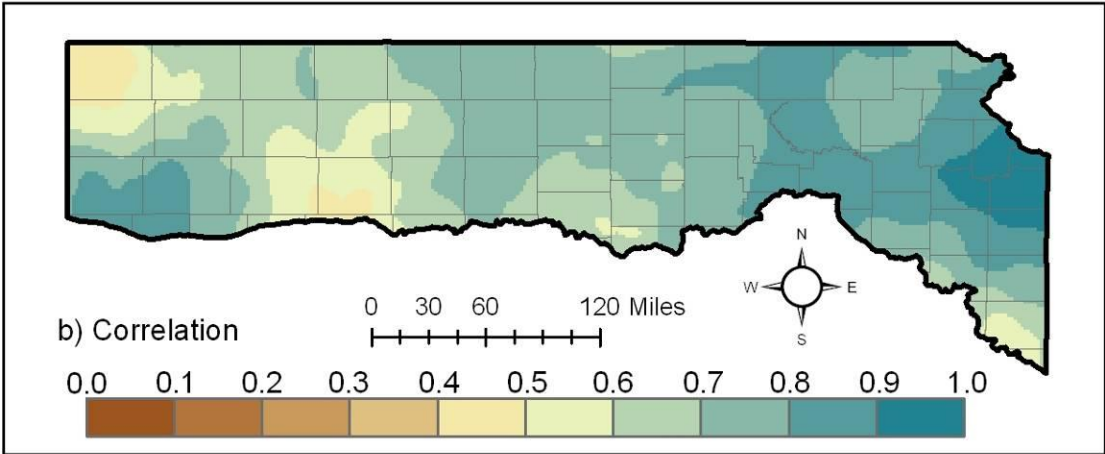
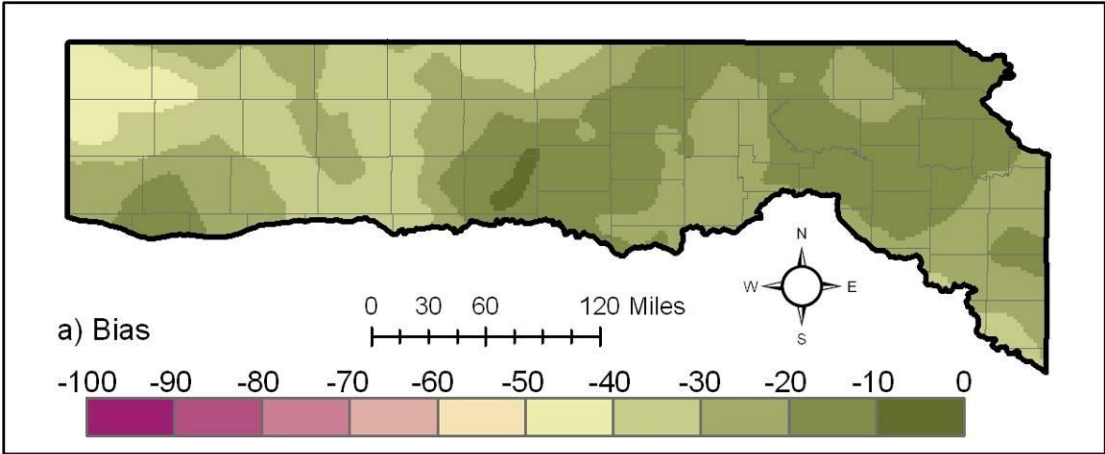


Figure 3.5: 1998 Warm Season

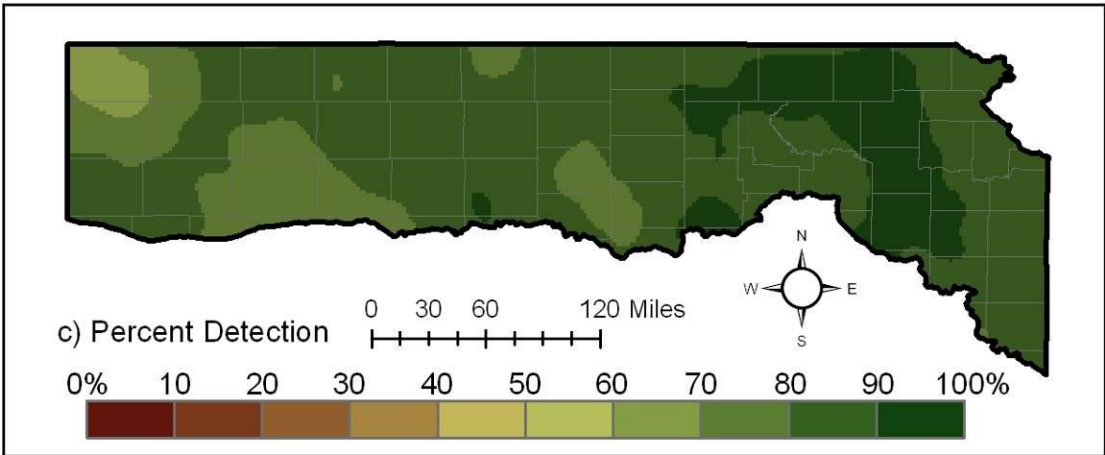
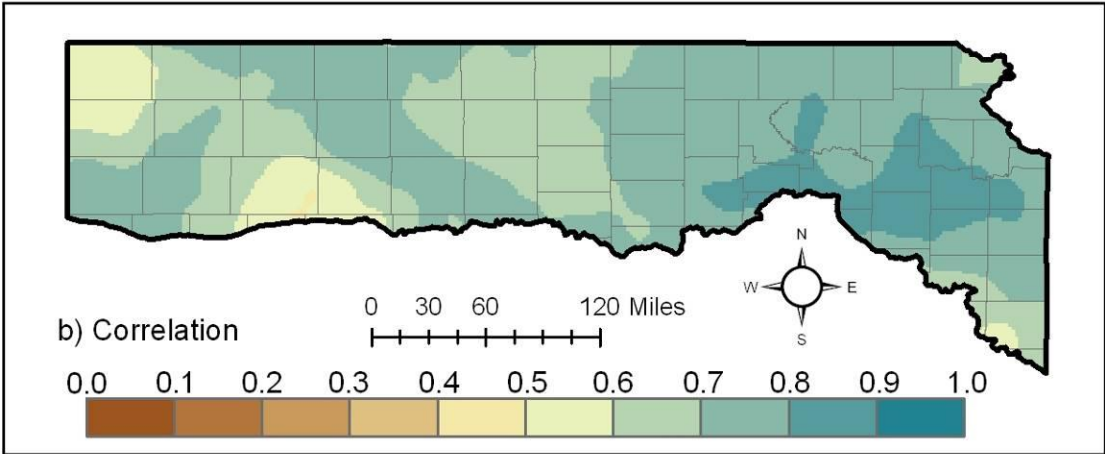
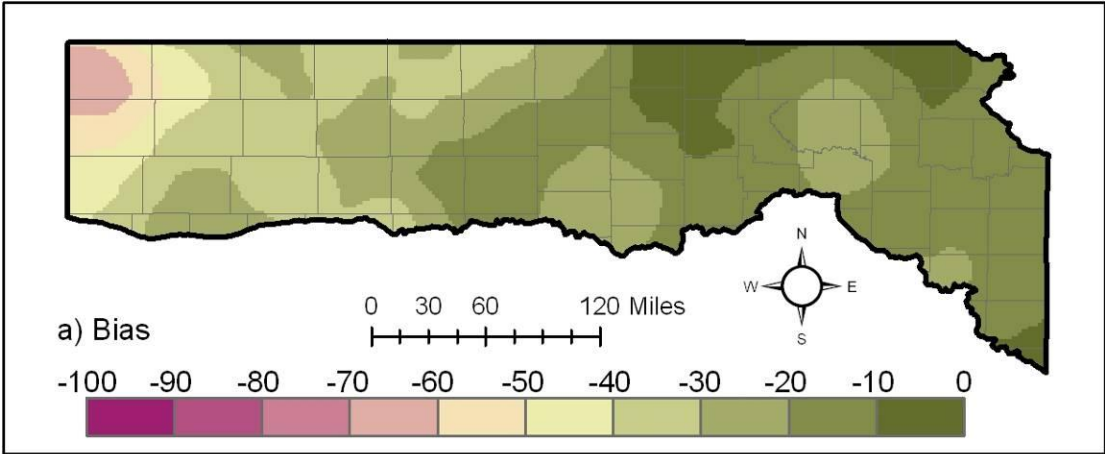


Figure 3.6: 1999 Warm Season

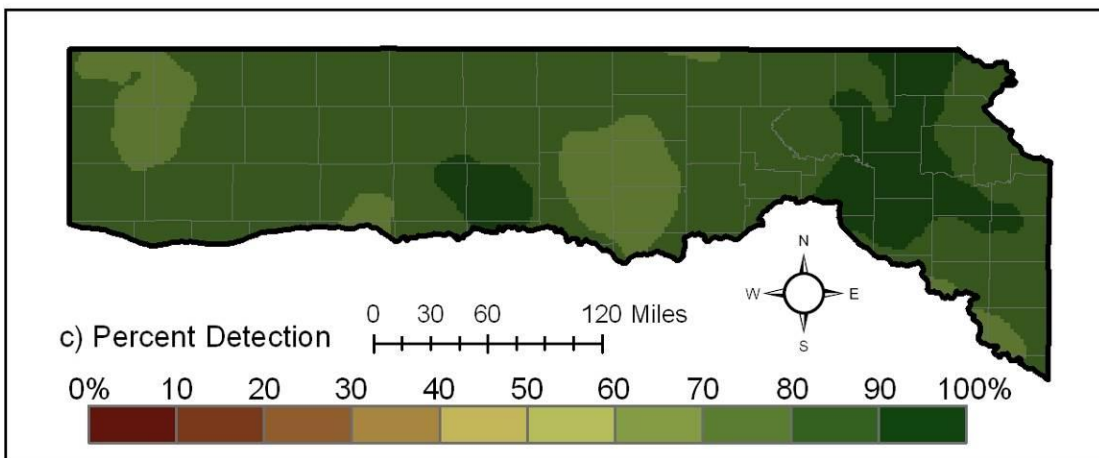
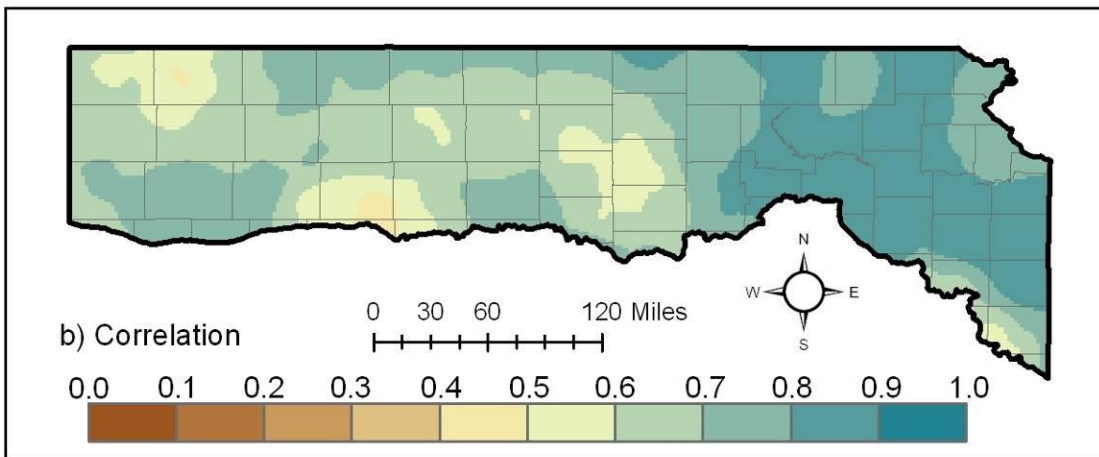
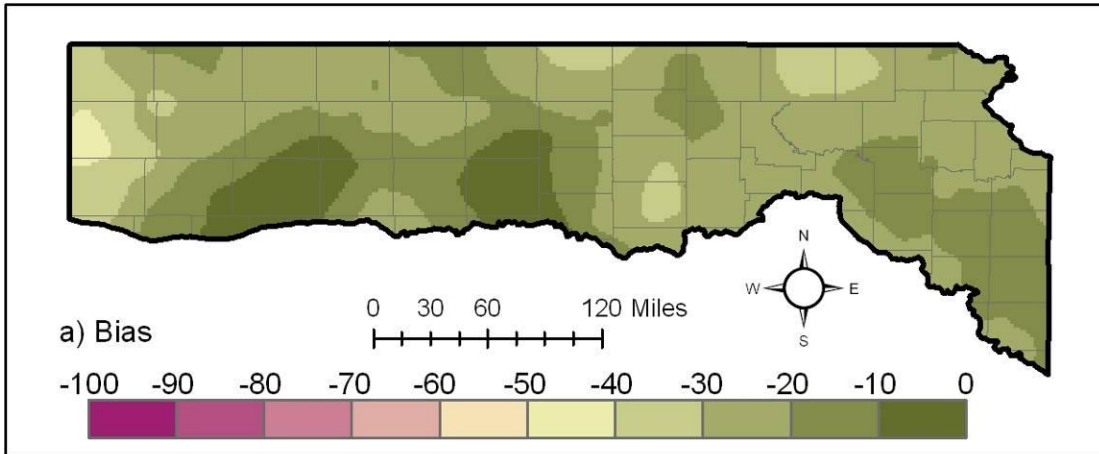


Figure 3.7: 2000 Warm Season

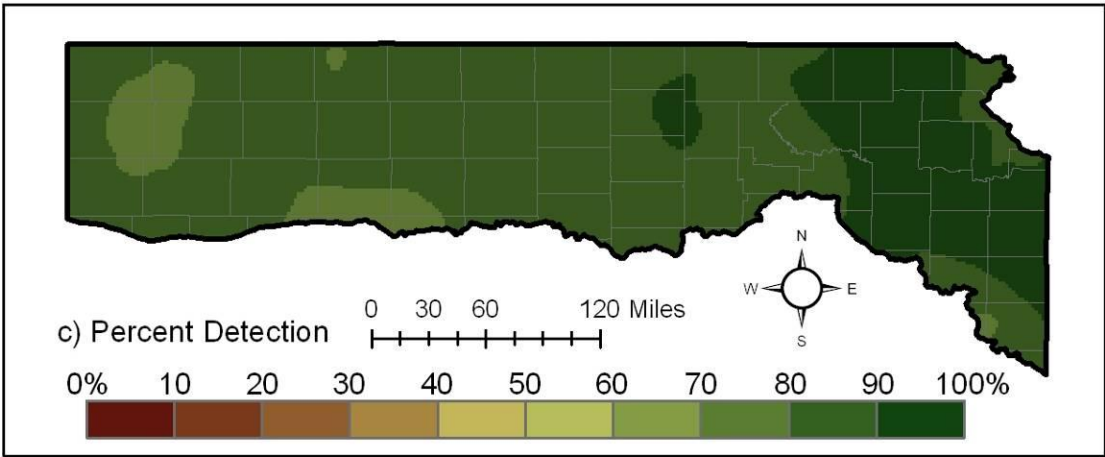
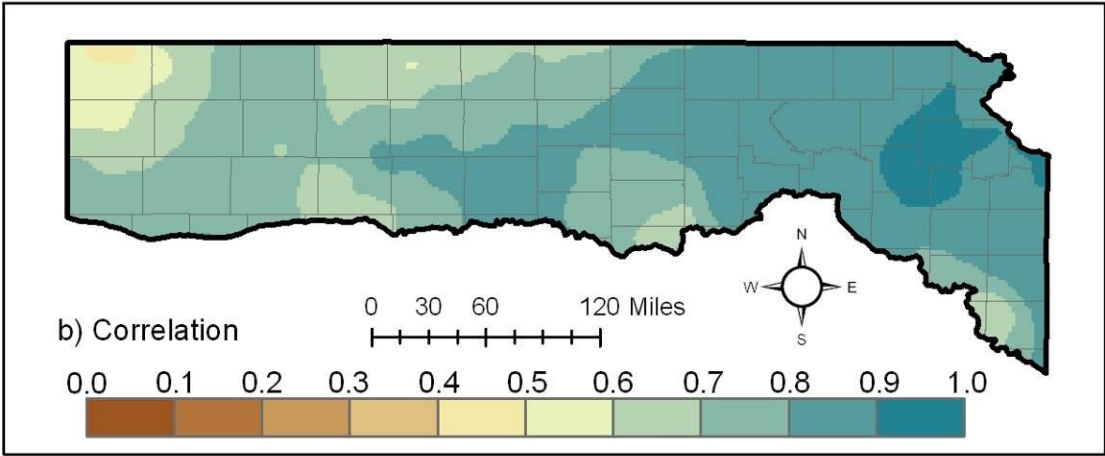
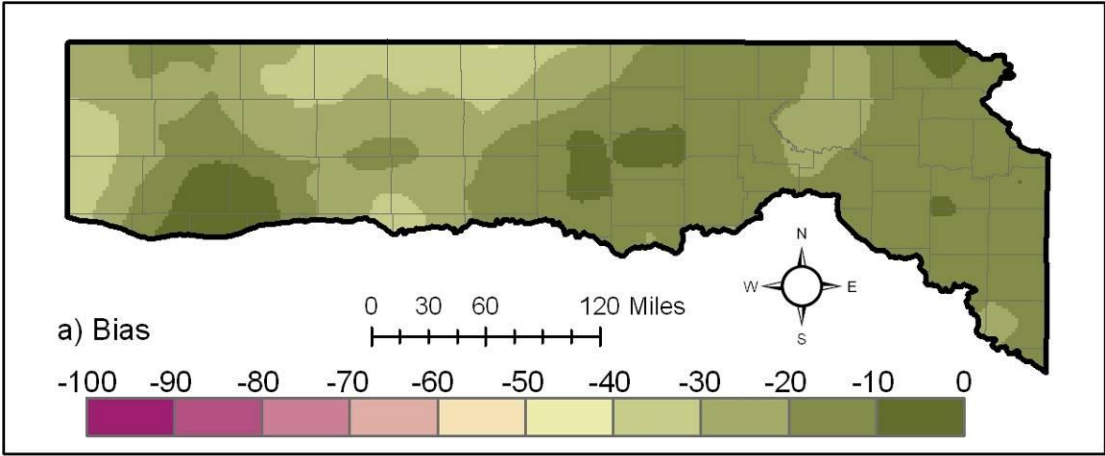


Figure 3.8: 2001 Warm Season

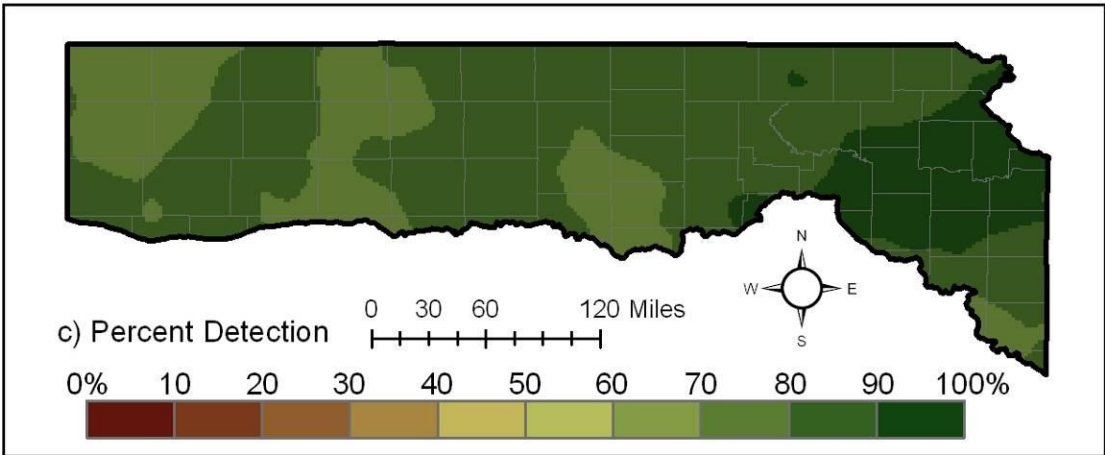
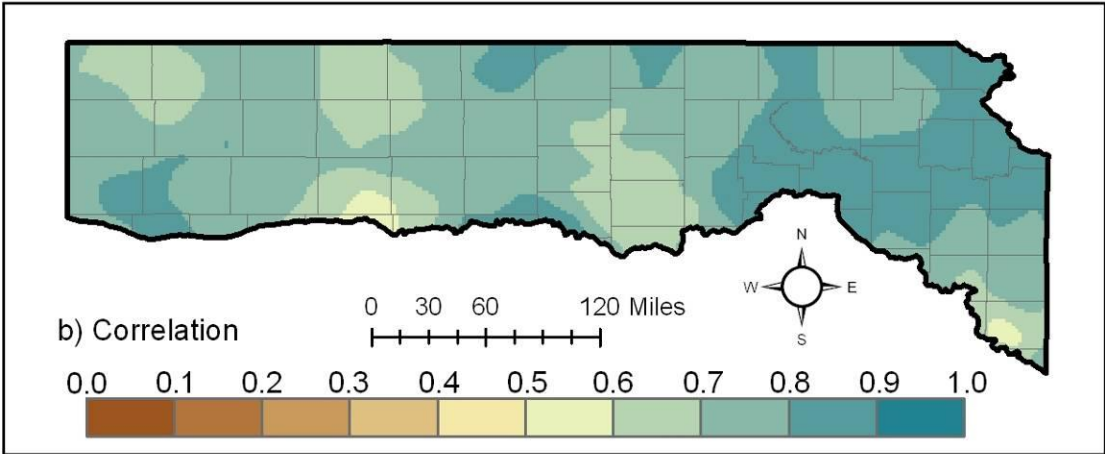
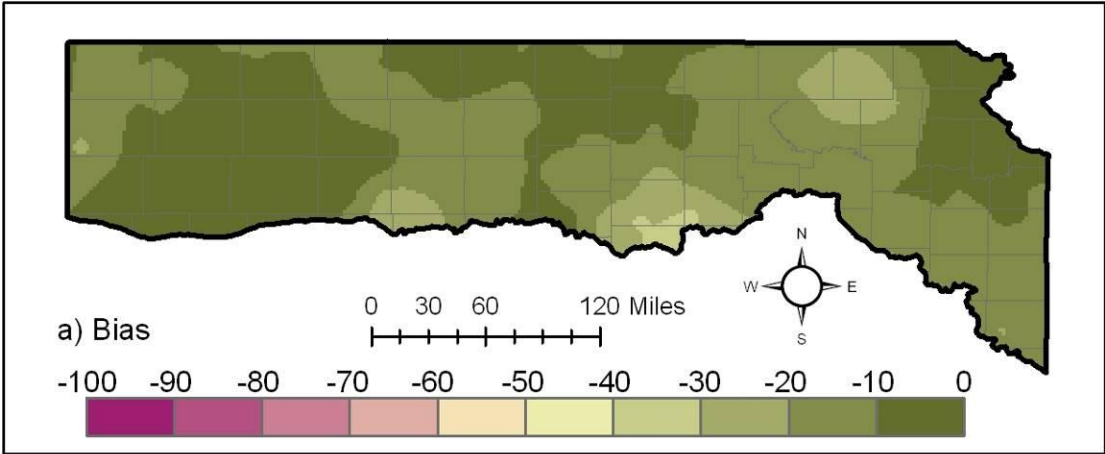


Figure 3.9: 2002 Warm Season

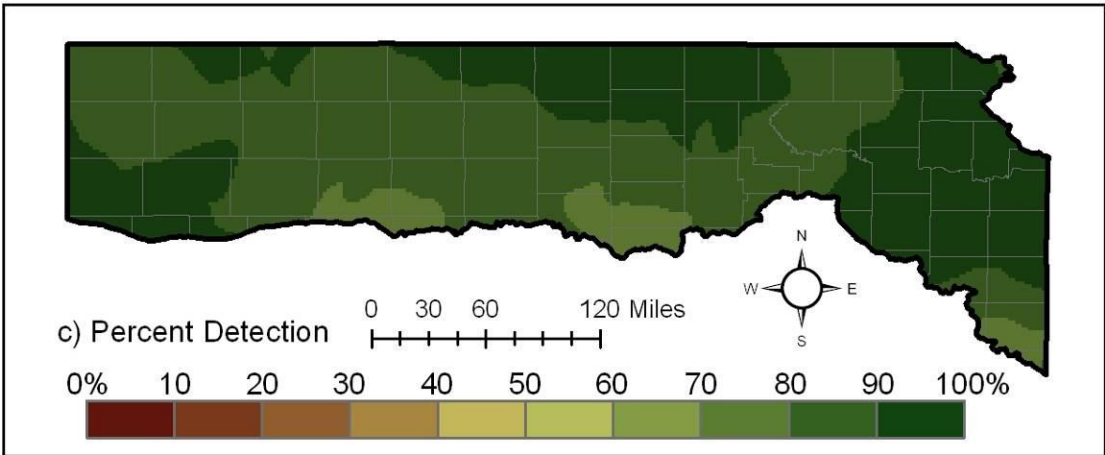
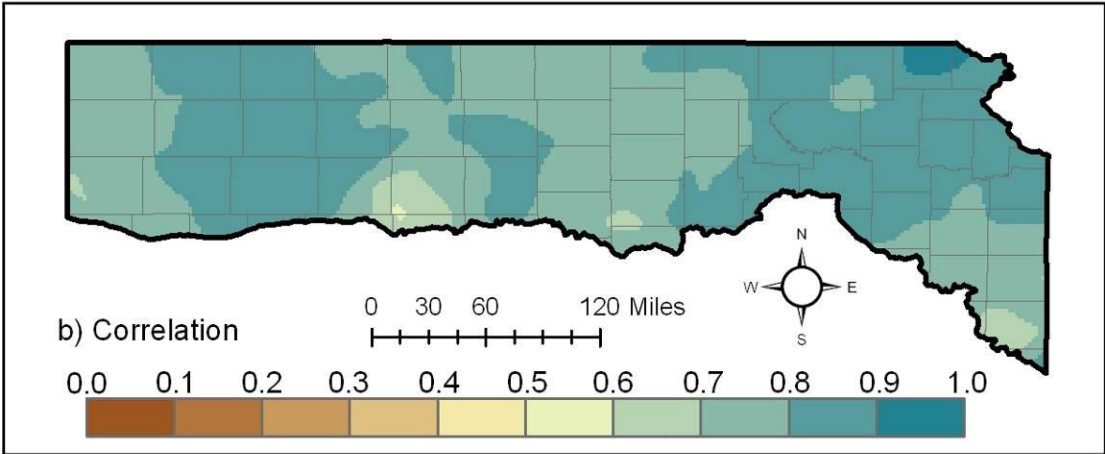
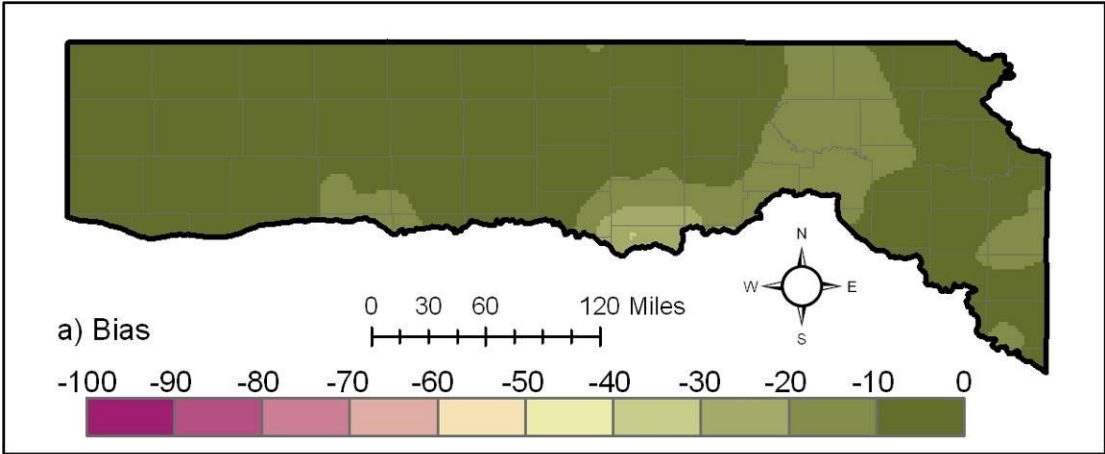


Figure 3.10: 2003 Warm Season

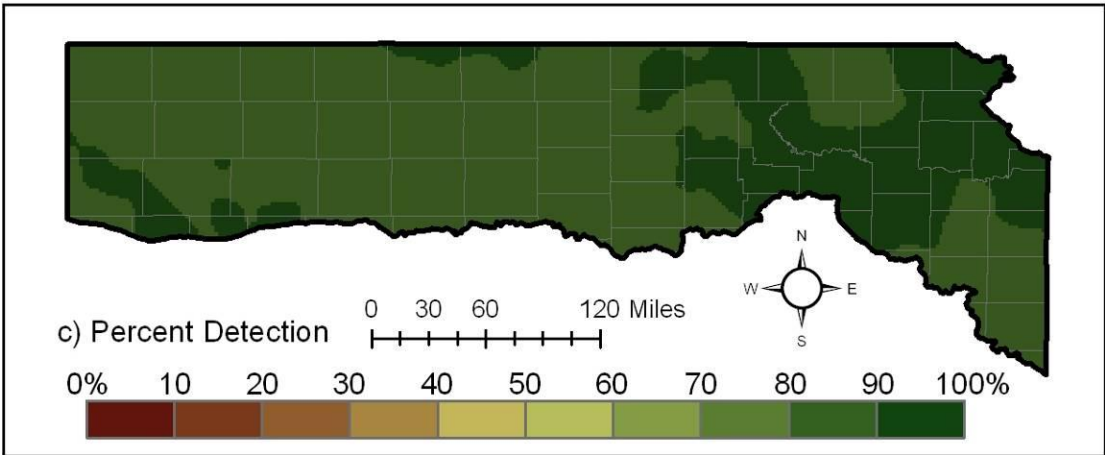
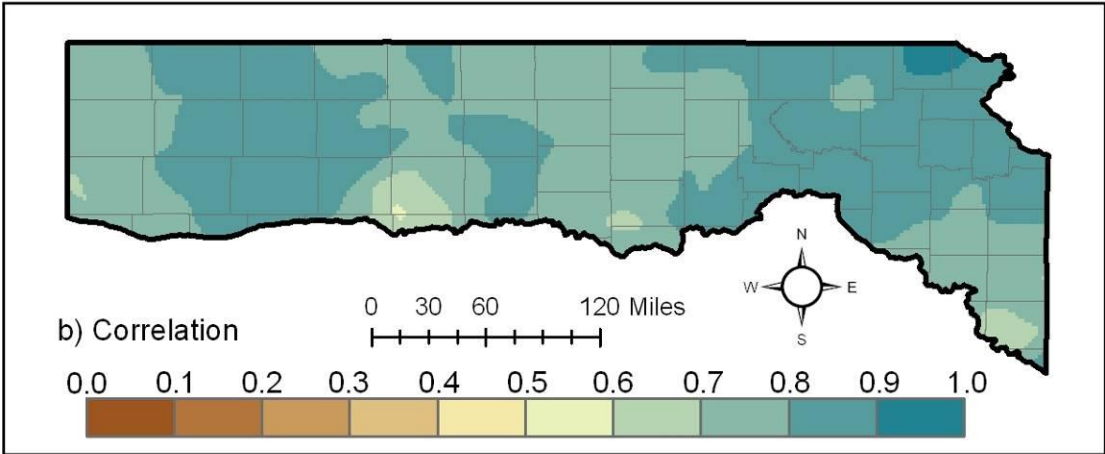
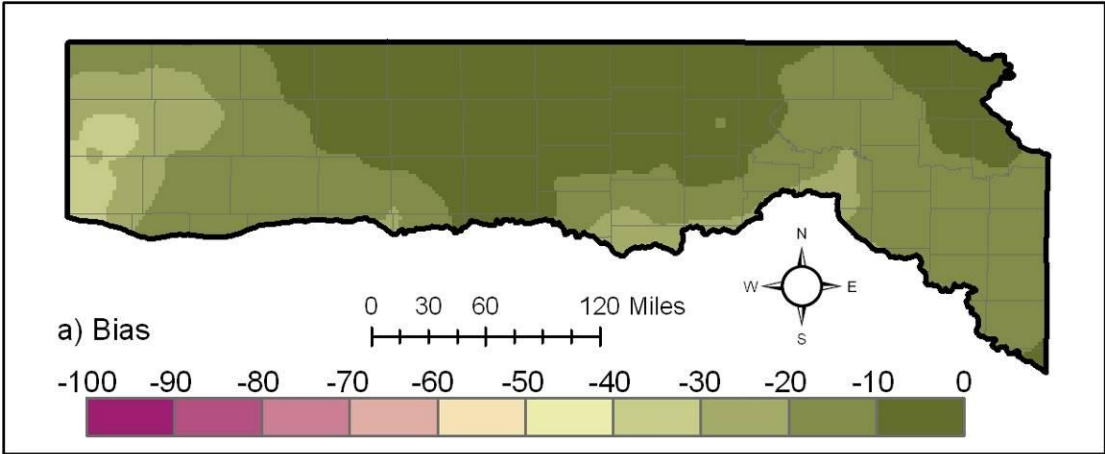


Figure 3.11: 2004 Warm Season

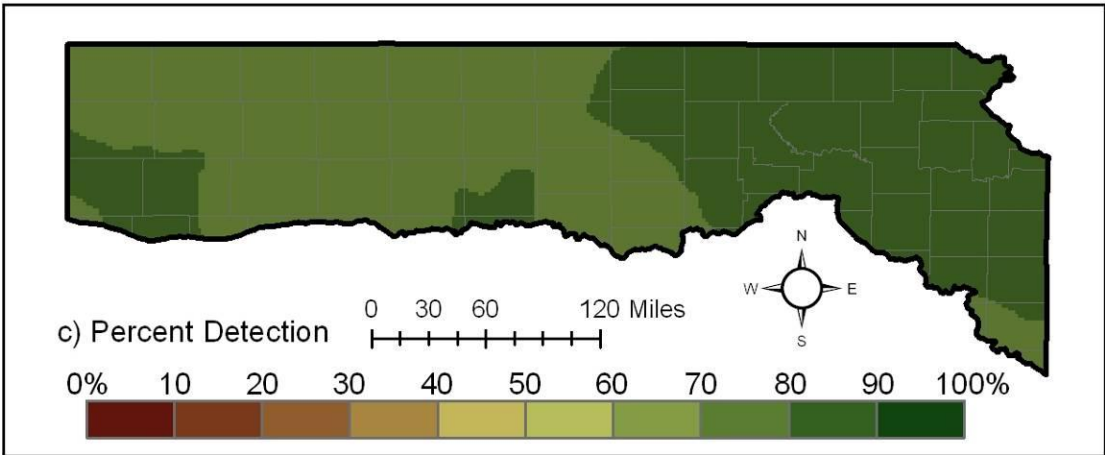
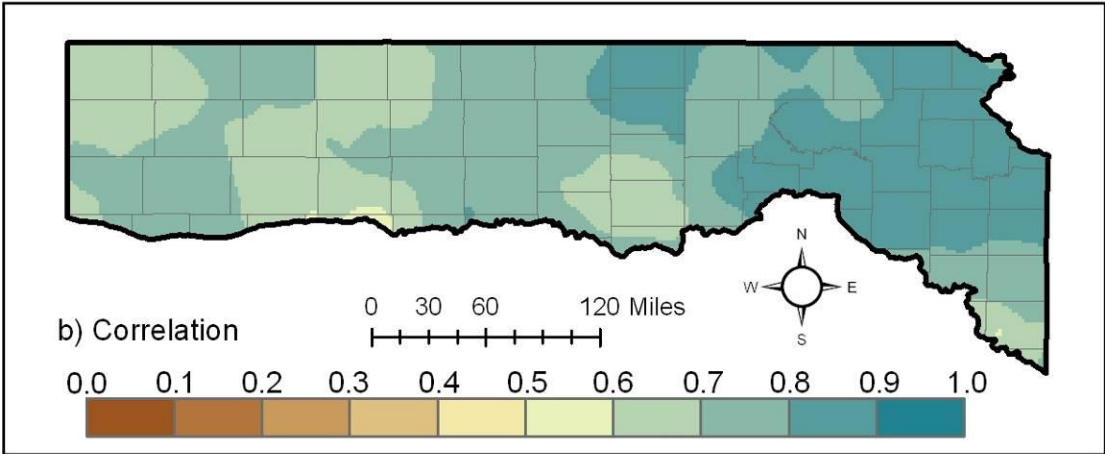
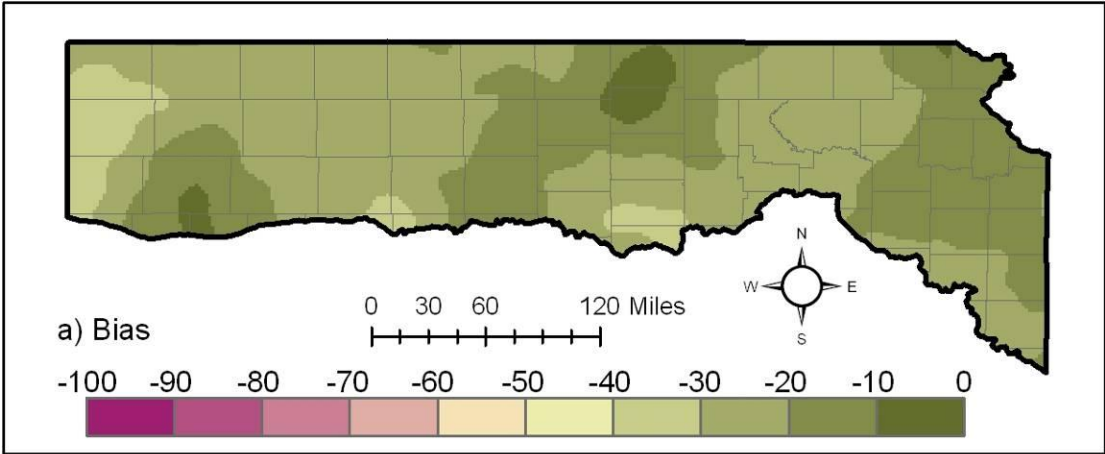


Figure 3.12: 1998 Cold Season

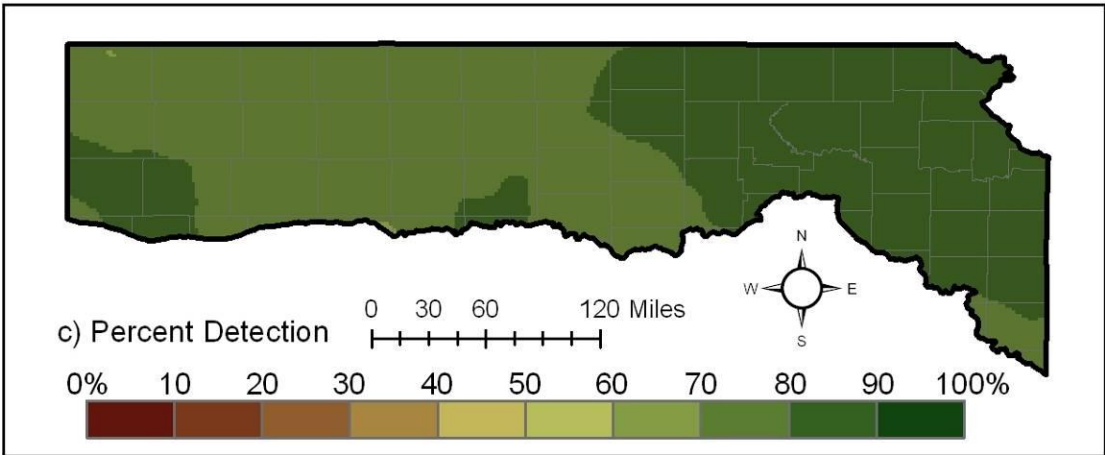
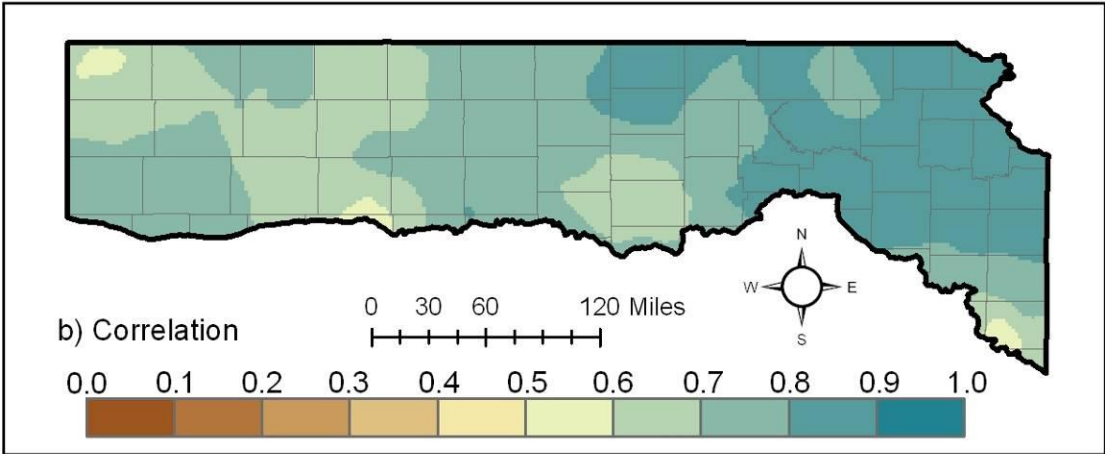
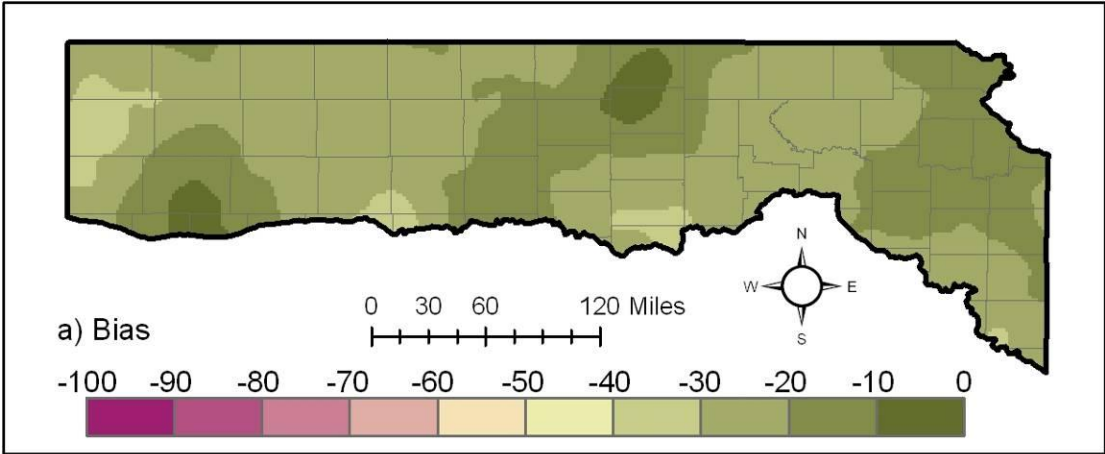


Figure 3.13: 1999 Cold Season

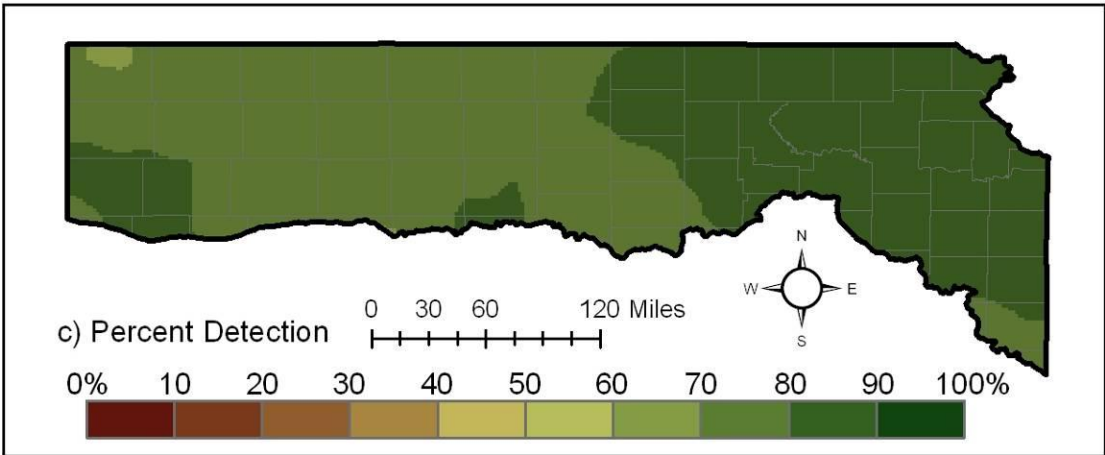
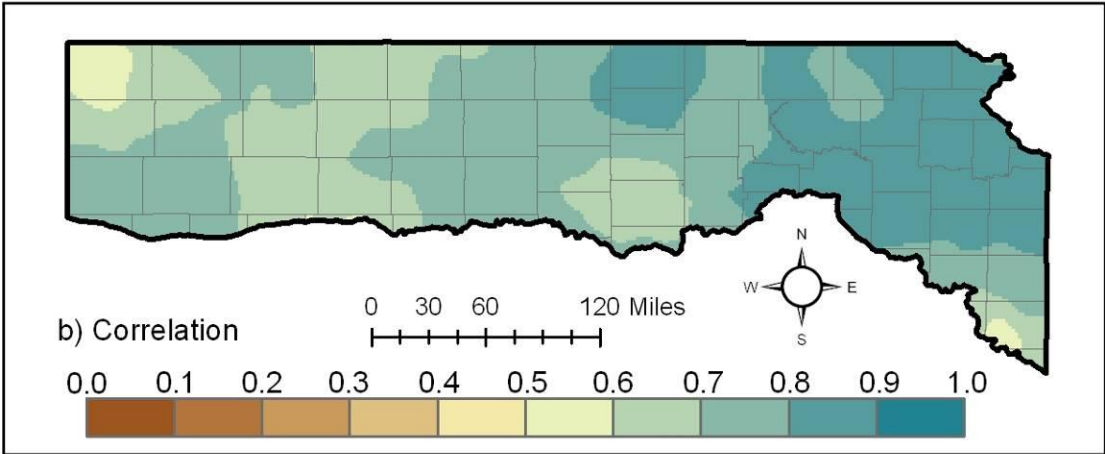
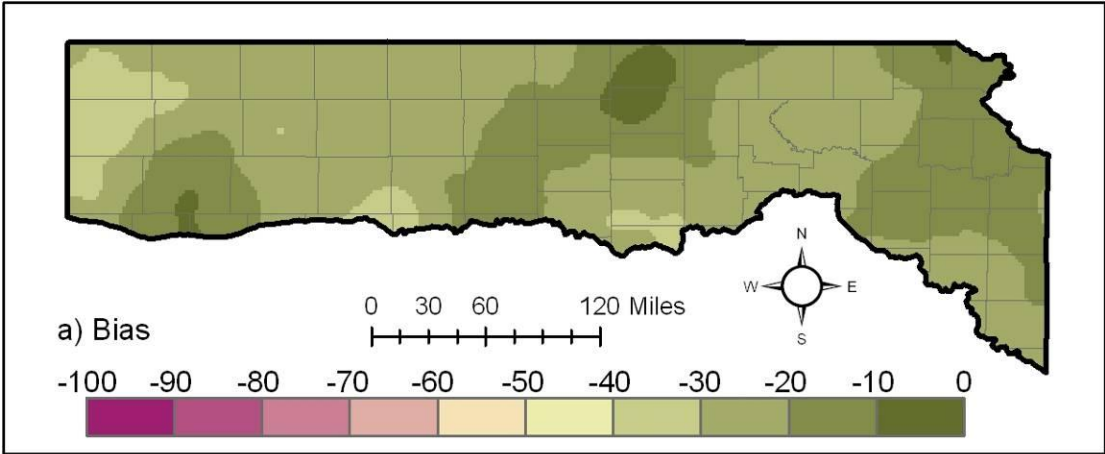


Figure 3.14: 2000 Cold Season

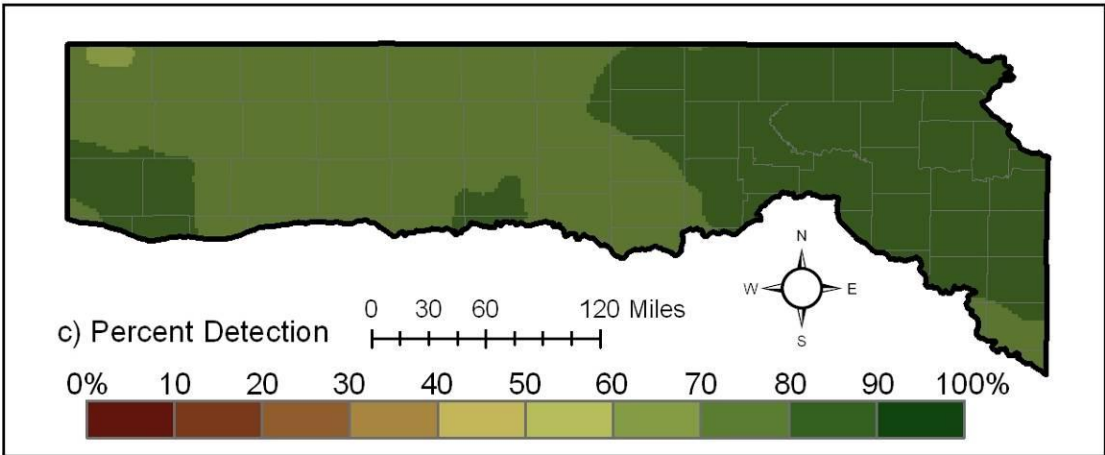
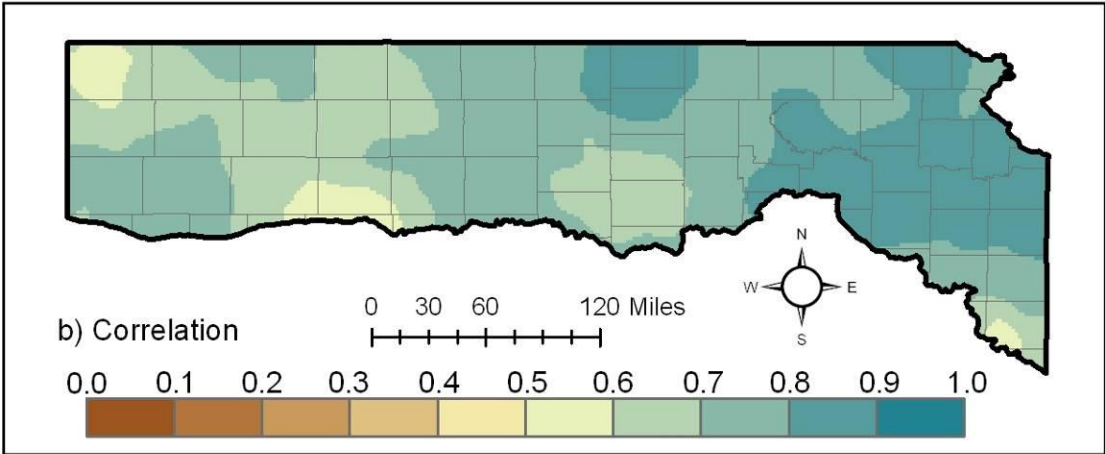
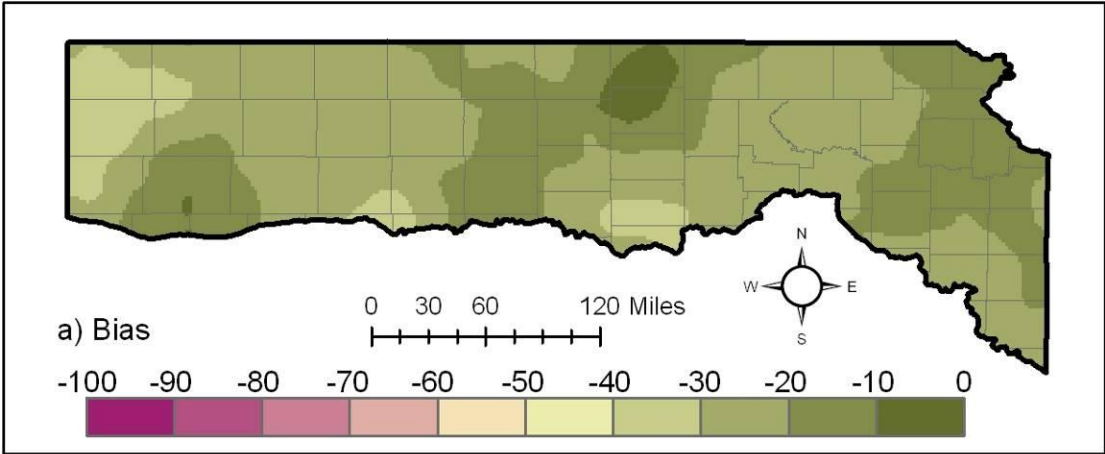


Figure 3.15: 2001 Cold Season

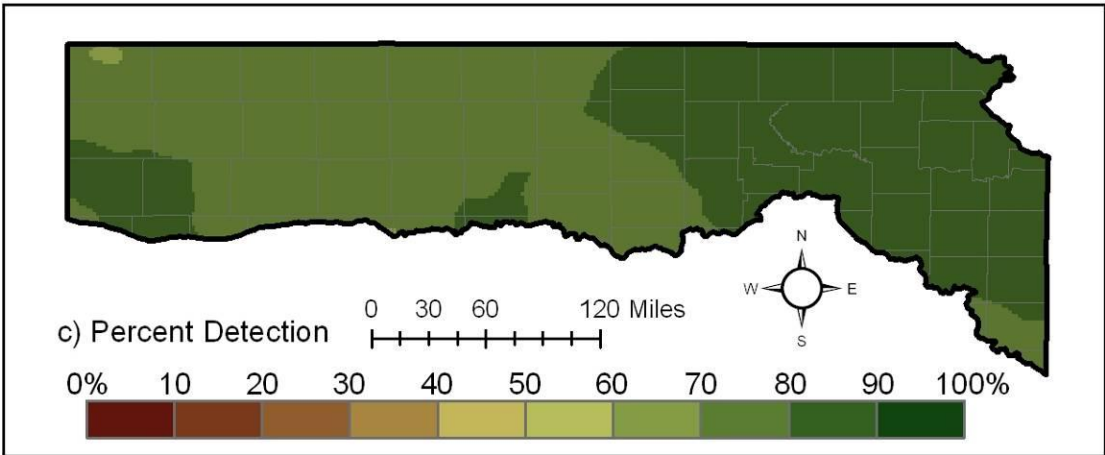
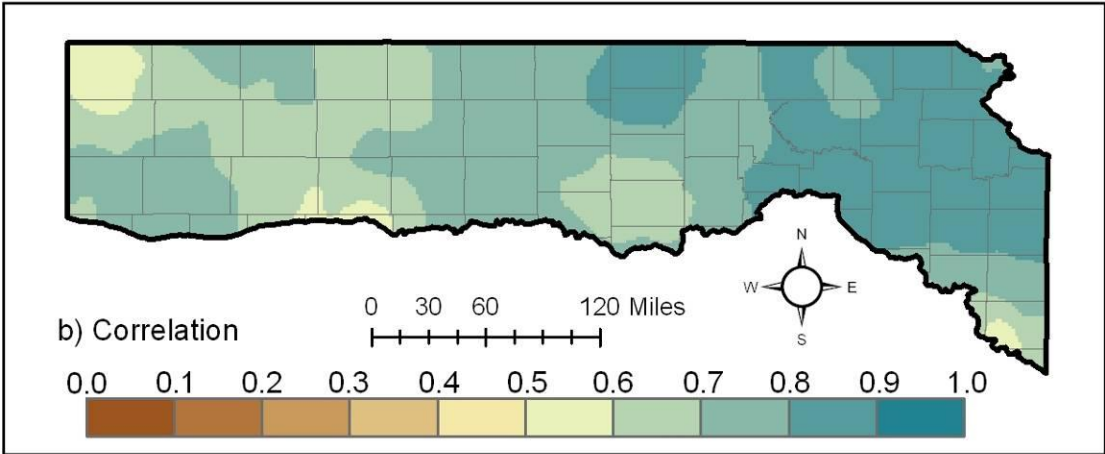
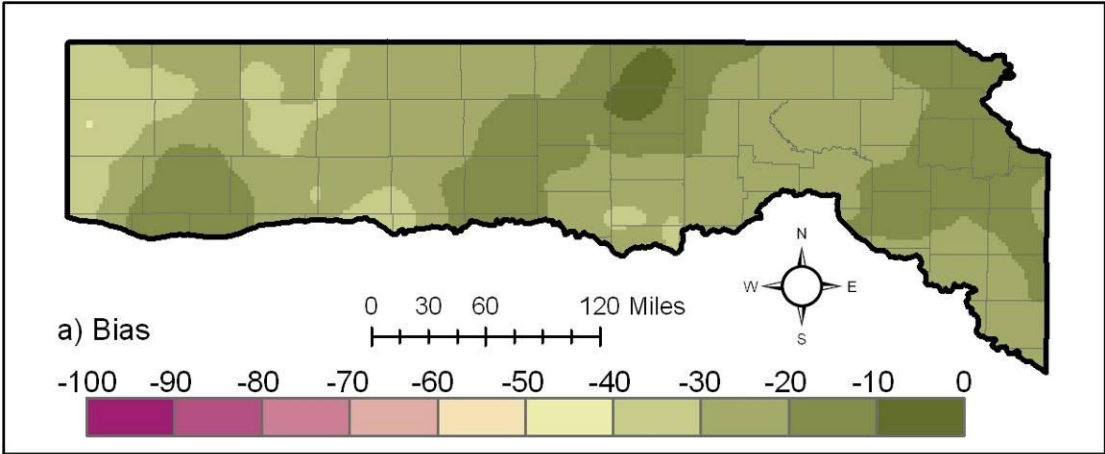


Figure 3.16: 2002 Cold Season

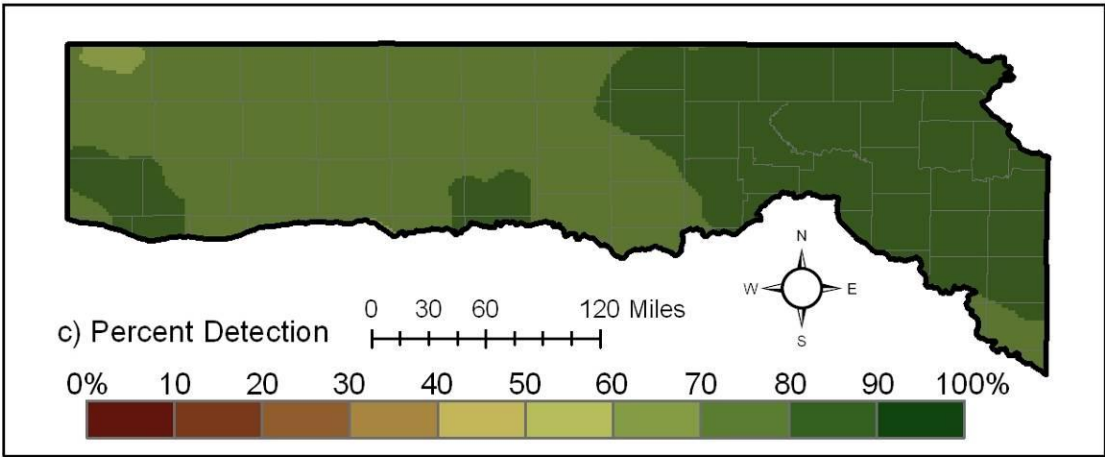
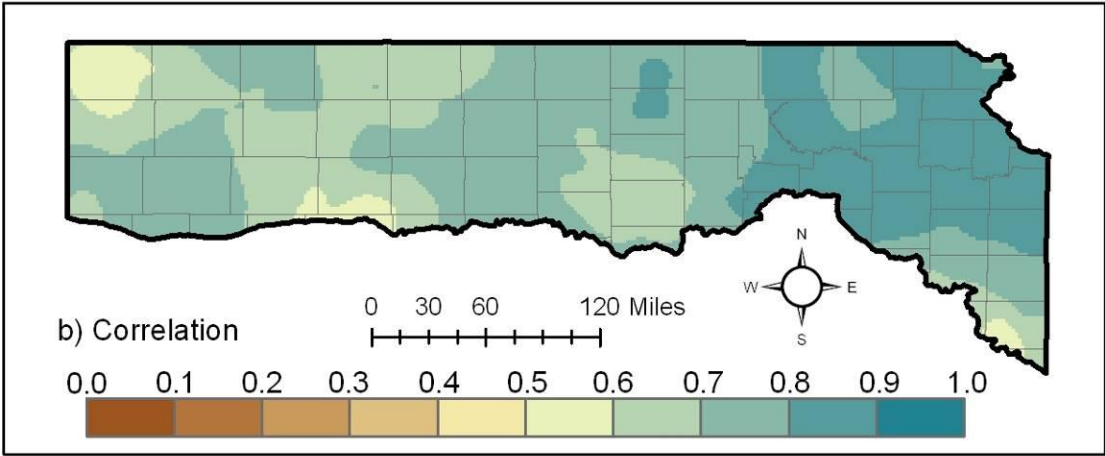
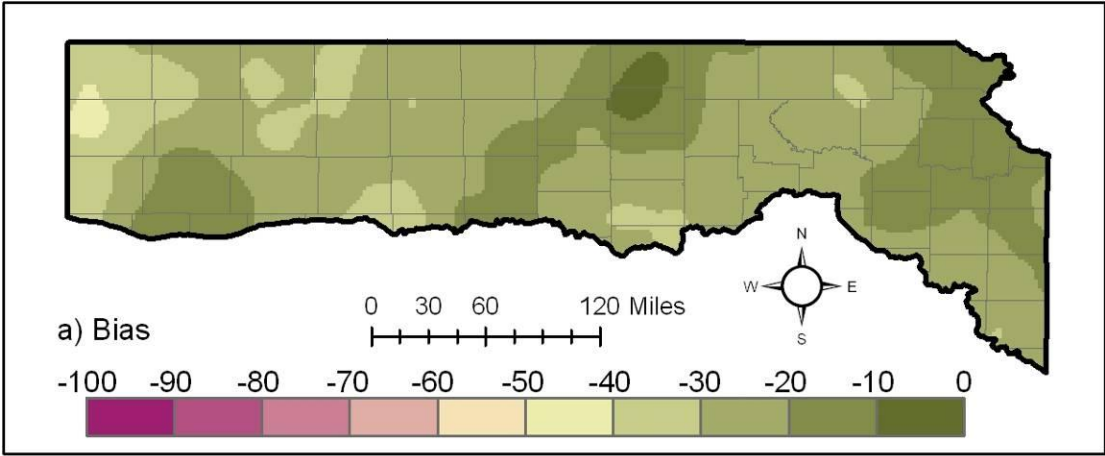


Figure 3.17: 2003 Cold Season

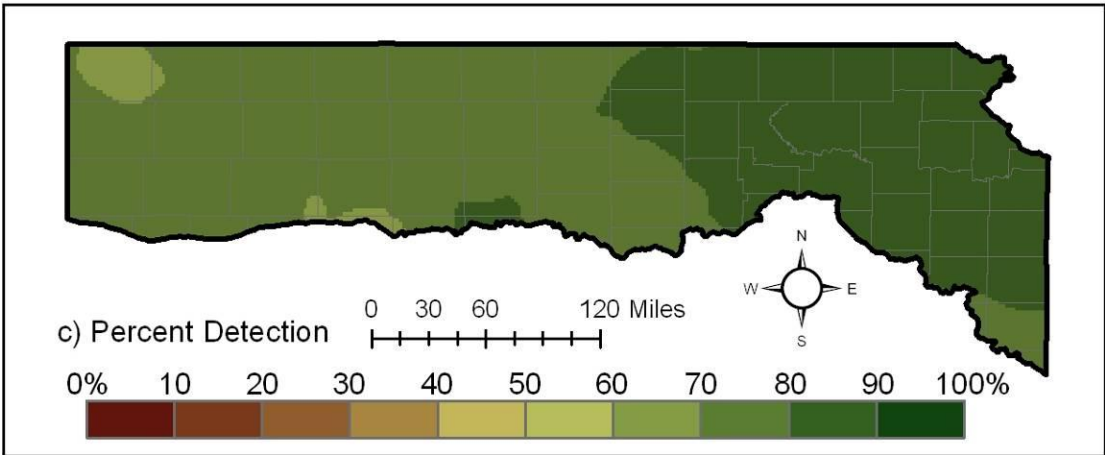
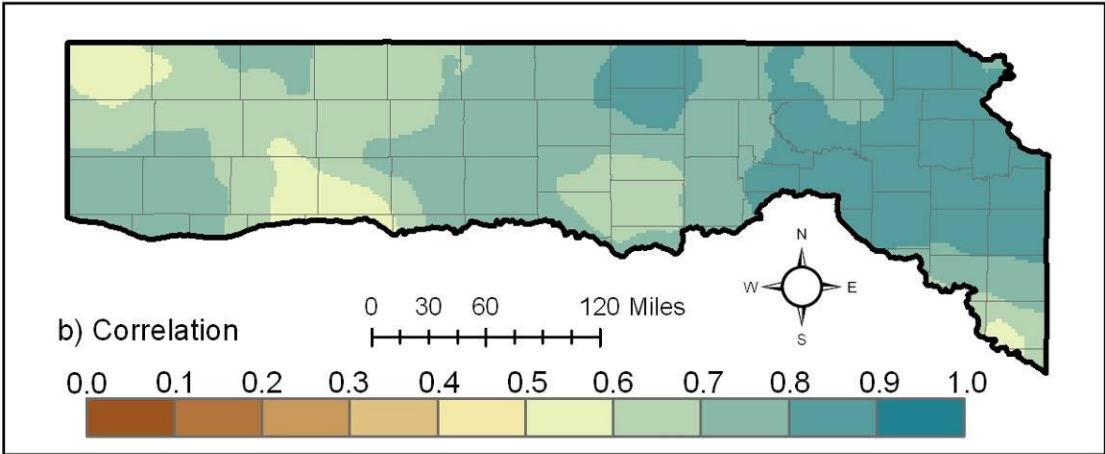
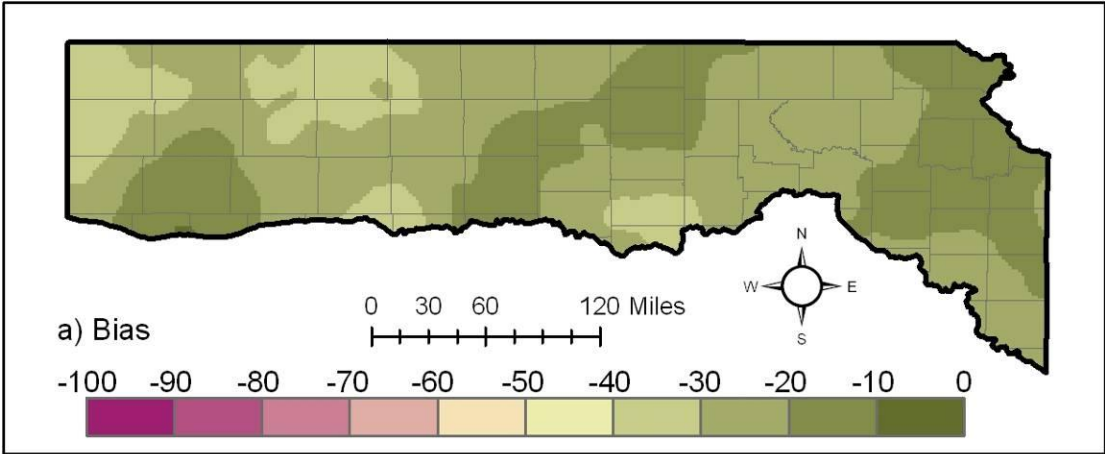


Figure 3.18: 2004 Cold Season

CHAPTER 4 - EVALUATION OF NEXRAD ESTIMATES USING ALERT RAIN GAUGES

4.1 Introduction

The previous chapter demonstrates the spatial and temporal variability of NEXRAD accuracy in northern Kansas. That analysis was performed using data from daily rain gauges across the region. Daily gauges were used because of the lack of hourly gauges that are independent of the NEXRAD product (not merged with the radar data). The objective of this chapter is to evaluate the quality of NEXRAD estimates of intense precipitation using the high-density ALERT rain gauge network in the Kansas City metropolitan area. This network provides a unique dataset, in that the vast majority of the gauges are independent (only a few of the gauges are available to the MBRFC for inclusion in the NEXRAD estimates). In addition, the network is dense, which allows for special statistical treatment of the NEXRAD-gauge comparison. The comparison in this chapter is not a point-to-pixel comparison; instead, this study uses spatially interpolated gauge data to get a direct area-to-area comparison with the NEXRAD data.

4.2 Study Area

The ALERT gauges used for this study are predominantly located in Johnson County, Kansas. There are several gauges in neighboring Jackson County, Missouri, and one gauge in Wyandotte County, Kansas. Figure 4.1 shows the study area and the ALERT gauges used for this analysis.

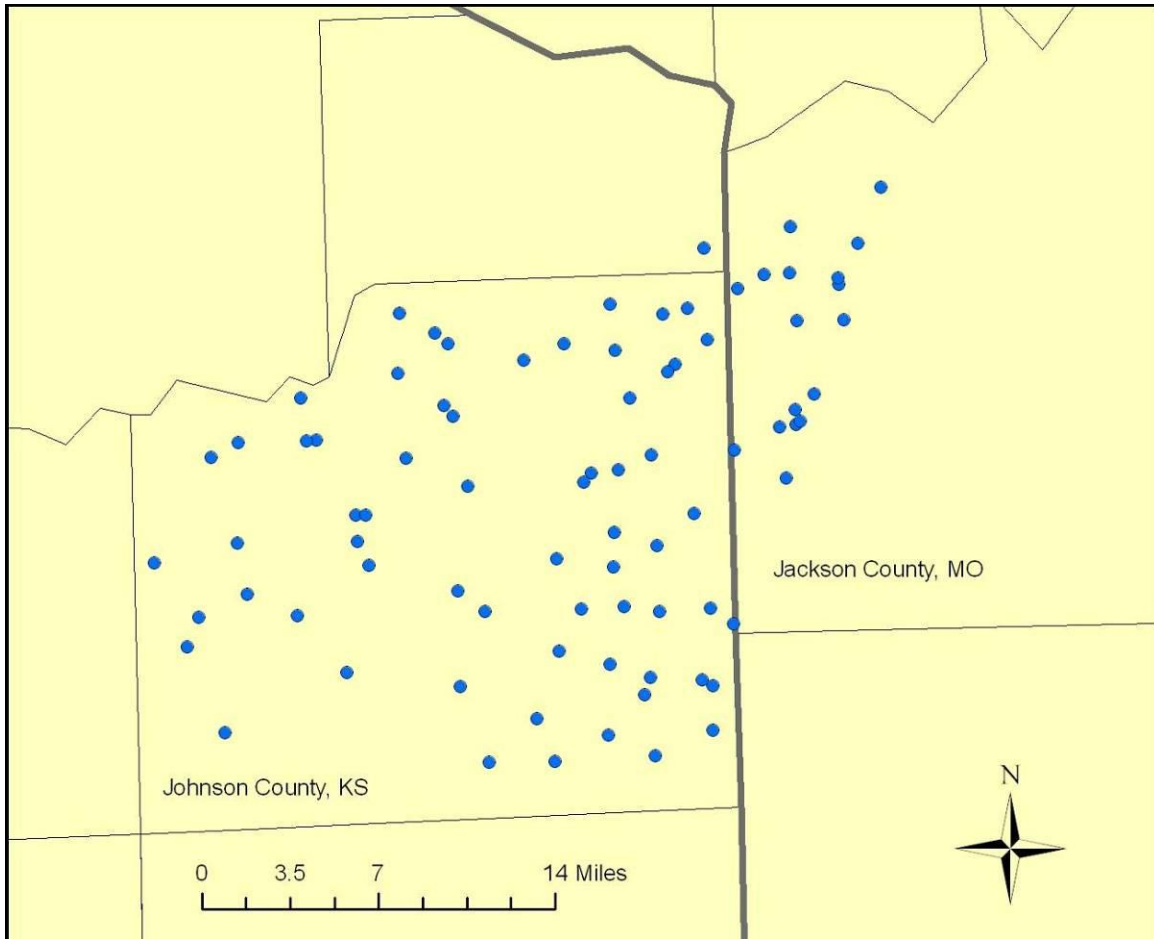


Figure 4.1: ALERT Network Rain gauges used in the Study

4.3 Data Preparation and Storm Selection

The ALERT network is managed and operated by the Johnson County Stormwater Management Program and the City of Overland Park, Kansas. The City of Overland Park provided all of the ALERT rain gauge data as 5-minute and daily accumulations from 1998-2004. The daily data were used to determine all rainfall events over the period 1998-2004 that produced 24-hour rainfall accumulation in excess of 2.0 inches at multiple gauge locations. The resulting storms were selected for further analysis.

For each selected storm, the 5-minute ALERT gauge data were accumulated to one-hour totals to match the temporal resolution of the NEXRAD precipitation estimates. Next, the NEXRAD data were extracted from the database described in the previous chapter for each storm, including files for three days prior to and three days after the date of the most intense rainfall. Radar loops, or storm animations, were created from the NEXRAD files at two different scales (see Figures 4.2 and 4.3). The regional map shows general storm movement and development, while the close-up map better shows the spatial distribution of rainfall in the study area. Each loop was evaluated visually to determine the start and stop times for the storm event. The start time for each storm was defined as one hour prior to the first appearance of precipitation in Johnson County. The end time was the time of the last appearance of precipitation in Johnson County. Determining the exact beginning and ending times was somewhat difficult. There were often several small storm systems that moved through the area, or there would be a short break in the precipitation, but it would continue again, still associated with the original storm system. Judgment was employed to define the start and end times, and the radar loops were then trimmed down to eliminate unnecessary frames and to reduce file size. The final loops are included with this report on a CD-ROM.

The majority of the storms chosen for this project were in the spring and summer months, when the likely cause of the heavy precipitation is either strong daytime heating or frontal systems moving through the region. Based on an evaluation of the radar loops, almost all of the storm systems chosen for the study were caused by cold fronts. A few of the storms were caused by a low-pressure center or warm front moving over

Johnson County, and even fewer were caused by light precipitation over long durations or strong daytime heating.

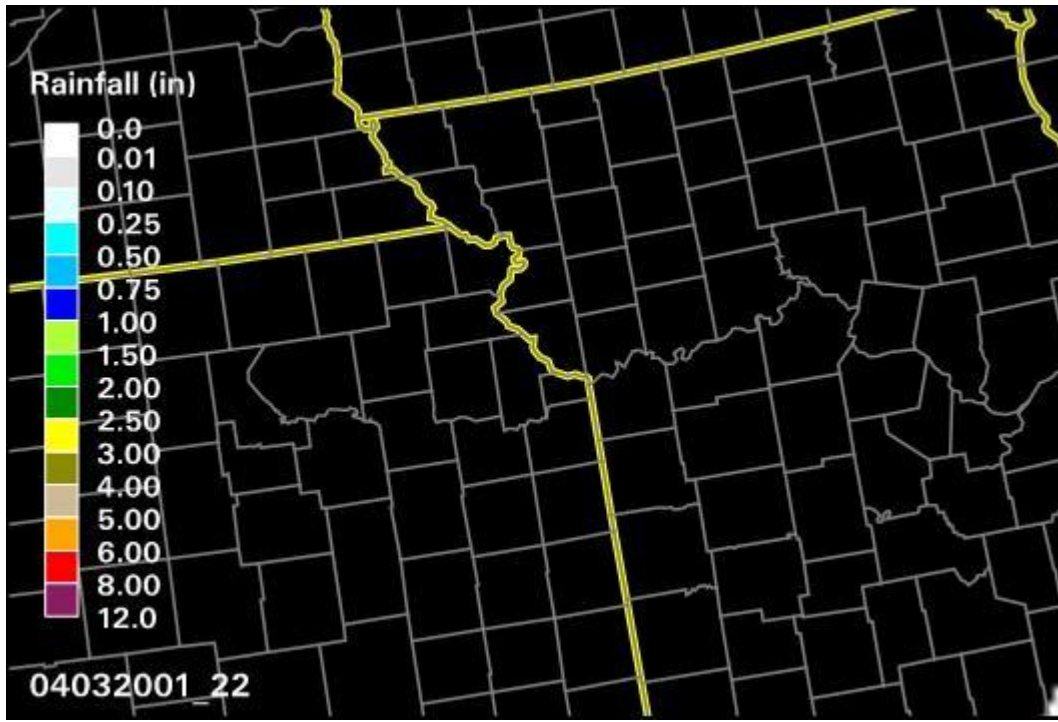


Figure 4.2: Example of Close-up Radar Image

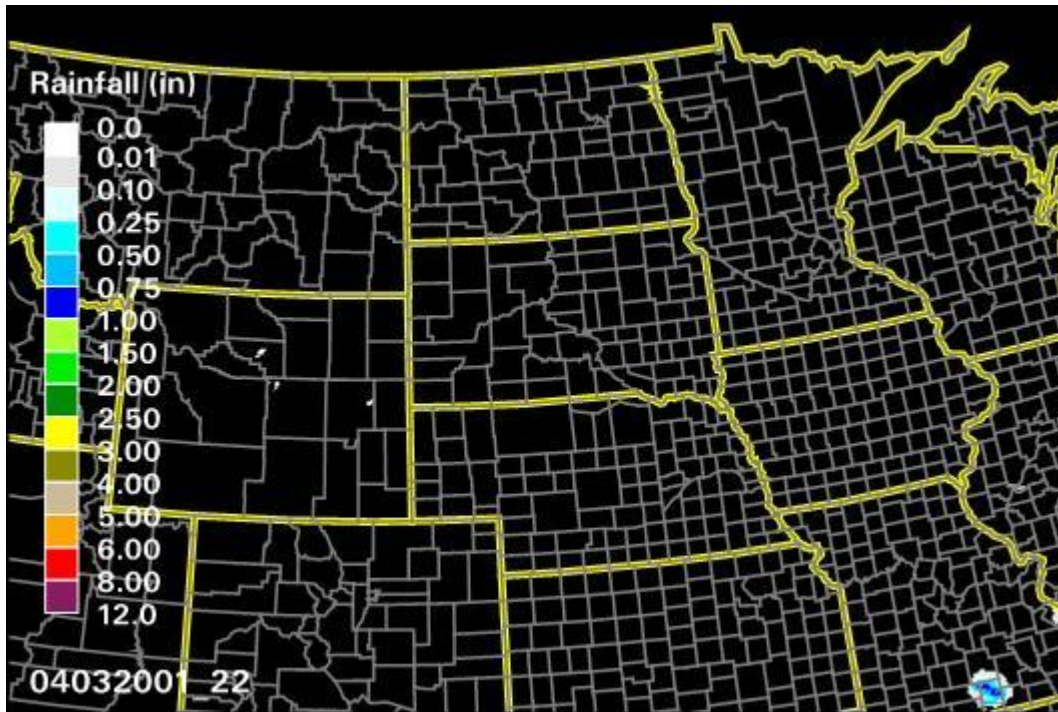


Figure 4.3: Example of Regional Radar Image

A few storms were eliminated from the study after examining both the rain gauge data and the radar data. There were a few instances in which the radar was not functioning properly for an hour or two, and the radar loop would show a blank image, when it actually should have been recording data. Storms that had missing radar data were eliminated from the study.

Quality control also indicated some errors in the rain gauge data. There were a few instances in which rain gauges recorded an unrealistic amount of precipitation. In other cases, some rain gauges recorded zero precipitation, when the radar image and nearby rain gauges were recording large amounts of precipitation. In the instances of rain gauge error, the data for each offending rain gauge was eliminated for the storm.

After quality control, 37 storms were selected for the study. The final dataset includes 34 storms; three storms were eliminated from the study because they did not meet the minimum hourly precipitation criteria described in a later section.

4.4 Methods

The NEXRAD-gauge comparison in the previous chapter is a direct comparison between the areal precipitation estimate produced by NEXRAD and the point observation at the rain gauge. This is common among evaluations of NEXRAD estimates, and necessary in the previous chapter due to the different reporting times for the gauges used. As such, some of the scatter in the results of Chapter 3 is due to the inter-cell spatial variability in rainfall. This chapter uses geostatistical techniques to interpolate the ALERT rain gauge data to the HRAP grid used for the NEXRAD product. This permits a comparison of areal-to-areal rainfall estimates. The geostatistical

technique employed, known as Kriging, also permits analysis of the estimation error in the interpolated gauge data.

Kriging is a method of spatial interpolation that is commonly used for geospatial datasets. Kriging was chosen for this project for many reasons. First, Kriging is a “Best Linear Unbiased Estimator,” or BLUE, where:

- “Best” means that the method seeks to minimize the prediction error variance,
- “Linear” means that the interpolated value is a linear combination of observed point observations, and
- “Unbiased” means that the kriging errors are, on average, zero.

In addition to minimizing the prediction error variance, kriging also provides an estimate of the error variance. This is something that other interpolation methods do not provide. This error variance can be used in turn to evaluate how much of the discrepancy between NEXRAD and gauge estimates is due to uncertainty in the gauge estimates.

All Kriging for this project was carried out in GSTAT, a freely available geostatistical software package (Pebesma and Wesseling, 1998). GSTAT allows processing in batch mode, which proved to be important in this project because of the large number of storms and hours processed.

Kriging uses information about the spatial correlation of the point data to compute the weights used in interpolation. If the point data are not very continuous in space, only the nearest gauges will get significant weighting. If the point data are highly continuous in space, the weights will decrease more gradually with distance. The weights are

computed using a model of the spatial correlation in the point data. In geostatistics, the spatial correlation is usually described using the semivariogram. The semivariogram at a given range of lag distances (say, 1 to 2 mi) is equal to one-half of the averaged squared difference for all of the data pairs that have a separation distance in that range:

$$\gamma(d) = \frac{1}{2N(d)} \sum_{(i,j):d_{ij}=d} (v_i - v_j)^2 \quad \text{Equation 4.1}$$

where $\gamma(d)$ is the semivariogram value at average lag distance, d , $N(d)$ is the number of pairs in the range of lag distances, and v_i and v_j represent each pair of observations that are separated by a lag distance in the specified range.

To kriging a dataset, the user must first select a semivariogram model. This is usually done in an interactive fashion. With GSTAT, the program computes an experimental semivariogram using the observed point data. The user then fits the semivariogram by selecting a model type and varying the model parameters until a good fit is achieved. For this research, four basic variogram models were used: linear, spherical, exponential, and Gaussian. Figures 4.4 through 4.7 show the basic shapes for these four models. Each model could also be assigned a nugget effect, which permits the semivariogram value at zero lag ($d = 0$) to be non-zero. Figure 4.8 shows the Gaussian model with a nugget effect. If a nugget effect is used to fit the observed semivariogram, this is usually the result of high spatial discontinuity in the point data. When modeling rainfall distributions, this high spatial discontinuity can be due to the type of storm passing through, but it is often the result of error in the rain gauge data.

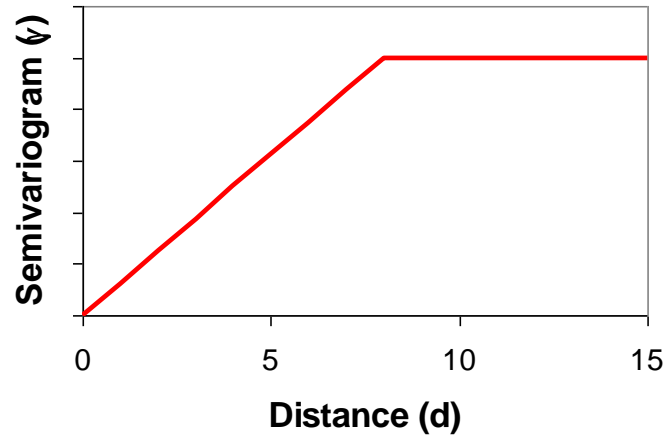


Figure 4.4: Linear Model for the Semivariogram

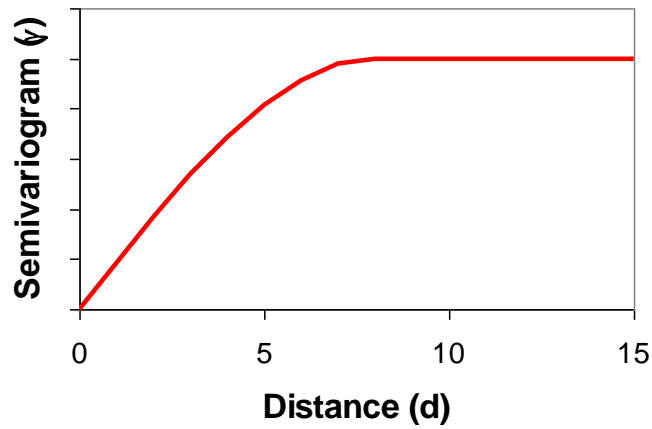


Figure 4.5: Spherical Model for the Semivariogram

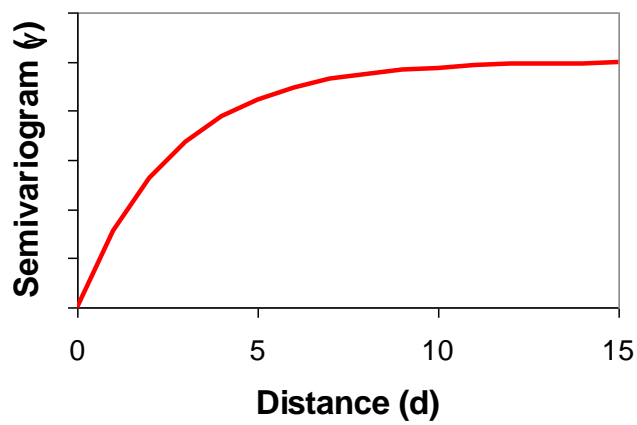


Figure 4.6: Exponential Model for the Semivariogram

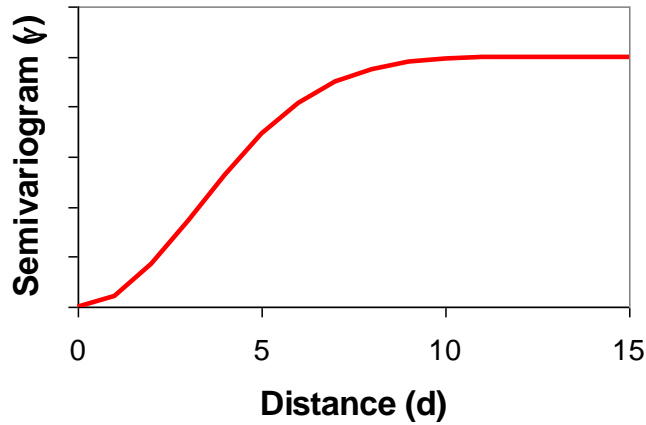


Figure 4.7: Gaussian Model for the Semivariogram

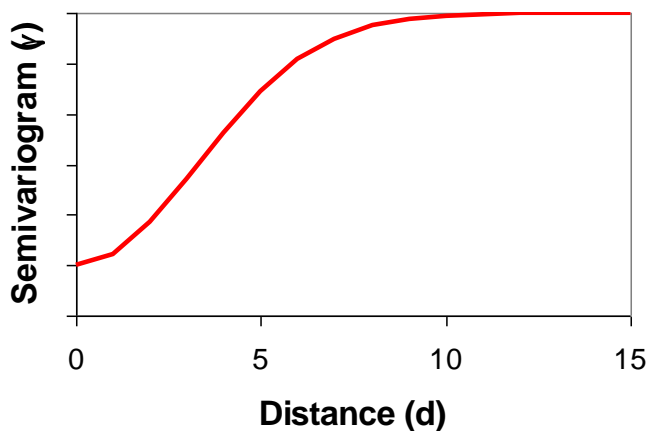


Figure 4.8: Gaussian Model with a Nugget Effect

GSTAT was used to compute the experimental semivariograms and to fit the semivariogram models in this study. The model type was selected by the user, and GSTAT computed the model parameters to achieve a least-squares fit of the experimental semivariogram. In most cases, a linear model or linear model with nugget adequately described the experimental semivariogram. A unique semivariogram was fit to each hour of data to ensure that the spatial variability was modeled as accurately as possible. Figure 4.9 shows a sample screenshot from GSTAT of the semivariogram

fitting procedure. The points on the graph indicate values computed for the experimental semivariogram. The curve fit to these points is a Gaussian model with a nugget effect.

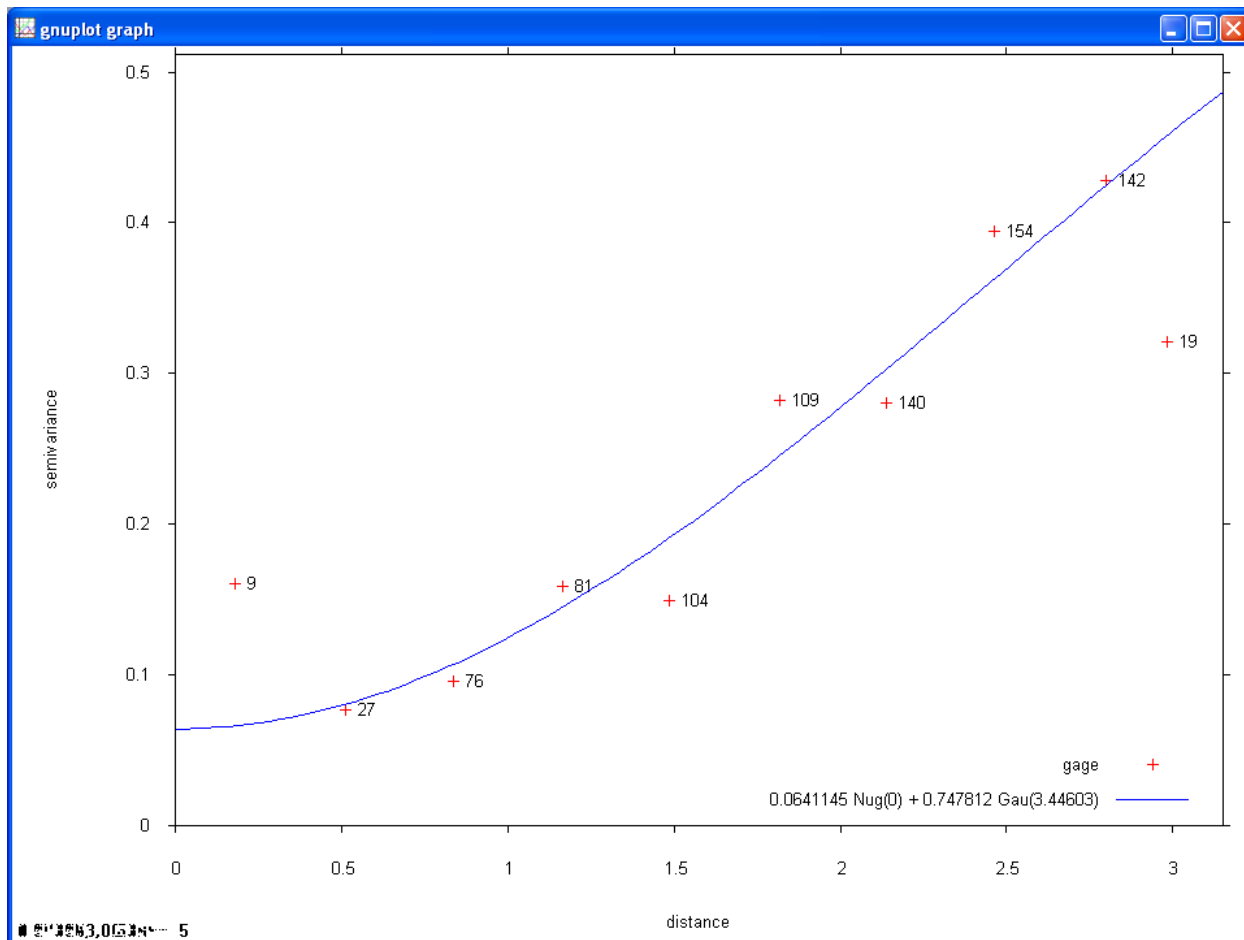


Figure 4.9: Screen Shot of the Semivariogram Fitting Procedure

Once the semivariogram model is fit by the user, GSTAT executes the kriging routine. In this case, the point data were interpolated to the HRAP grid, but only for cells that were within the ALERT rain gauge network. Kriging can be somewhat unstable when used to extrapolate data, so a mask file was generated for each storm that clipped the kriging output to the extent of the ALERT network.

The kriging process was applied to all storm hours that had mean rainfall totals in excess of 0.25 inches. In addition, kriging was applied to compute storm total

precipitation. The interpolated gauge estimates of precipitation were combined with estimates of the kriging error variance and the NEXRAD rainfall estimates into files for each storm event. These files were analyzed in Excel to remove any cases where kriging ended up extrapolating values to the edge of the study area.

Next, several statistical values were calculated to quantify the differences between the kriged ALERT rain gauge data and the NEXRAD rainfall estimates. The statistical measures calculated included: mean absolute difference (MAD), normalized mean absolute difference (NMAD), bias, root mean square difference (RMSD), fractional square difference (FSD), and the percentage of points outside the 90% confidence interval. The formulas given below were used to calculate each of these parameters:

$$\text{MAD} = \frac{1}{n} \sum |Nex_i - Gage_i| \quad \text{Equation 4.2}$$

$$\text{NMAD} = \frac{\text{MAD}}{\frac{1}{n} \sum Gage_i} \cdot 100\% \quad \text{Equation 4.3}$$

$$\text{Bias} = \frac{\sum Nex_i - \sum Gage_i}{\sum Gage_i} \cdot 100\% \quad \text{Equation 4.4}$$

$$\text{RMSD} = \sqrt{\frac{1}{n} \sum (Nex_i - Gage_i)^2} \quad \text{Equation 4.5}$$

$$\text{FSD} = \frac{\sqrt{\frac{1}{n} \sum (Nex_i - Gage_i)^2}}{\frac{1}{n} \sum Gage_i} \times 100\% \quad \text{Equation 4.6}$$

The 90% confidence interval for each Kriged gauge estimate was computed using 1.645 times the square root of the Kriging error variance. This confidence interval

can be used to assess how much of the NEXRAD-gauge scatter is due to error in the kriged rainfall estimates. If the NEXRAD estimates are equal in quality to the kriged gauge estimates, about 10% of the points will fall outside of the 90% confidence interval due to random variability. Thus, if the number of points outside the 90% confidence interval is close to 10%, then it can be concluded that the NEXRAD estimates are not significantly different than the kriged gauge estimates.

Scatter plots were developed for both the hourly data and the storm total data for each storm. These graphs show the values of the kriged rain gauge data as the independent variable, and the NEXRAD estimates as the dependent variable. Points within the 90% confidence interval are plotted in green, and points outside the 90% confidence interval are plotted in red. A trendline is also fit to the data to show the average deviation from the 1:1 line as a function of gauge accumulation. Plots of the hourly data comparisons are in Appendix A, and plots of the storm total comparisons are in Appendix B.

4.5 Results

Tables 4.1 and 4.2 summarize the statistics mentioned above for the hourly accumulations and the storm total data, respectively. These tables present the range, quartiles, and average statistics for all 34 storms. The mean bias for all hours evaluated was +8.15% and the mean bias for all storms was +17.1% (NEXRAD overestimating relative to kriged gauge estimates). The bias figures are different for hourly and storm totals because only hours with intense rainfall were evaluated (mean rainfall in excess of 0.25 in). Analysis of the figures in Appendix A and B indicates that, in general, the NEXRAD product overestimates rainfall at low gauge accumulations and

underestimates rainfall for high gauge accumulations. This conditional bias is the cause for storm total bias exceeding the bias in the hourly figures. The storm totals include hours with small accumulations (where NEXRAD tends to overestimate rainfall) that were excluded from the evaluation of hourly estimates. The bias numbers presented here appear to conflict with those presented in Chapter 3. Again, it must be considered that the NEXRAD data set evaluated in this chapter is a subset of that used in Chapter 3. The evaluation in this chapter focuses on 34 large rainfall events. It has been documented (in Chapter 3 and elsewhere) that the NEXRAD product suffers underdetection and underestimation of rainfall not associated with heavy storms.

The normalized mean absolute difference (NMAD) between NEXRAD and gauge estimates is 42.1% for the hourly accumulations and 31.3% for the storm totals. This reduction in NMAD indicates that random errors in the NEXRAD product are reduced through aggregation to longer time steps. The RMSD increases from hourly to storm total rainfall accumulations, but this increase is due to the fact that storm totals are by definition larger. The FSD, which is essentially a normalized RMSD, decreases from 58.3% for hourly accumulations to 39.8% for the storm totals.

The number of points outside of the 90% confidence interval is high for both the hourly and storm accumulations (52% and 59% respectively). This indicates that a large degree of the difference between NEXRAD and the kriged gauge estimates cannot be attributed to the natural spatial variability in the rainfall.

The statistics in Tables 4.1 and 4.2 compare hourly and storm accumulations for $4 \times 4 \text{ km}^2$ cells in the HRAP grid. Figure 4.10 presents a comparison of storm totals

averaged over the entire study area (the extent of the ALERT gauge network). The correlation in this relationship is 0.87.

Tables 4.3 and 4.4 present summary statistics for each of the 34 storms analyzed in this study. These tables are included at the end of this chapter.

4.6 Conclusions

The statistics presented in Tables 4.1 and 4.2 point to large errors in the NEXRAD product. In general, NEXRAD overestimated hourly and storm accumulations, although this bias was conditional. NEXRAD overestimated rainfall for low gauge observations and underestimated rainfall at high gauge values. In addition, the NEXRAD MAD and RMSD are high in comparison to the mean gauge accumulations as expressed in the NMAD and FSD. However, Figure 4.10 shows that the NEXRAD product does a good job of predicting the spatially averaged estimates of storm totals.

Although the comparison in this chapter finds large errors in the NEXRAD product, it must be remembered that gauge estimates of rainfall are not free of error either. Gauge error may contribute significantly to the statistics reported in this chapter, although using a kriged gauge field does acknowledge the error introduced through spatial variability. Other errors such as wind induced undercatch, poor gauge calibration, and false tips cannot be accounted for.

Table 4.1: Summary of Statistics for Hourly Accumulations

	Bias (%)	NMAD (%)	RMSD (in)	FSD (%)	Correlation	% of Points outside CI
Minimum	-21.0	24.8	0.10	32.2	0.01	29
10%	-15.2	27.7	0.14	38.2	0.47	36
25%	-4.4	30.6	0.19	41.8	0.63	42
Median	2.2	39.8	0.24	57.9	0.72	54
75%	24.1	49.3	0.30	68.4	0.77	60
90%	31.9	54.8	0.41	76.3	0.84	69
Max	62.8	91.0	0.54	130.3	0.93	83
Mean	8.15	42.1	0.26	58.3	0.66	52

Table 4.2: Summary of Statistics for Storm Totals

	Bias (%)	NMAD (%)	RMSD (in)	FSD (%)	Correlation	% of Points outside CI
Minimum	-15.7	8.83	0.19	12.8	-0.22	8
10%	-8.76	15.9	0.30	22.5	-0.07	22
25%	-1.00	21.4	0.43	25.8	0.22	36
Median	10.7	24.4	0.55	33.4	0.59	65
75%	31.6	37.1	0.67	47.9	0.79	83
90%	47.9	62.1	1.23	70.7	0.89	92
Maximum	81.0	81.0	3.07	94.1	0.97	99
Mean	17.1	31.3	0.68	39.8	0.51	59

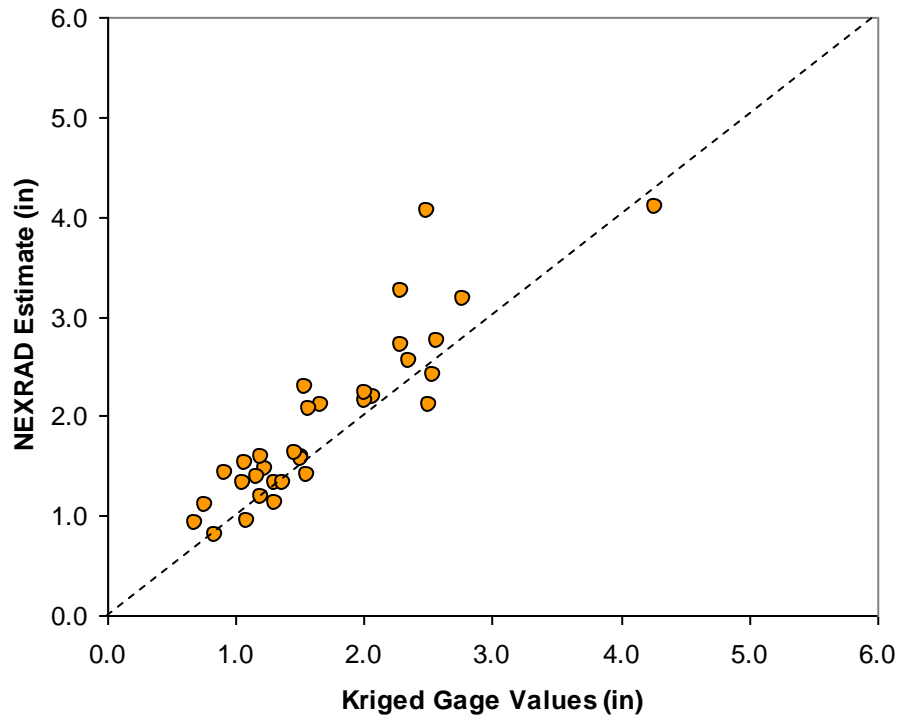


Figure 4.10: Comparison of Storm Total Spatial Averages

Table 4.3: Statistics for Hourly Totals for all 34 Events

Storm Date	Average Gage (in)	Average NEX (in)	Bias (%)	MAD (in)	NMAD (%)	RMSD (in)	FSD (%)	Correlation	% of Points outside CI
8-Jun-98	0.43	0.34	-21.0	0.12	27.9	0.14	32	0.20	57
22-Jun-98	0.37	0.36	-3.5	0.23	61.8	0.28	75	0.59	60
29-Jun-98	0.41	0.67	62.8	0.38	91.0	0.54	130	0.47	79
26-Jul-98	0.37	0.38	3.7	0.09	25.2	0.12	33	0.89	34
30-Jul-98	0.40	0.40	-0.1	0.16	40.8	0.24	59	0.51	61
13-Sep-98	0.42	0.37	-12.6	0.21	49.2	0.27	64	0.47	83
21-Sep-98	0.27	0.34	24.8	0.15	54.7	0.19	68	0.22	56
4-Oct-98	0.59	0.50	-16.5	0.24	41.0	0.41	68	0.76	49
1-Nov-98	0.27	0.26	-4.6	0.12	43.2	0.16	58	0.64	42
22-Apr-99	0.45	0.53	18.8	0.12	27.6	0.18	40	0.78	41
23-Jun-99	0.69	0.70	0.4	0.20	28.5	0.23	34	0.74	46
27-Jun-99	0.37	0.36	-2.9	0.28	74.4	0.41	109	0.01	58
9-Jul-99	0.60	0.75	25.0	0.23	38.1	0.31	51	0.72	29
26-May-00	0.43	0.54	24.5	0.15	35.4	0.20	47	0.70	30
20-Jun-00	0.40	0.33	-16.3	0.15	36.9	0.20	49	0.50	56
14-Oct-00	0.36	0.34	-5.6	0.15	42.2	0.21	58	0.72	62
3-Apr-01	0.31	0.31	-1.7	0.12	38.9	0.20	63	0.76	36
3-May-01	0.50	0.53	5.1	0.26	51.5	0.39	77	0.77	64
17-May-01	0.83	1.16	38.8	0.41	49.3	0.47	57	0.74	70
4-Jun-01	0.42	0.54	29.2	0.20	48.3	0.27	65	0.68	56
5-Jun-01	0.75	0.76	2.1	0.25	33.5	0.31	42	0.81	49
20-Jun-01	0.58	0.63	9.0	0.21	36.0	0.28	47	0.64	56
25-Aug-01	0.45	0.51	14.6	0.24	53.1	0.31	70	0.67	37
11-May-02	0.39	0.40	2.3	0.17	43.8	0.28	70	0.77	52
24-May-02	0.35	0.36	1.6	0.10	28.4	0.14	38	0.71	43
13-Aug-02	0.45	0.59	33.0	0.21	46.9	0.27	61	0.76	44
19-Apr-03	0.35	0.44	25.0	0.12	35.6	0.20	59	0.63	67
30-Aug-03	0.33	0.37	11.4	0.11	32.7	0.14	42	0.71	53
4-Mar-04	0.30	0.25	-17.9	0.08	24.8	0.12	38	0.93	37
18-May-04	0.35	0.50	41.3	0.19	54.8	0.29	83	0.85	61
6-Jul-04	0.50	0.47	-6.7	0.15	29.9	0.23	46	0.80	51
24-Jul-04	0.27	0.26	-5.7	0.08	29.3	0.10	38	0.75	70
23-Aug-04	0.61	0.75	22.7	0.31	50.3	0.43	70	0.78	56
28-Aug-04	0.56	0.53	-4.0	0.14	25.8	0.22	40	0.91	38

Table 4.4: Statistics for Storm Totals for all 34 Events

Storm Date	Average Gage (in)	Average NEX (in)	Bias (%)	MAD (in)	NMAD (%)	RMSD (in)	FSD (%)	Correlation	% of Points outside CI
8-Jun-98	1.5	1.6	5.3	0.15	9.65	0.19	12.80	0.57	20.0
22-Jun-98	1.2	1.2	-1.5	0.21	17.83	0.32	26.80	0.59	8.3
29-Jun-98	1.5	2.3	49.2	1.10	71.69	1.45	94.14	-0.15	94.4
26-Jul-98	1.5	1.6	3.6	0.13	8.83	0.22	14.52	0.91	11.1
30-Jul-98	2.1	2.2	5.9	0.46	22.08	0.58	27.97	0.17	33.3
13-Sep-98	4.3	4.1	-4.1	0.91	21.30	1.16	27.11	-0.16	90.9
21-Sep-98	1.2	1.5	19.2	0.24	19.28	0.30	24.12	0.65	41.2
4-Oct-98	2.5	2.1	-15.7	0.89	35.58	1.21	48.35	0.57	93.3
1-Nov-98	2.8	3.2	14.7	0.48	17.22	0.68	24.59	0.19	30.6
22-Apr-99	0.9	1.4	54.2	0.57	61.28	0.67	72.29	0.31	76.9
23-Jun-99	1.1	1.0	-12.2	0.34	30.93	0.49	45.09	0.71	85.7
27-Jun-99	2.5	4.0	62.5	1.56	62.49	1.67	66.93	0.15	92.3
9-Jul-99	1.2	1.6	31.0	0.45	37.58	0.56	46.40	0.46	52.0
26-May-00	0.8	1.1	44.7	0.36	47.58	0.42	55.65	0.84	71.2
20-Jun-00	2.0	2.1	6.3	0.44	21.76	0.51	25.57	0.60	83.3
14-Oct-00	1.6	1.4	-10.4	0.37	23.74	0.48	30.57	0.57	78.8
3-Apr-01	0.8	0.8	-3.7	0.18	21.74	0.29	34.74	0.85	21.2
3-May-01	0.7	0.9	32.2	0.44	63.15	0.58	84.19	0.61	77.4
17-May-01	1.1	1.5	41.4	0.50	46.73	0.57	52.90	0.71	85.3
4-Jun-01	1.7	2.1	26.1	0.52	31.14	0.70	41.85	0.58	52.9
5-Jun-01	1.3	1.3	0.5	0.34	25.63	0.46	35.41	0.75	54.4
20-Jun-01	2.0	2.2	10.7	0.44	22.04	0.63	31.05	-0.22	44.1
25-Aug-01	1.5	1.6	10.7	0.37	25.13	0.44	30.13	0.14	47.1
11-May-02	1.2	1.4	19.4	0.27	23.53	0.31	26.56	0.97	69.1
24-May-02	1.4	1.3	-3.2	0.32	23.01	0.47	34.15	0.37	83.9
13-Aug-02	1.1	1.3	25.2	0.30	28.06	0.35	32.71	0.61	65.7
19-Apr-03	1.6	2.1	31.8	0.50	31.97	0.67	42.75	0.66	80.6
30-Aug-03	3.5	6.4	81.0	2.84	80.97	3.07	87.56	0.10	98.6
4-Mar-04	2.6	2.7	6.8	0.25	9.81	0.33	13.01	0.88	23.6
18-May-04	2.3	3.2	41.3	1.00	43.48	1.24	53.91	0.85	69.4
6-Jul-04	1.3	1.1	-13.5	0.33	25.20	0.50	38.33	0.80	34.7
24-Jul-04	2.4	2.6	8.5	0.38	16.08	0.54	23.12	-0.22	45.8
23-Aug-04	2.3	2.7	18.5	0.50	21.83	0.56	24.50	0.89	63.9
28-Aug-04	2.5	2.4	-5.0	0.40	15.76	0.57	22.25	0.90	30.6

CHAPTER 5 - SUMMARY AND CONCLUSIONS

5.1 Summary

This report presents the results of two separate evaluations of NEXRAD precipitation estimates in Kansas. The first study compares NEXRAD estimates of precipitation to daily rain gauge accumulations to determine spatial and temporal trends in NEXRAD error. The second study evaluated NEXRAD estimates of intense rainfall in Johnson County, Kansas, using a local ALERT rain gauge network. Results from these studies are presented in Chapters 3 and 4 of this report.

Chapter 3 provides maps of NEXRAD bias, correlation, and percent detection for the warm season (April through September) and cold season (October through March) for 1998 through 2004. These maps show the spatial distribution of NEXRAD error characteristics. In general, estimates in the eastern portion of the state exhibit lower bias and higher correlation. Over time, estimates of warm season precipitation have improved significantly. The average 2004 warm season bias was -10.9%, and the average correlation was 0.79. The average cold season bias in 2004 was -23.5%, and the average correlation was 0.74.

Chapter 4 presents an evaluation of NEXRAD estimates for 34 storms from 1998 through 2004. The results show that NEXRAD, on average, overestimates precipitation in Johnson County by 8% for hours with intense precipitation and 17% for storm totals for large events. Graphs of hourly and storm total accumulations presented in the appendices show that the bias is conditional: NEXRAD tends to overestimate low hourly accumulations and tends to underestimate high hourly accumulations relative to gauge data. NEXRAD estimates of storm total accumulation averaged over the study area are

in good agreement with rain gauge data, indicating that temporal and spatial averaging tends to reduce uncertainty in the NEXRAD estimates.

5.2 Conclusions and Recommendations

The two studies presented in this report show that the quality of NEXRAD precipitation estimates varies across the state and through time. Both studies indicate a high degree of scatter between NEXRAD operational estimates of precipitation and gauge-based estimates of rainfall. Although some of this scatter may be due to gauge error and the spatial variability of precipitation, the study presented in Chapter 4 shows that a large fraction of the scatter must be due to NEXRAD error. The gauges used in this report are independent of the NEXRAD processing algorithm, with the exception of a few ALERT gauges that are available to the MBRFC.

The question remains, then, as to when NEXRAD estimates might be used and how they should be used in hydrologic analysis. NEXRAD operational estimates of precipitation are a combination of radar and gauge observations. The algorithms used to combine these sources of information are designed to minimize the error variance of the combined estimate. As such, the NEXRAD estimate should be better than a gauge-only or radar-only estimate of precipitation. The studies in this report indicate that there is still a high degree of uncertainty in the NEXRAD estimates, as compared to gauge-derived rainfall. Although this uncertainty is documented, it should not exceed the uncertainty of the gauge-only estimate of rainfall used to generate the NEXRAD product.

Chapter 4 compares the NEXRAD product to a high-density gauge network. The vast majority of Kansas is poorly instrumented for rainfall data. Although the NEXRAD

uncertainty demonstrated in Chapter 4 is higher than that present in gauge-only estimates, this will not hold true in most areas of Kansas. Prior research (Young 2000; Bedient et al. 2000) indicates that NEXRAD-driven watershed models can out-perform gauge-driven models when gauges are sparse. For example, if the nearest gauge is 20 miles away, then NEXRAD becomes a very attractive source of precipitation data.

Given the NEXRAD error documented in this report, it is recommended that KDOT rely primarily on rain gauge data when it is available at or near the area of interest. NEXRAD estimates of precipitation should be used to augment available rain gauge data. NEXRAD radar loops (such as those provided on the CD with this report) could be used to evaluate the storm path and to identify which rain gauges should be used. The nearest available gauge may not accurately represent rainfall at the point of interest; a gauge that is further away but captured the same storm cell that affected the area of interest may provide better rainfall estimates.

In many cases, data from daily rain gauges may be available near the area of interest. NEXRAD data could also be used to temporally disaggregate rainfall observations from these gauges. The NEXRAD hourly data could be used as a guide to determine what proportion of the total rainfall occurred in each hour of the storm.

In cases where gauges are not available, NEXRAD may also be used as the primary source of rainfall data. In such situations, the maps presented in Chapter 3 should be used to determine the average NEXRAD error characteristics for the area and time period of interest.

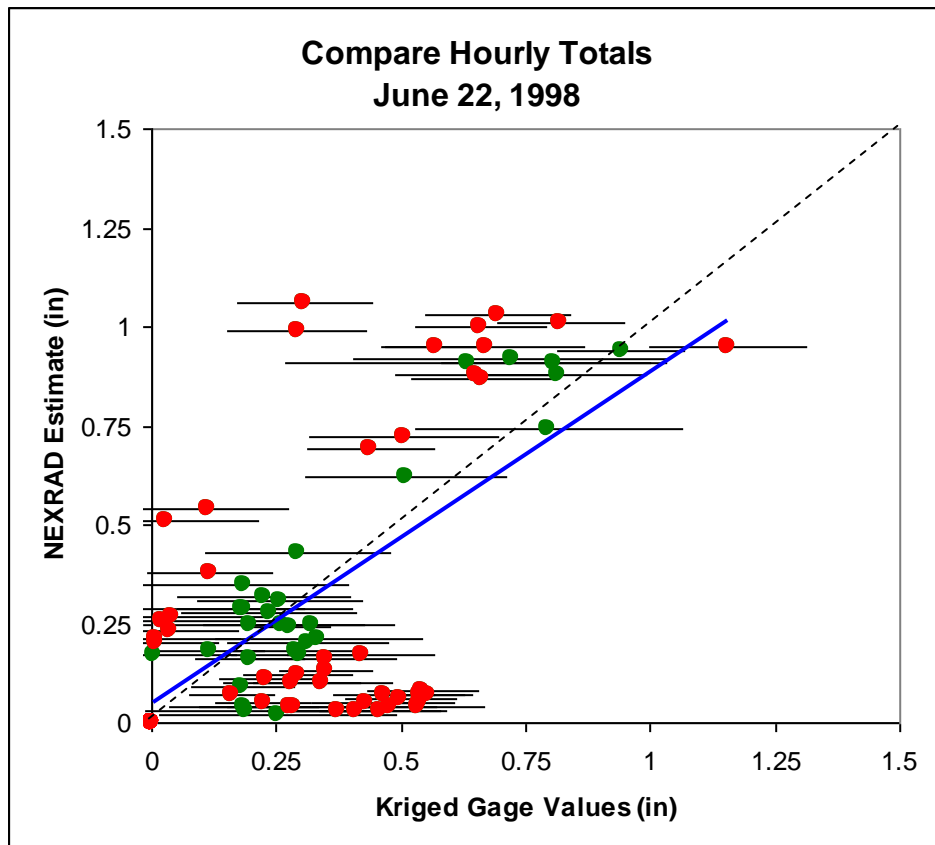
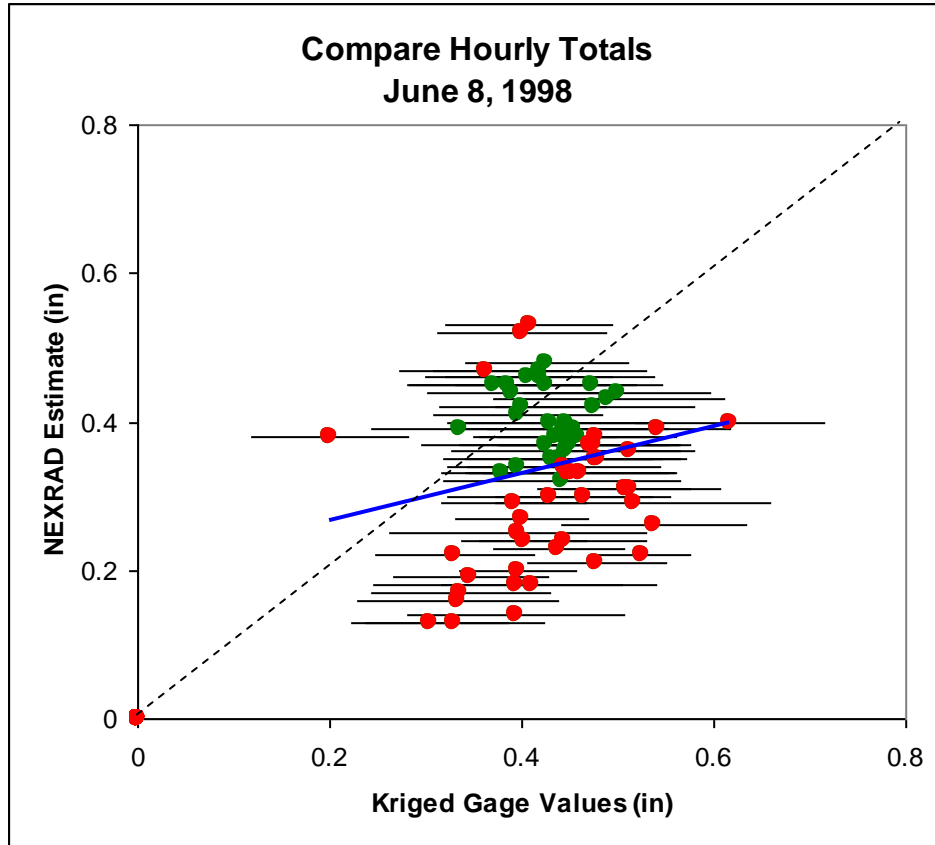
REFERENCES

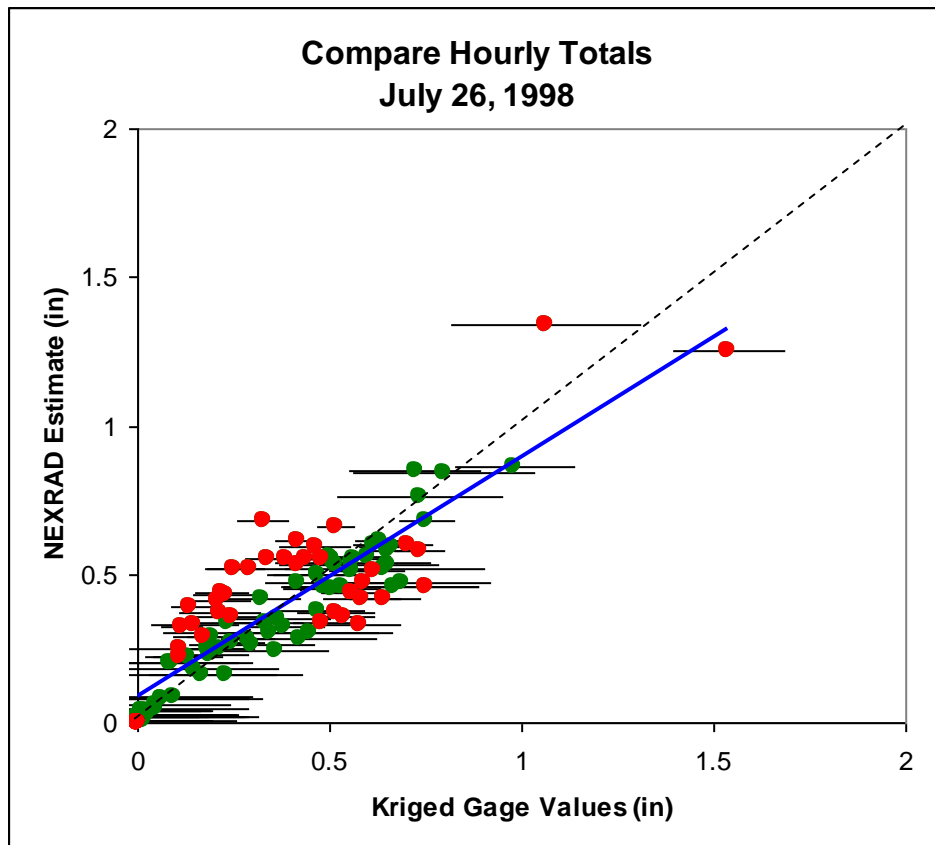
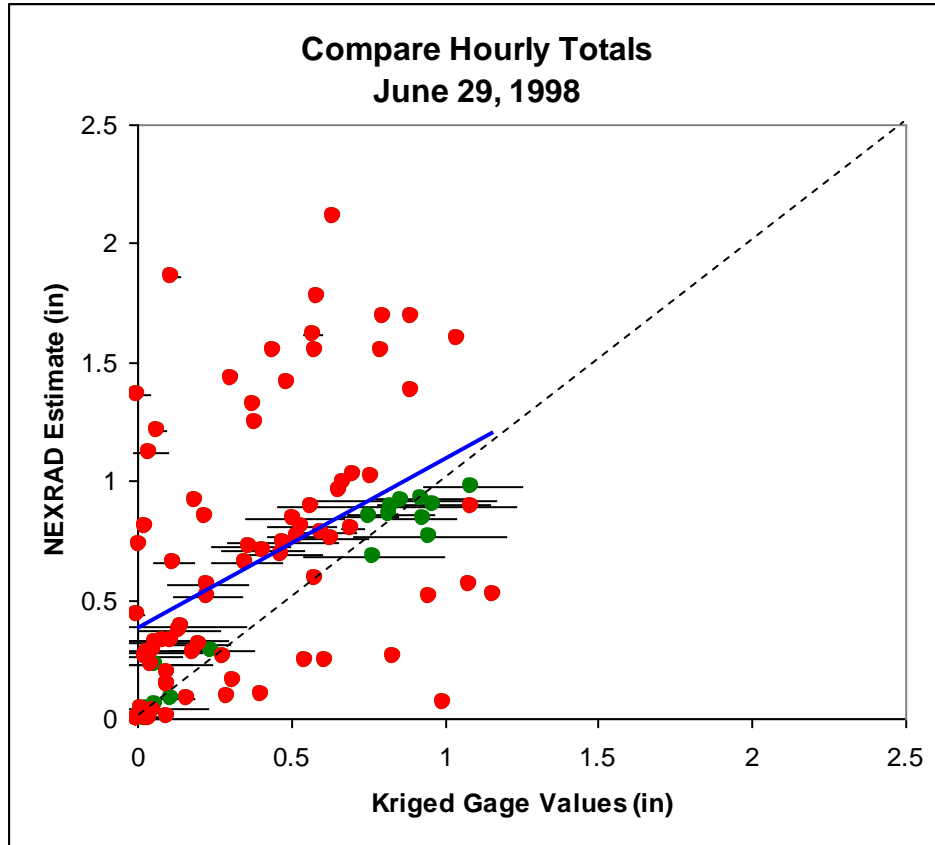
- Bedient, P. B., B. C. Hoblit, D. C. Gladwell, and B. E. Vieux (2000). "NEXRAD Radar for Flood Prediction in Houston." *Journal of Hydrologic Engineering*, 5(3), 269-277.
- Duchon, C. E., and G. R. Essenberg (2001). "Comparative Rainfall Observations from Pit and Aboveground Rain Gauges with and without Wind Shields." *Water Resources Research*, 37(12), 3253-3263.
- Fulton, R. A., J. B. Breidenbach, D.-J. Seo, D. A. Miller, and T. O'Bannon (1998). "The WSR-88D Rainfall Algorithm." *Weather and Forecasting*, 13(2), 377-395.
- Grassotti, C., R. N. Hoffman, E. R. Vivoni, and D. Entekhabi (2003), "Multiple-Timescale Intercomparisons of Two Radar Products and Rain Gauge Observations over the Arkansas-Red River Basin." *Weather and Forecasting*, 18(6), 1207-1229.
- Johnson, D., M. Smith, V. Koren, and B. Finnerty (1999). "Comparing Mean Areal Precipitation Estimates from NEXRAD and Rain Gauge Networks." *Journal of Hydrologic Engineering*, 4(2), 117-124.
- Neary, V. S., E. Habib, and M. Fleming (2004). "Hydrologic Modeling with NEXRAD Precipitation in Middle Tennessee." *Journal of Hydrologic Engineering*, 9(5), 339-349.
- Nelson, B. R., W. F. Krajewski, J. A. Smith, E. Habib, and G. Hoogenboom (2005). "Archival Precipitation Data Set for the Mississippi River Basin: Evaluation." *Geophysical Research Letters*, 32, L18403, doi:10.1029/2005GL023334, 2005.
- Pebesma, E. J., and C. G. Wesseling (1998). "GSTAT: A Program for Geostatistical Modelling, Prediction, and Simulation." *Computers & Geosciences*, 24(1), 17-31.

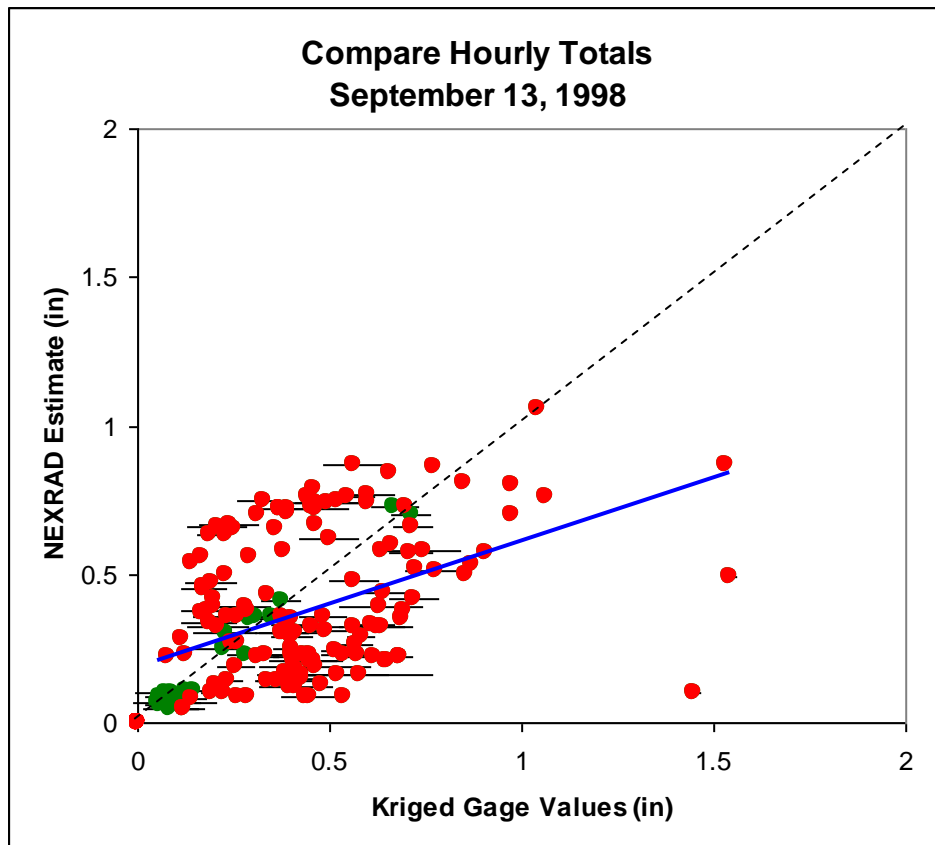
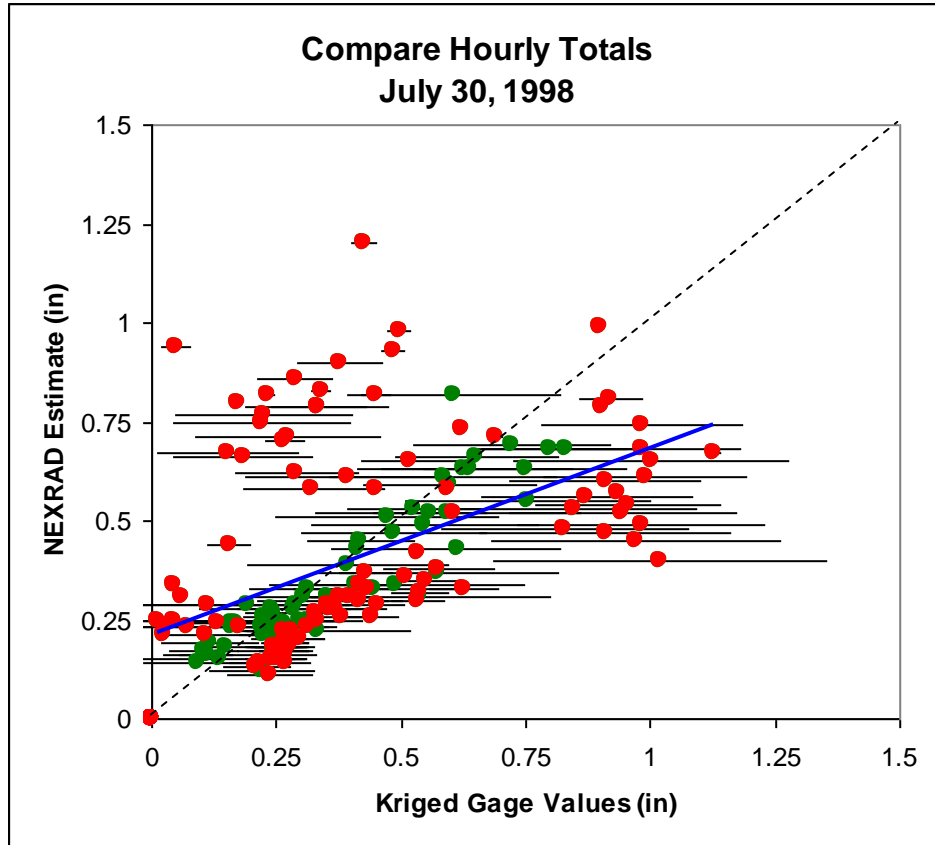
- Seo, D.-J., and J. B. Breidenbach (2002). "Real-Time Correction of Spatially Nonuniform Bias in Radar Rainfall Data Using Rain Gauge Measurements." *Journal of Hydrometeorology*, 3(2), 93-111.
- Smith, J. A., D.-J. Seo, M. L. Baeck, and M. D. Hudlow (1996). "An Intercomparison Study of NEXRAD Precipitation Estimates." *Water Resources Research*, 32, 2035-2045.
- Young, C. B., B. R. Nelson, A. A. Bradley, J. A. Smith, C. D. Peters-Lidard, A. Kruger, and M. L. Beck (1999). "An Evaluation of NEXRAD Precipitation Estimates in Complex Terrain." *Journal of Geophysical Research*, 104, 19691-19703.
- Young, C. B. (2000). Evaluation of NEXRAD Precipitation Estimates and their Potential Use for Nonpoint Source Pollution Modeling. Ph.D. Dissertation, University of Iowa.
- Young, C. B., A. A. Bradley, W. F. Krajewski, and A. Kruger (2000). "Evaluating NEXRAD Multisensor Precipitation Estimates for Operational Hydrologic Forecasting." *Journal of Hydrometeorology*, 1(3), 241-254.

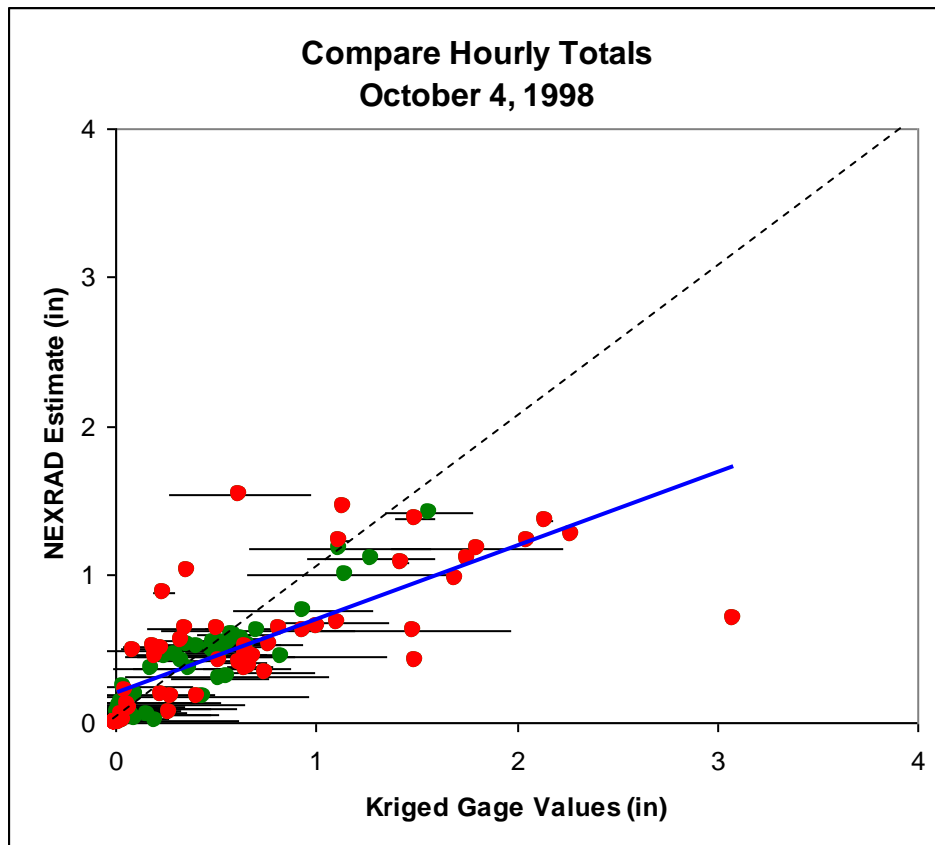
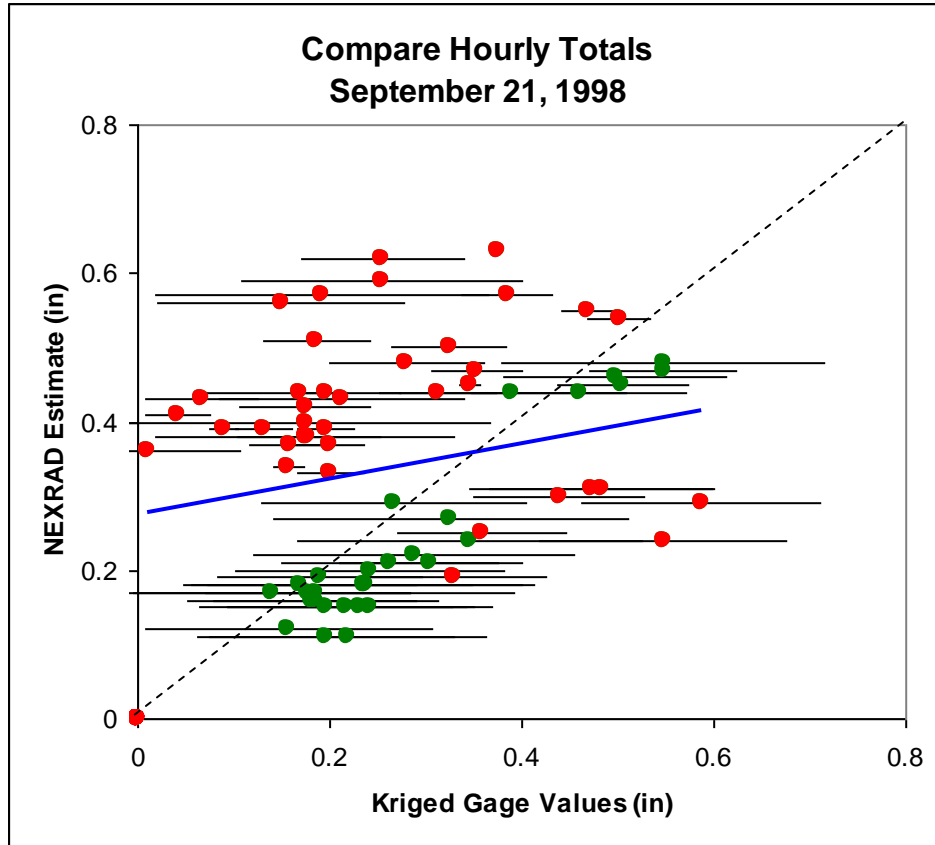
APPENDIX A

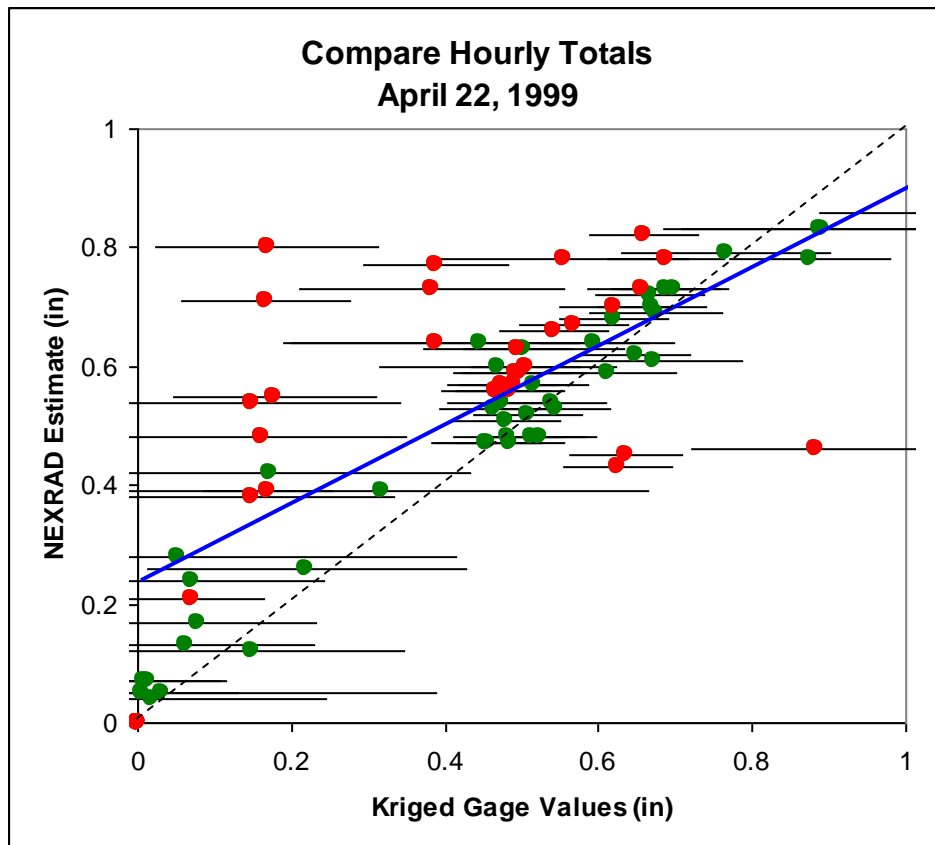
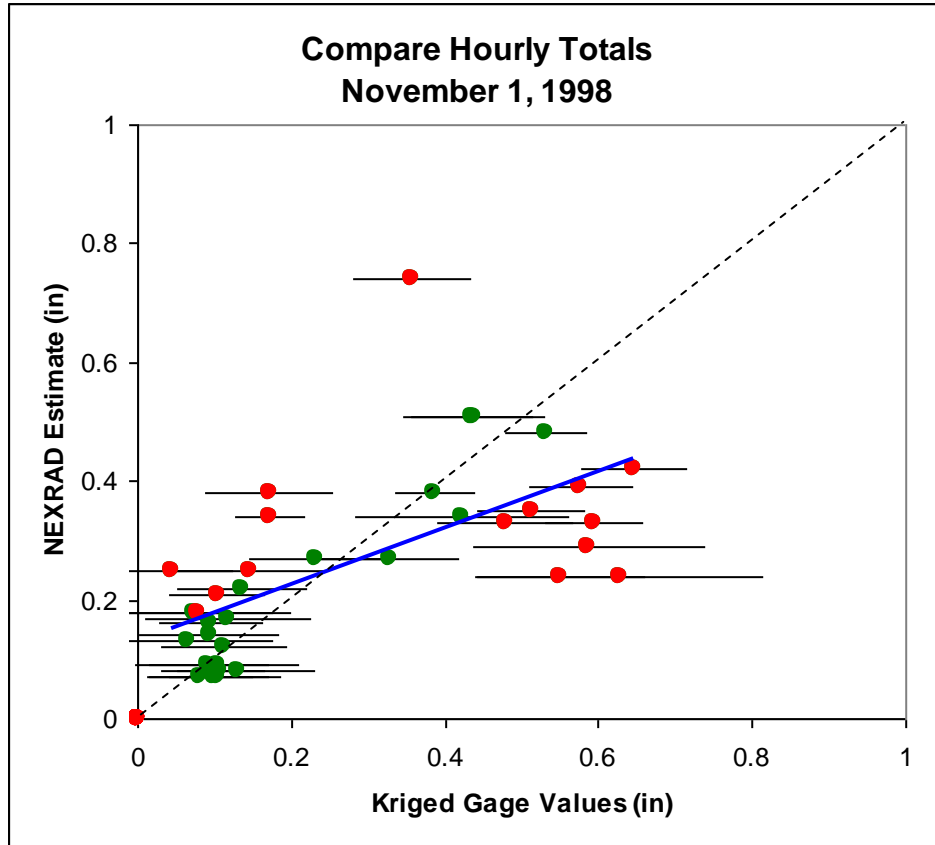
SCATTER PLOTS FOR HOURLY ACCUMULATIONS

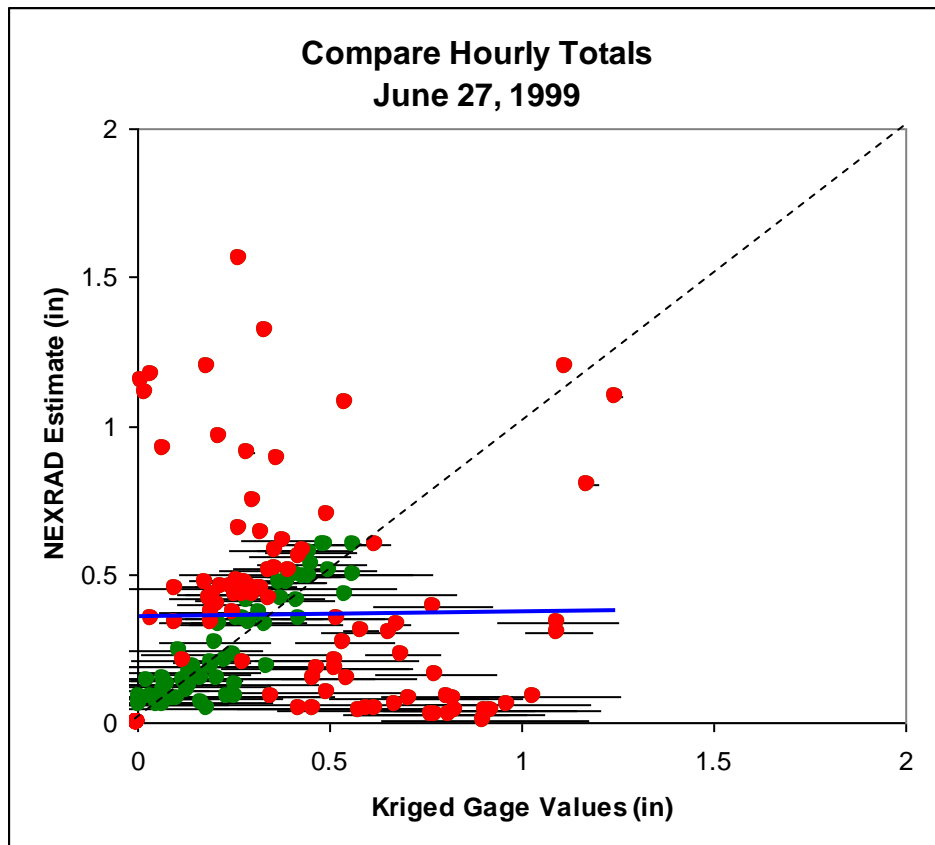
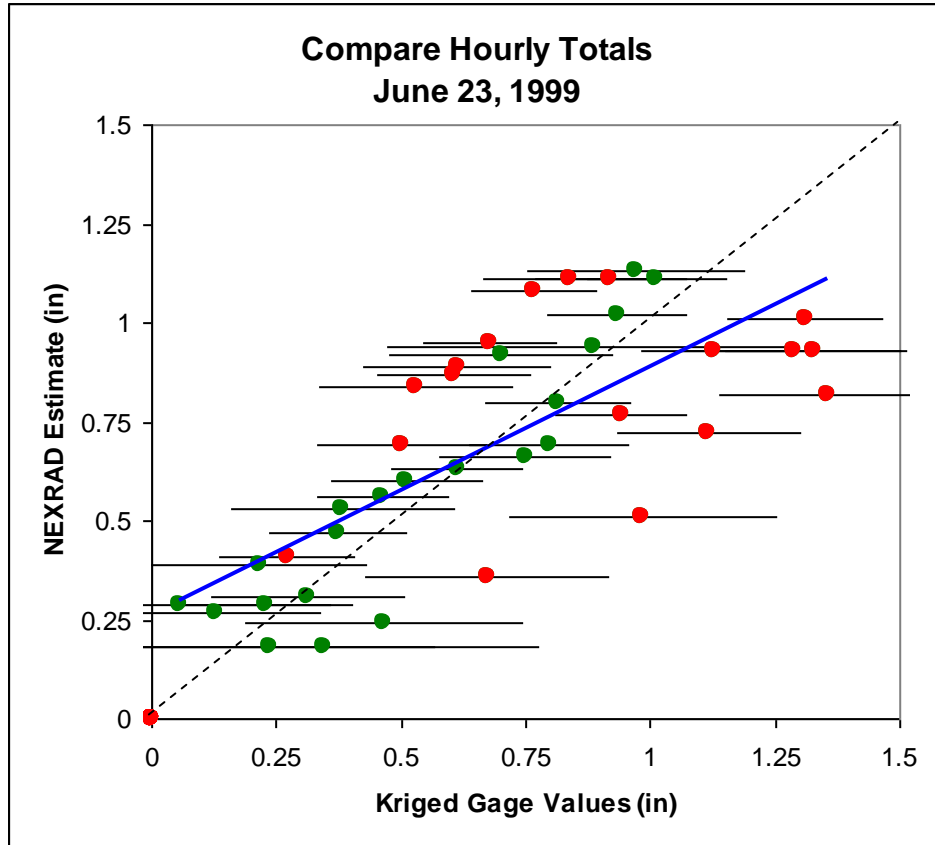


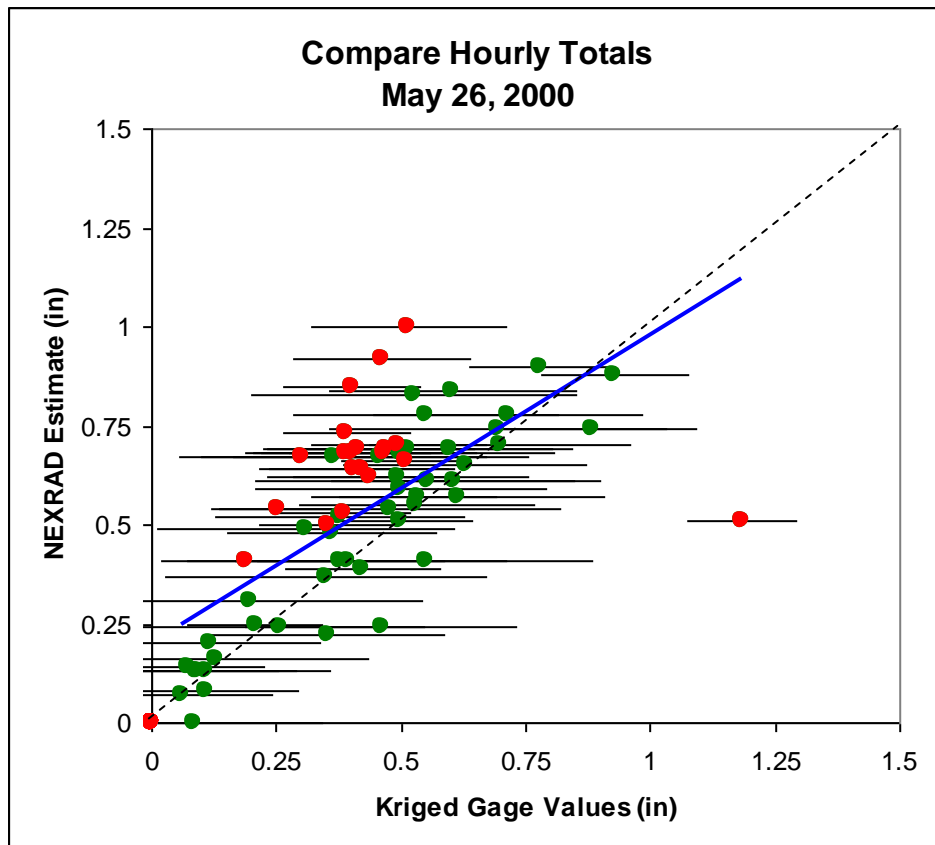
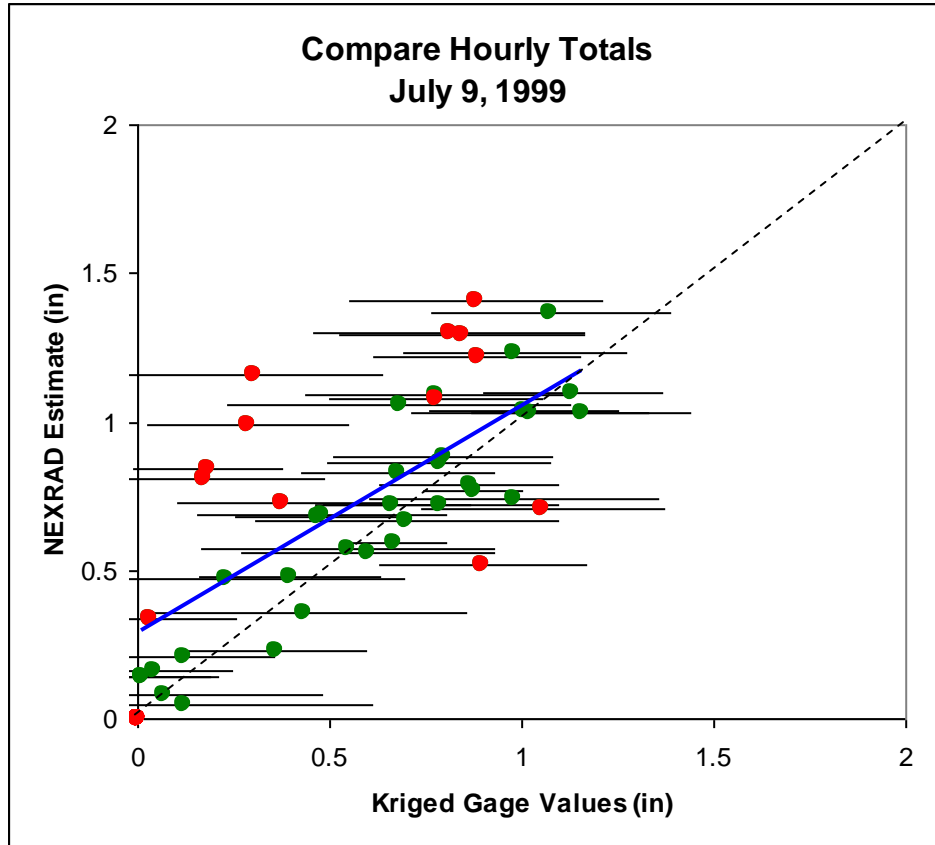


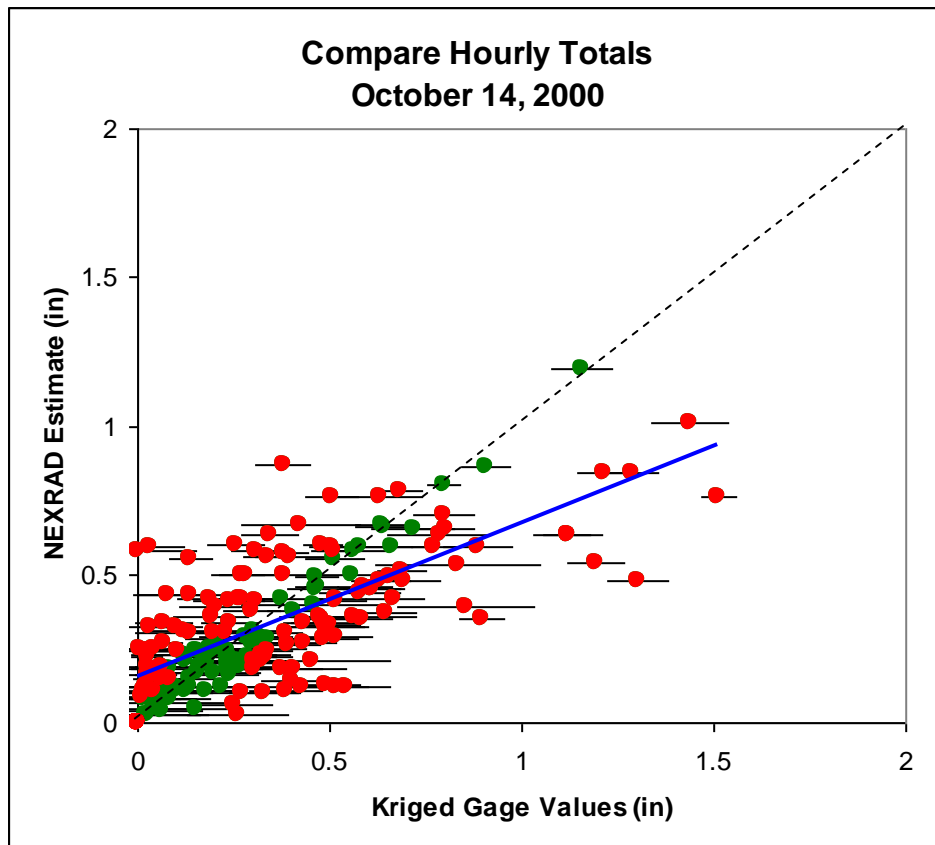
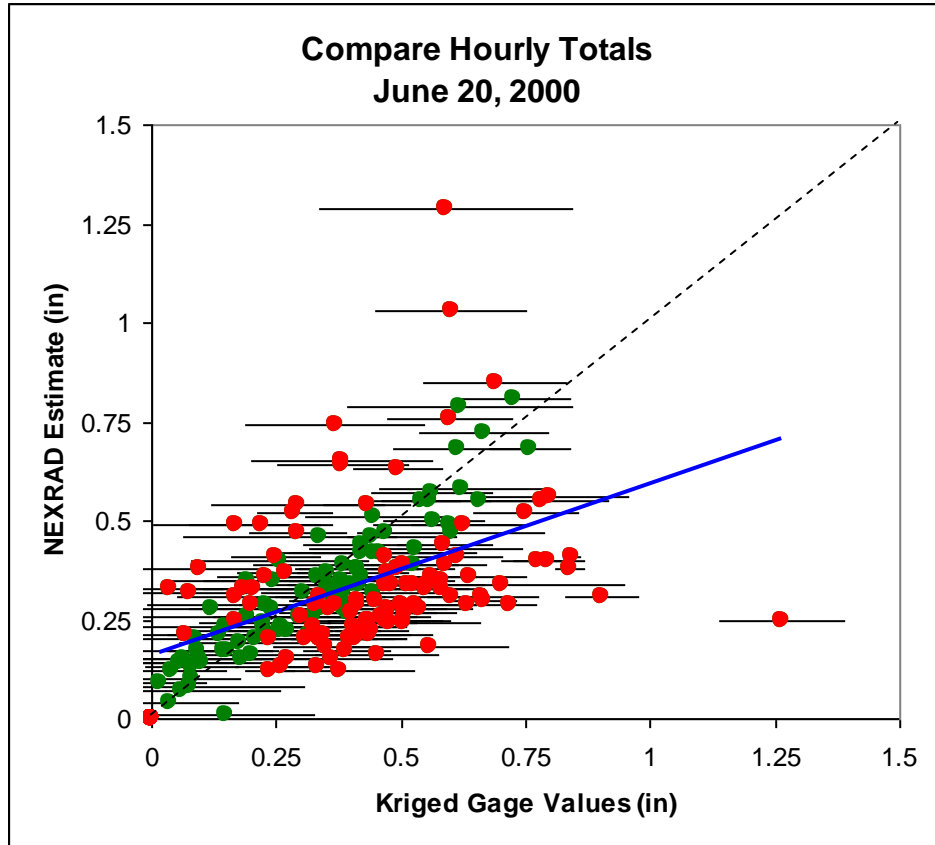


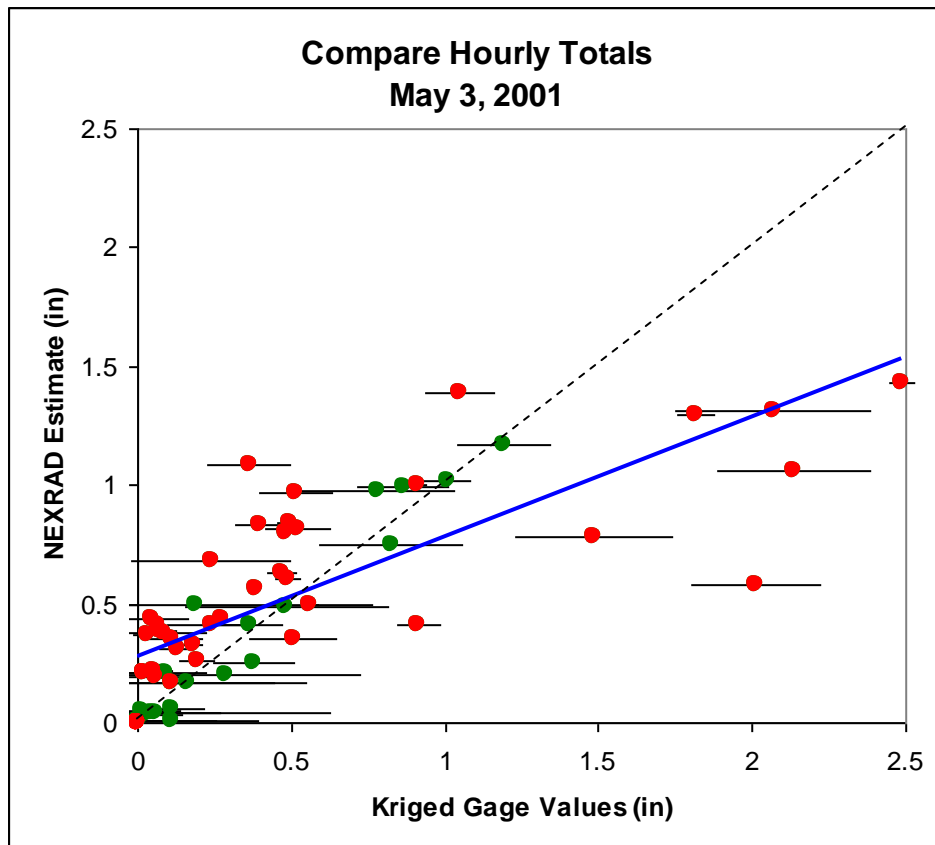
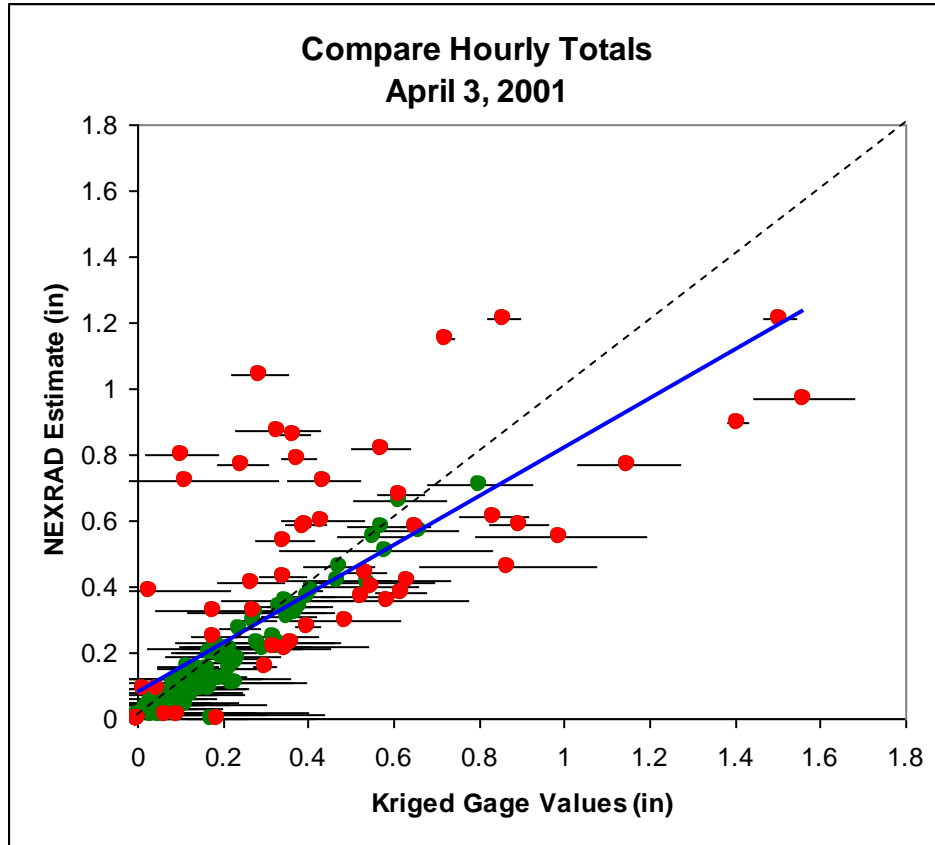


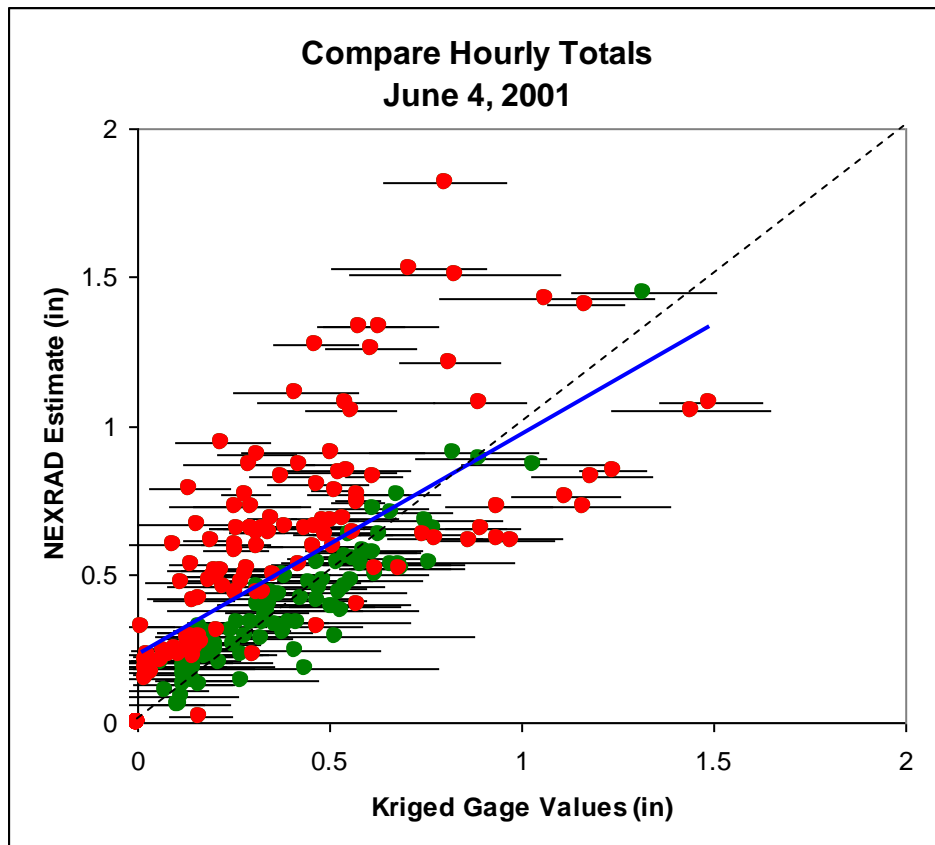
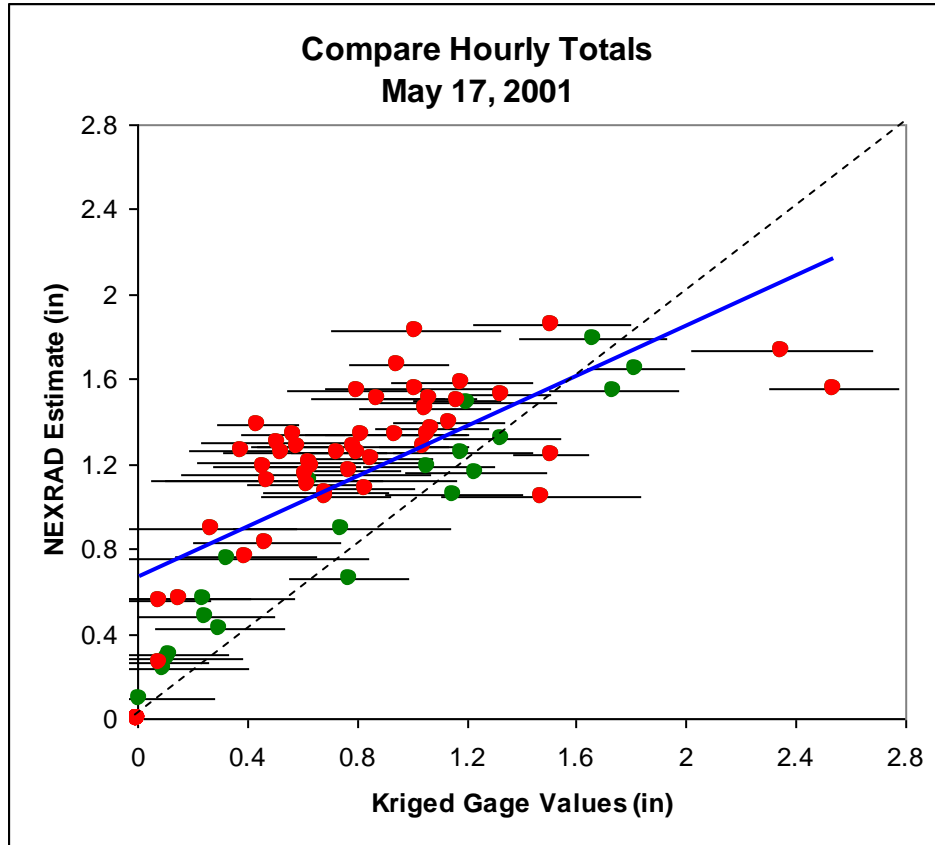


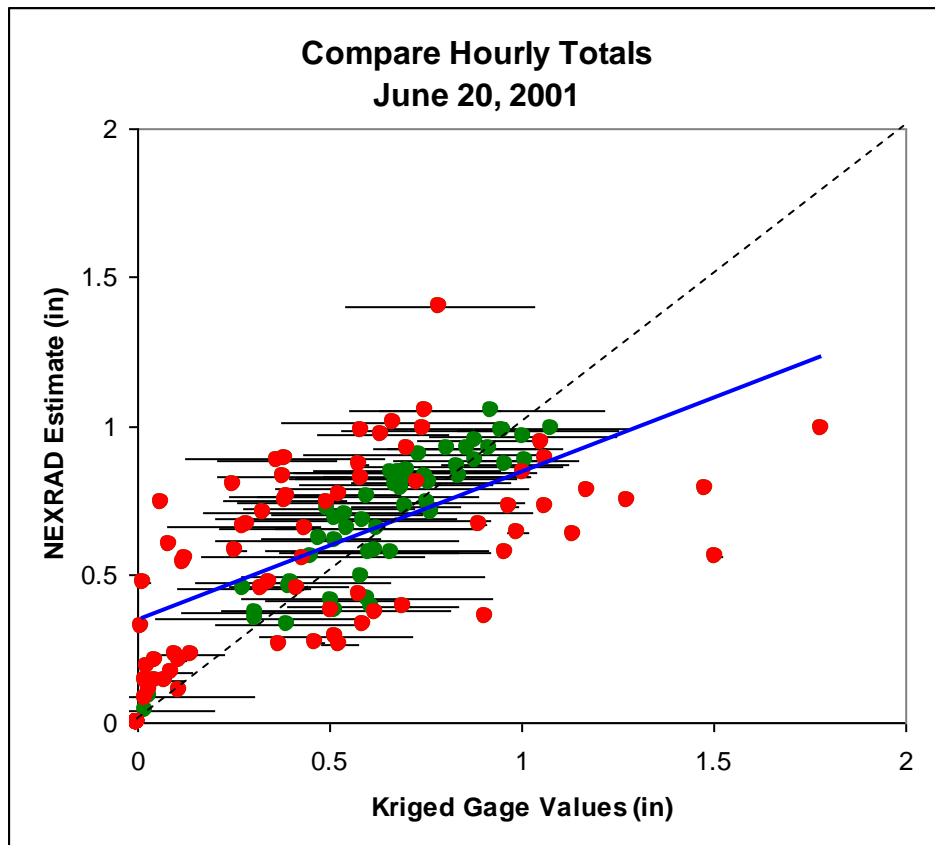
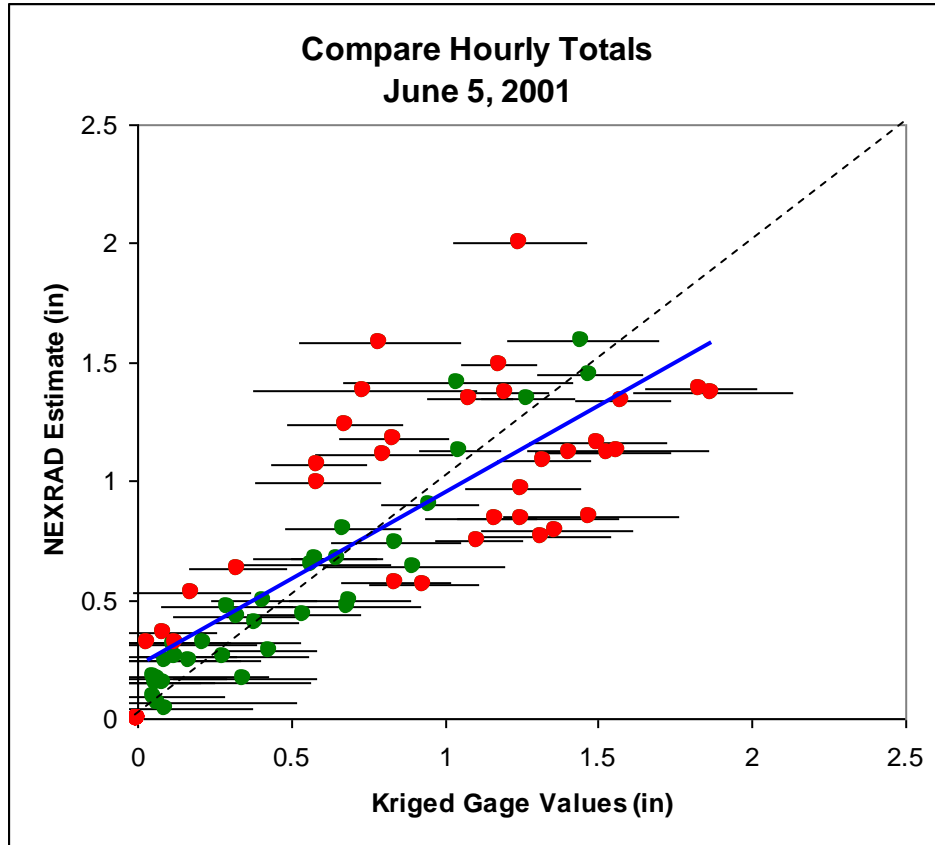


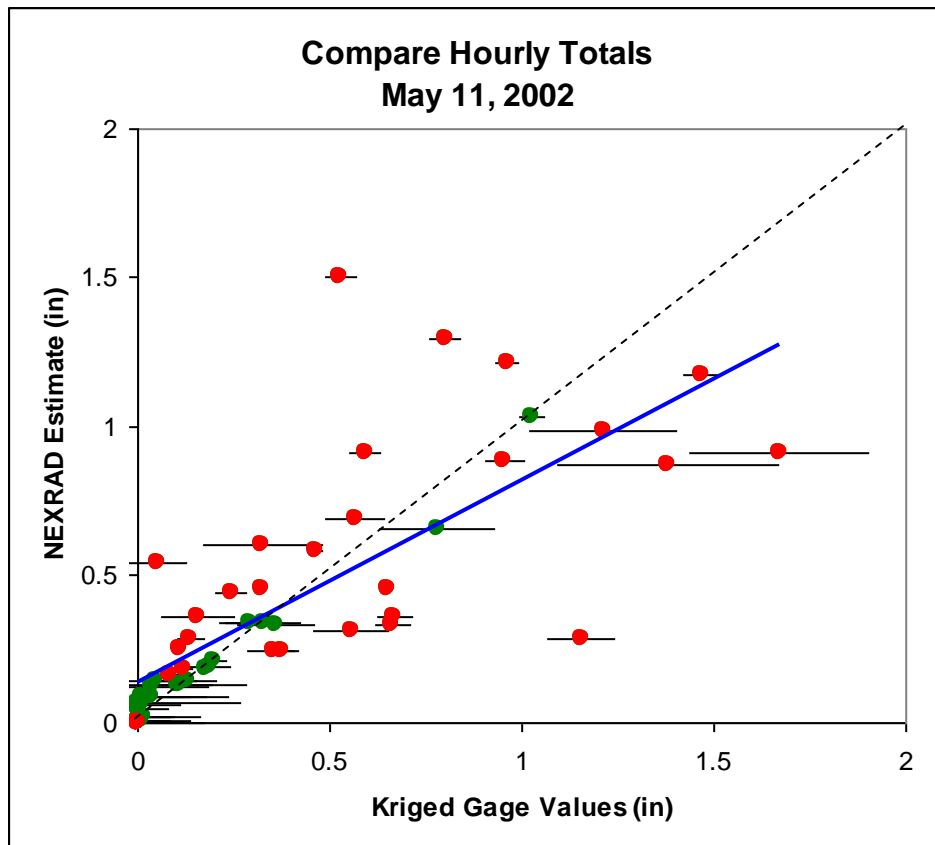
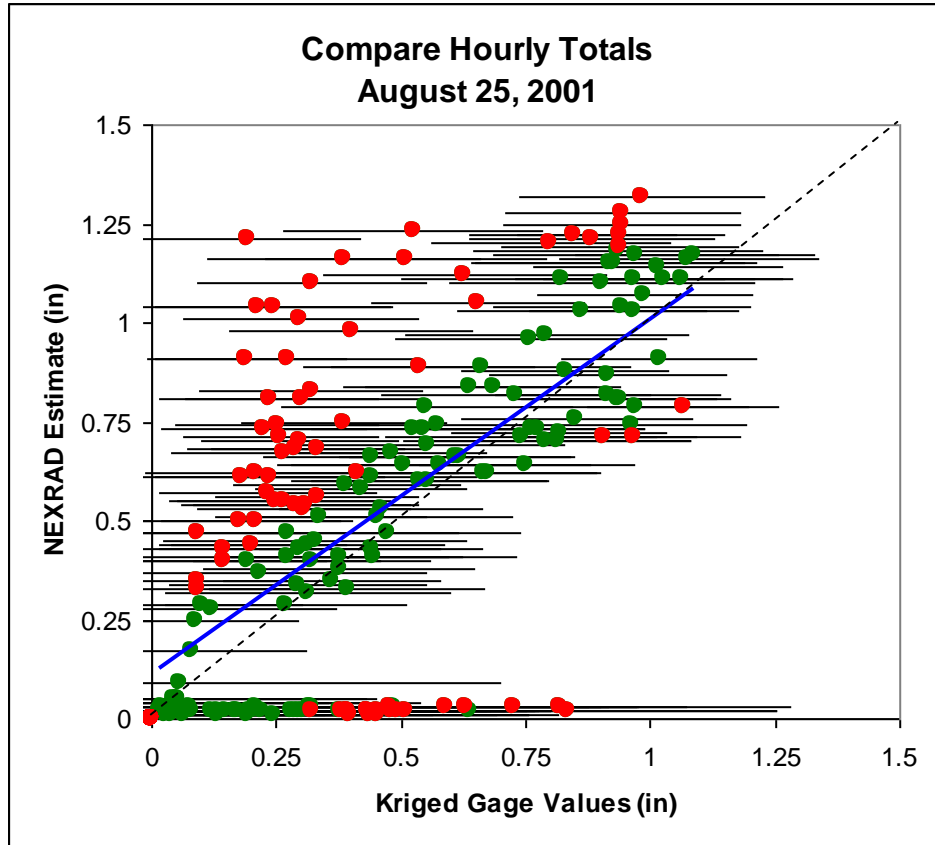


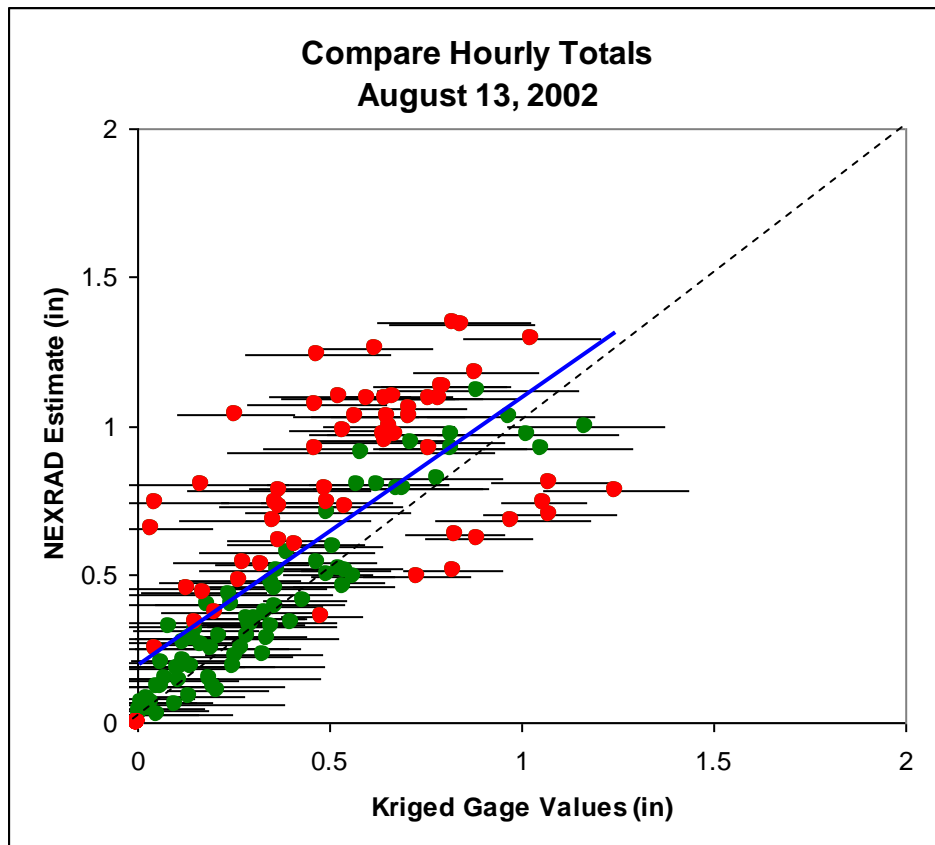
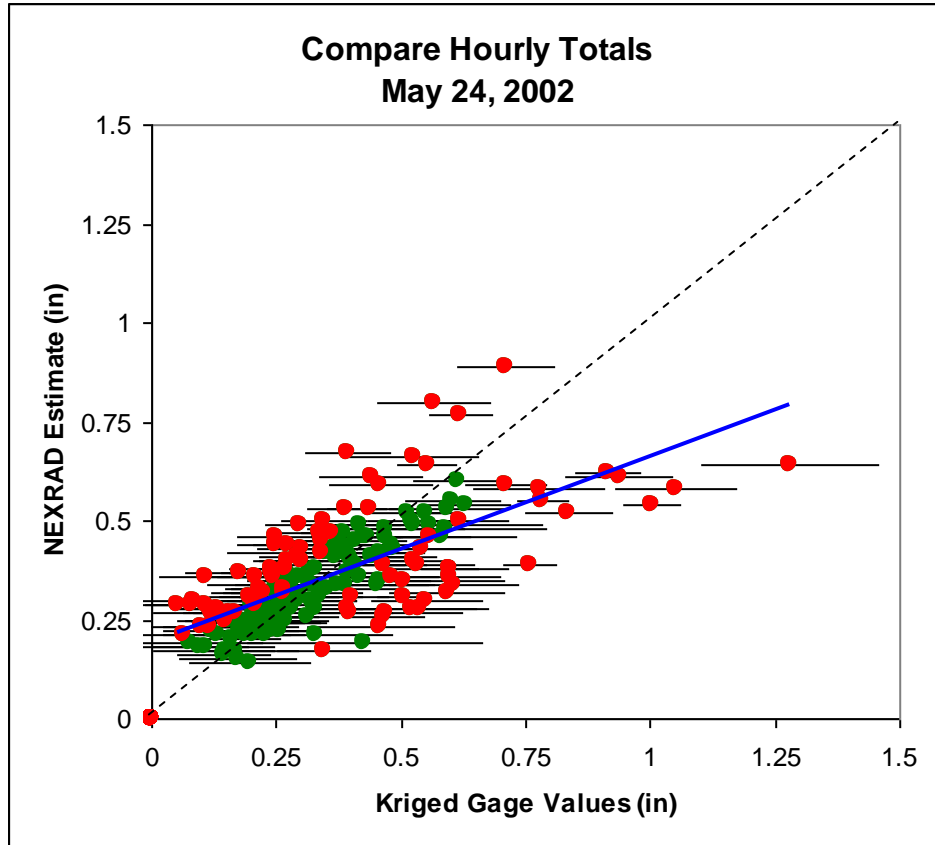


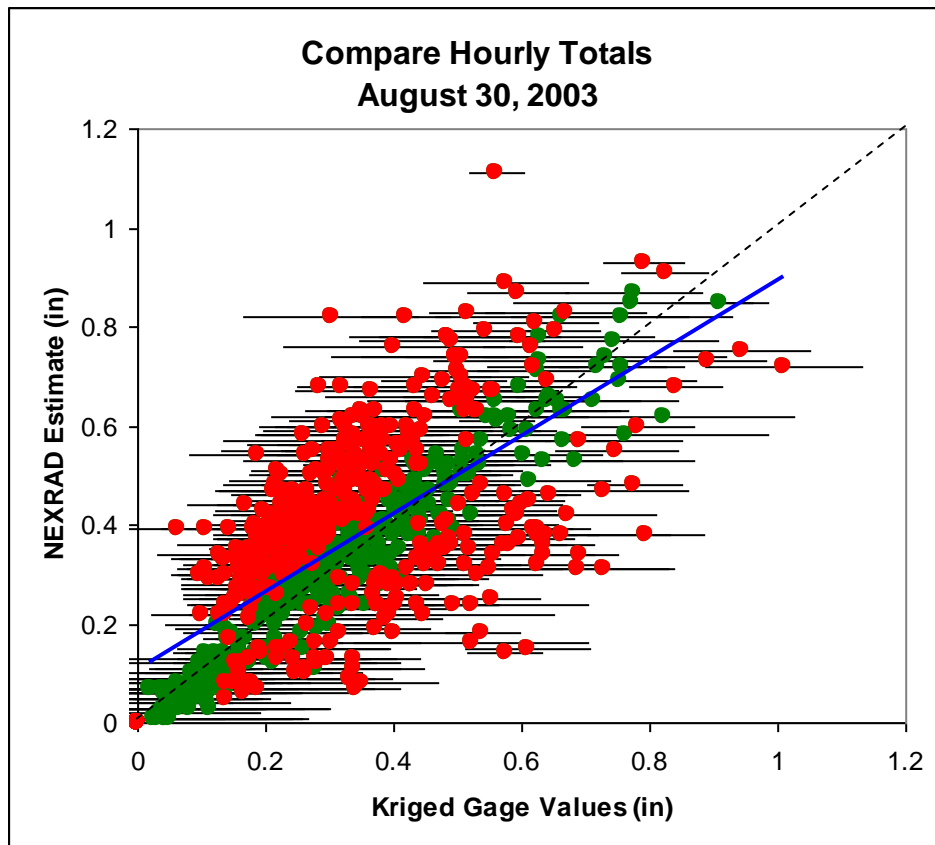
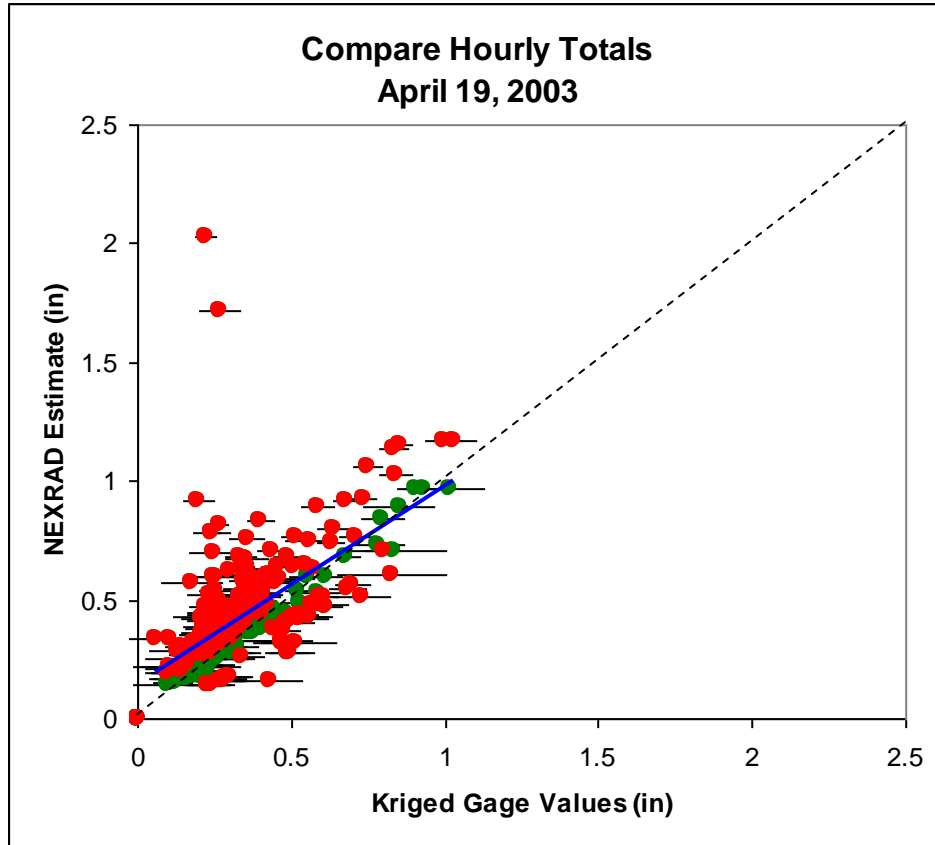


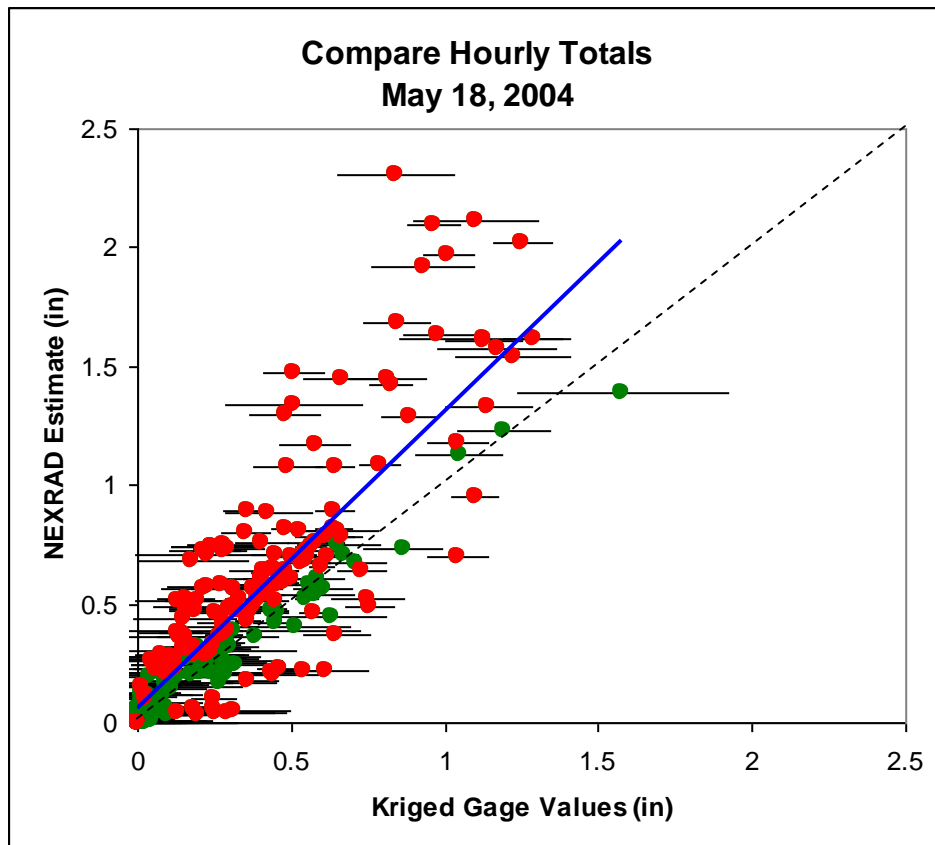
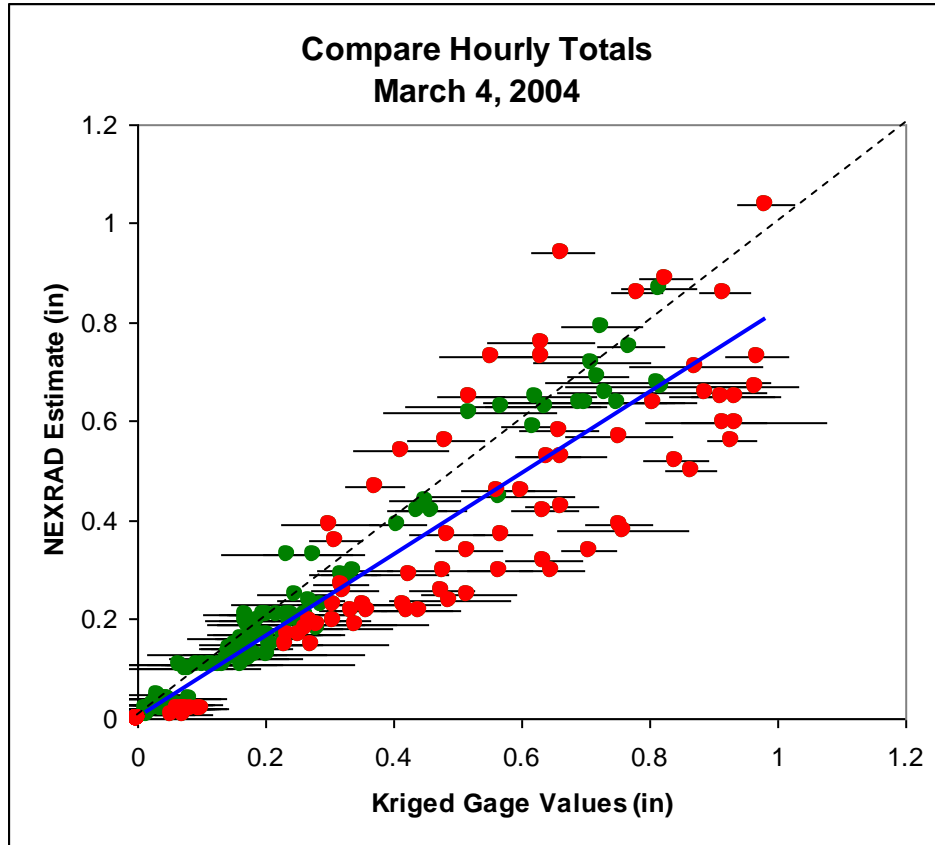


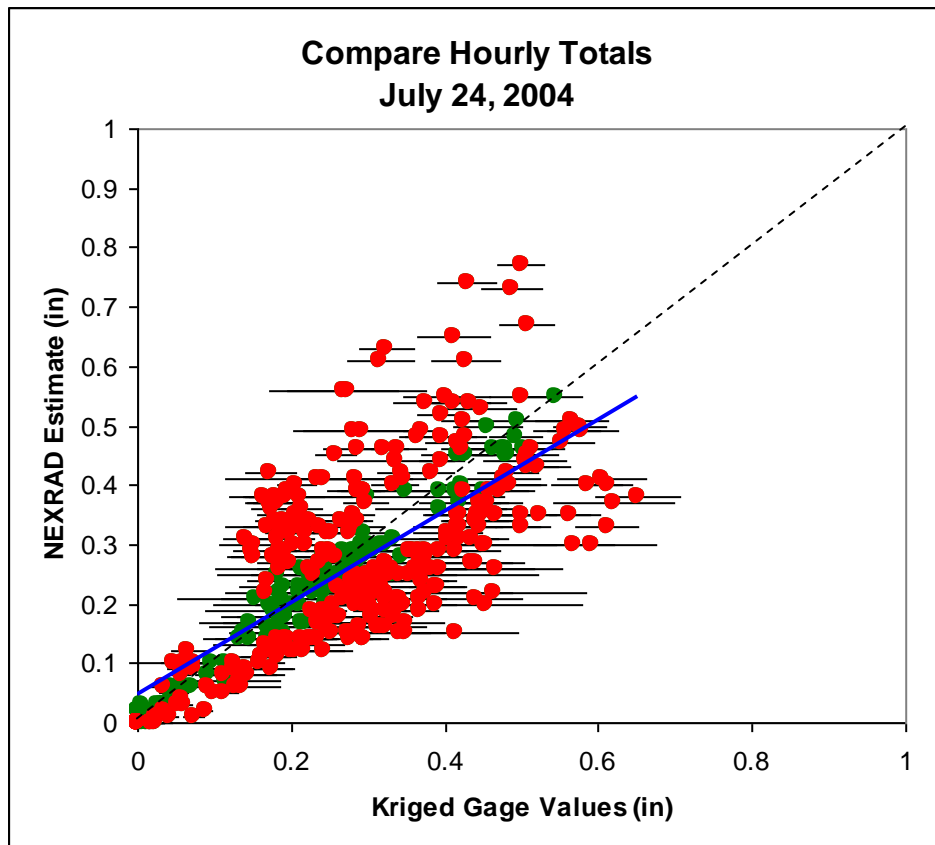
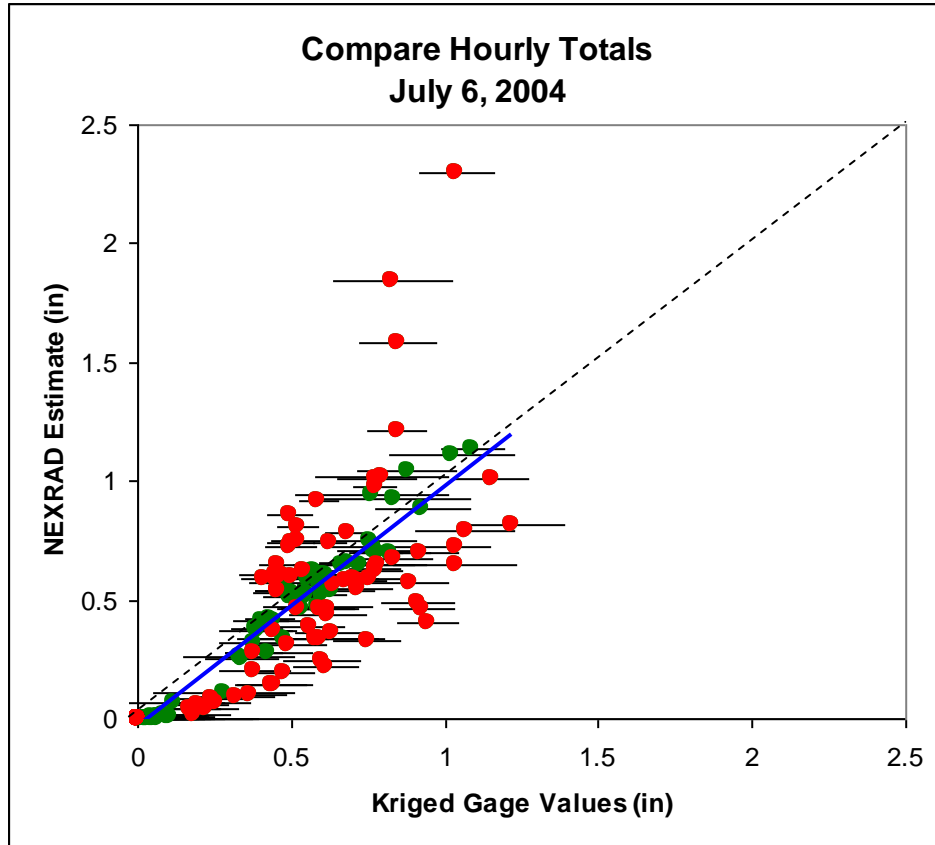


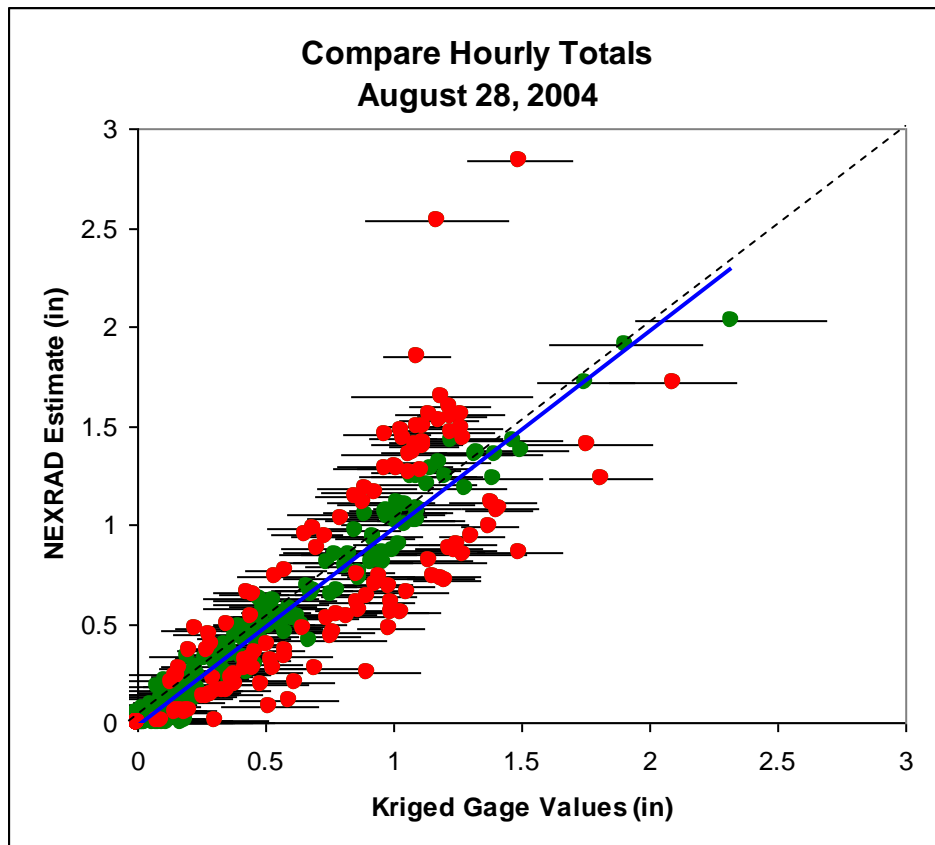
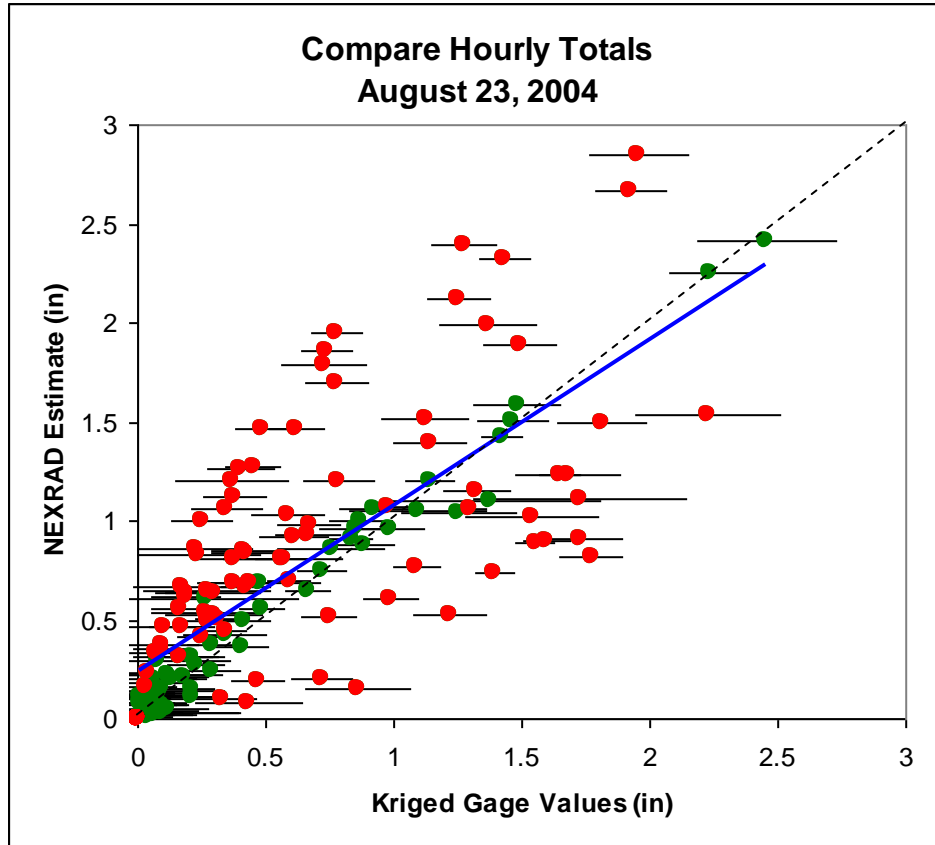






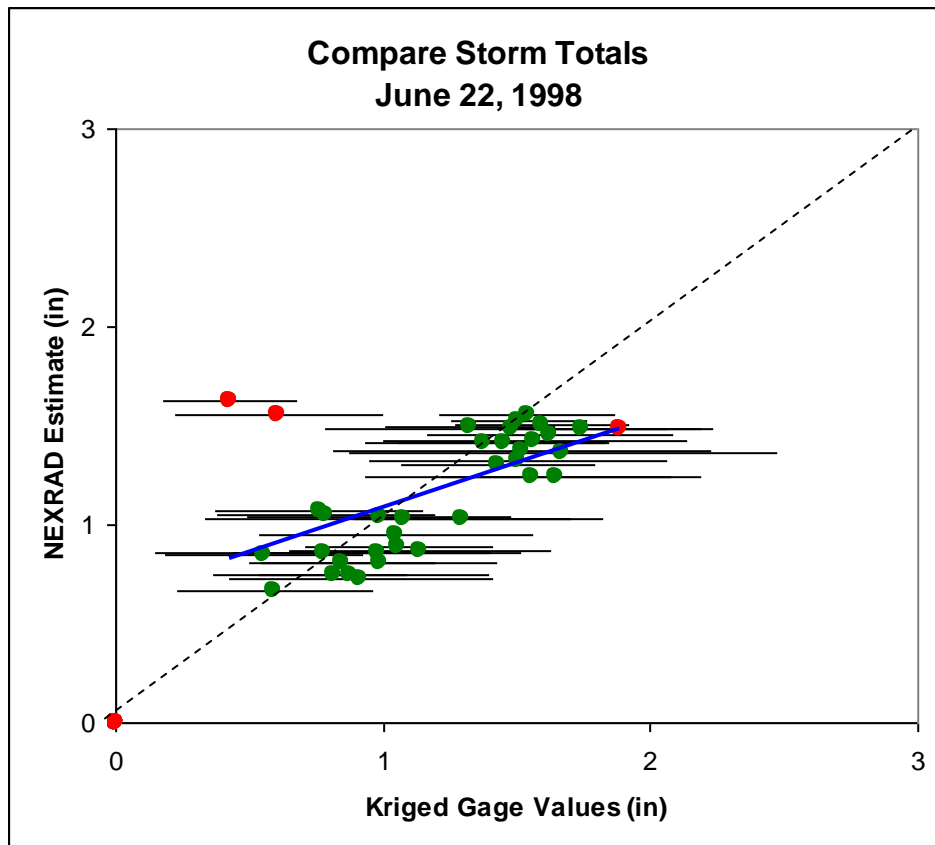
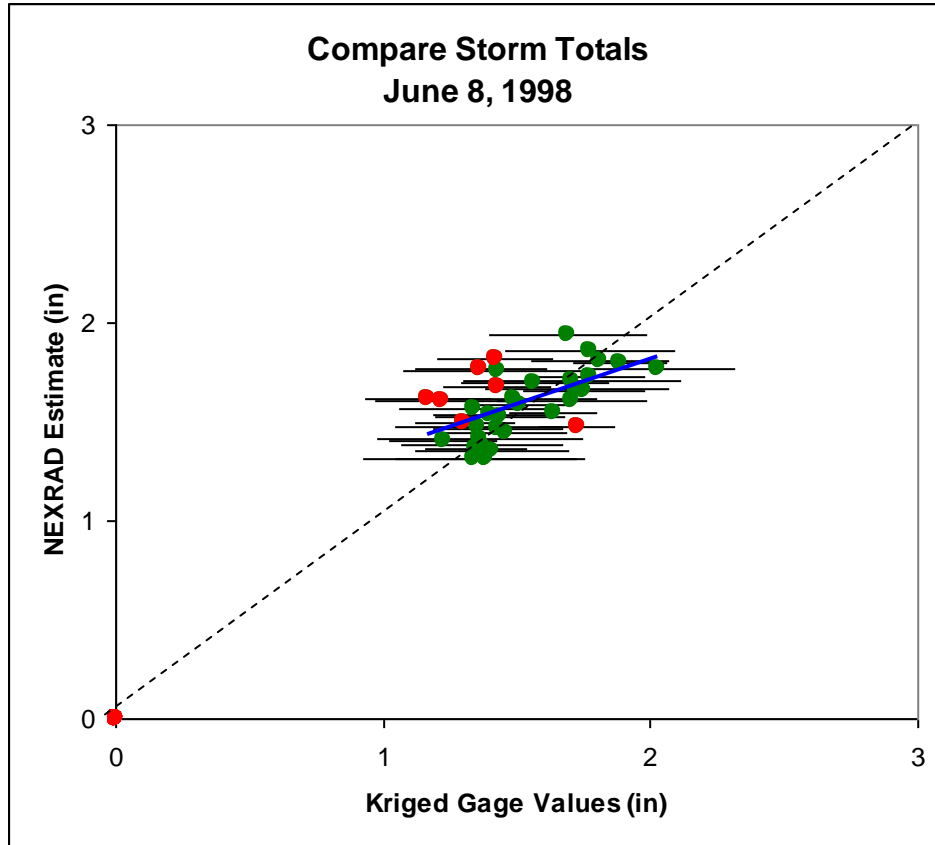


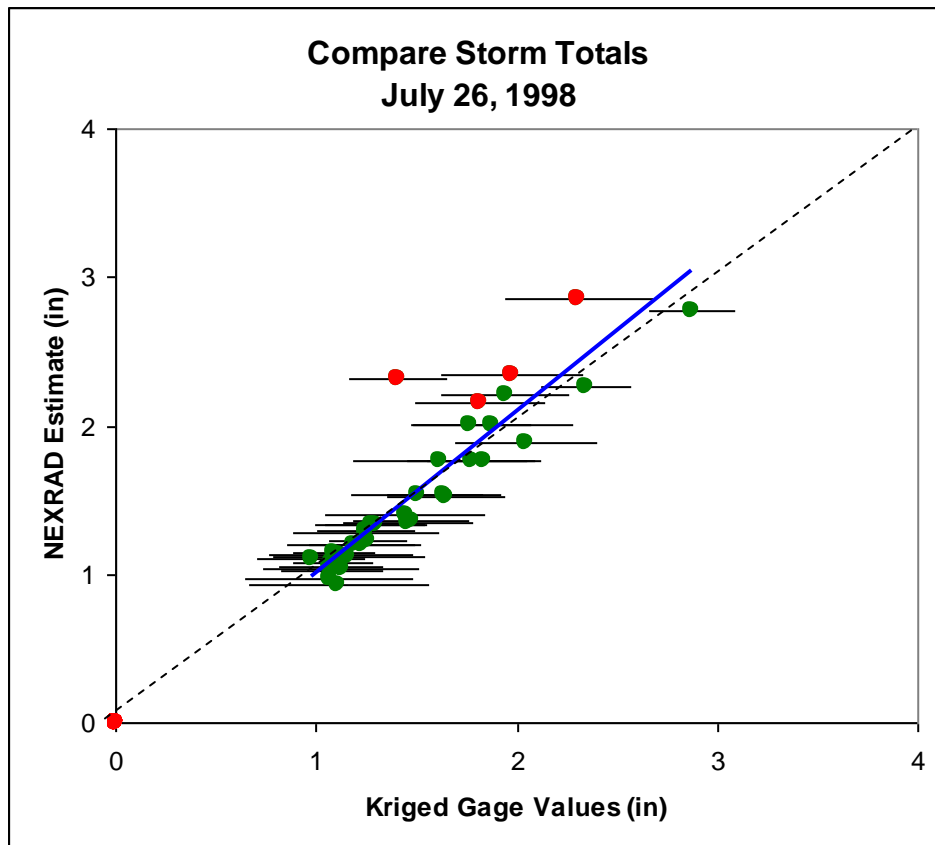
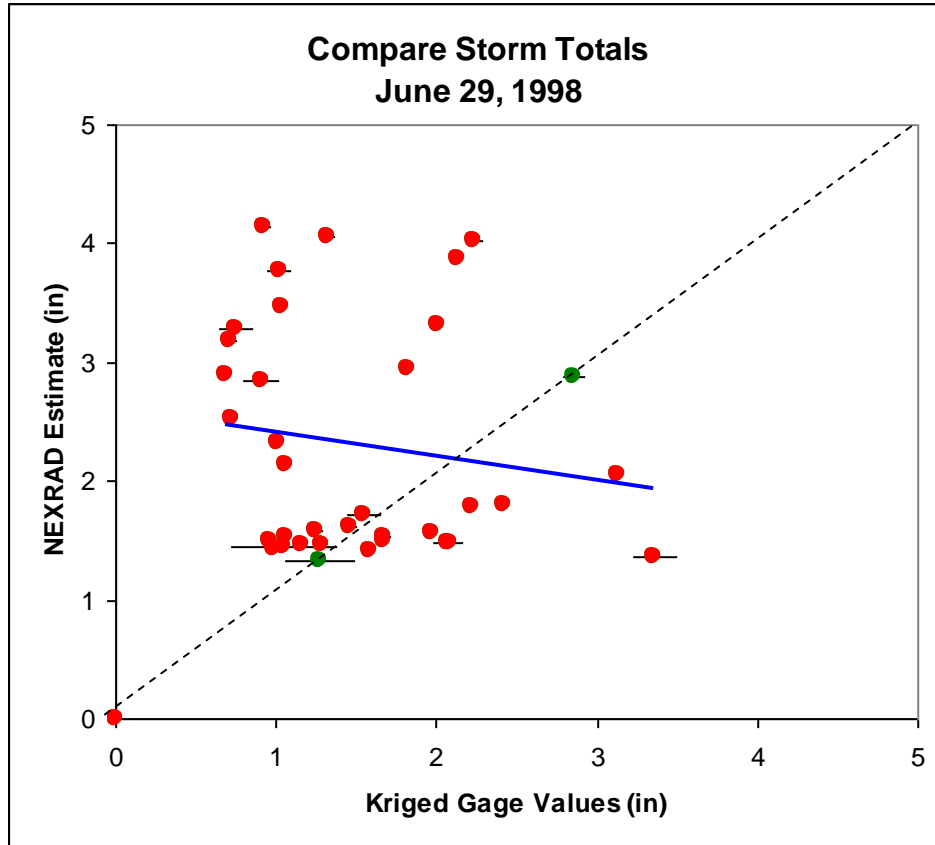


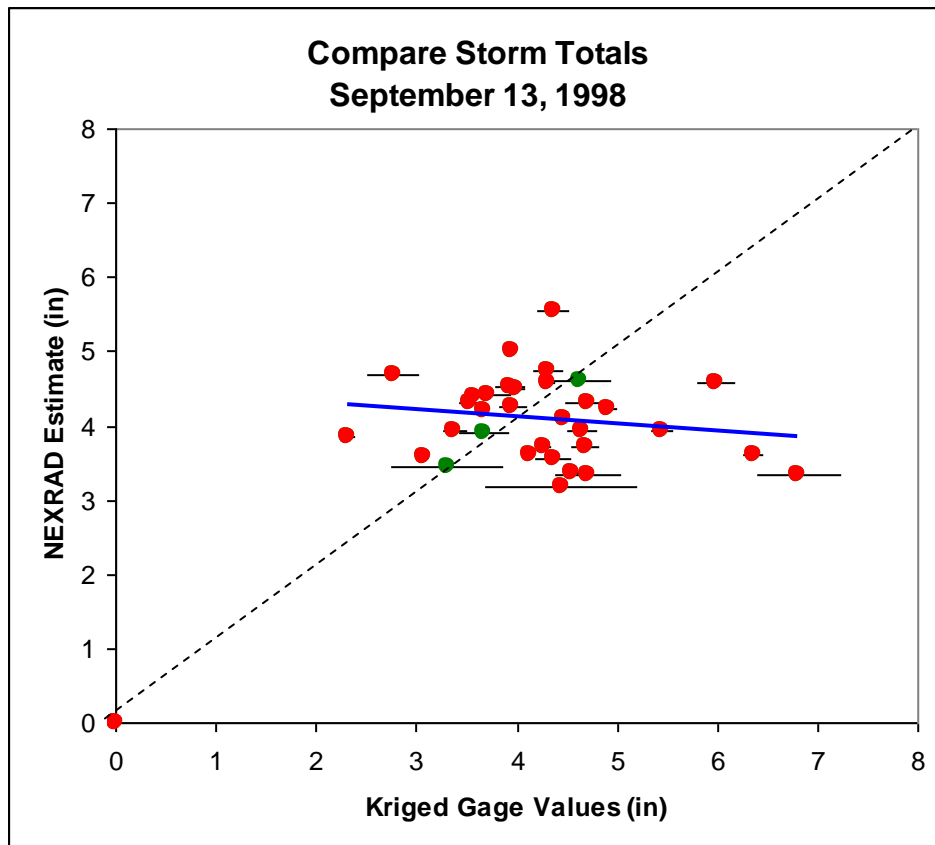
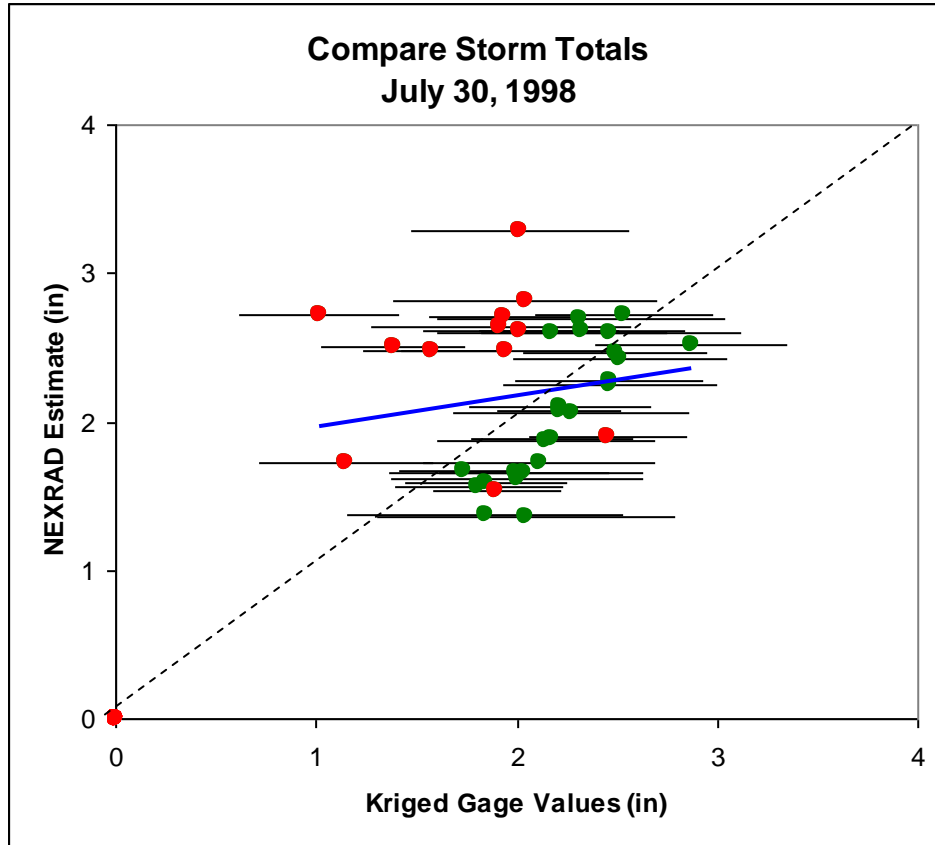


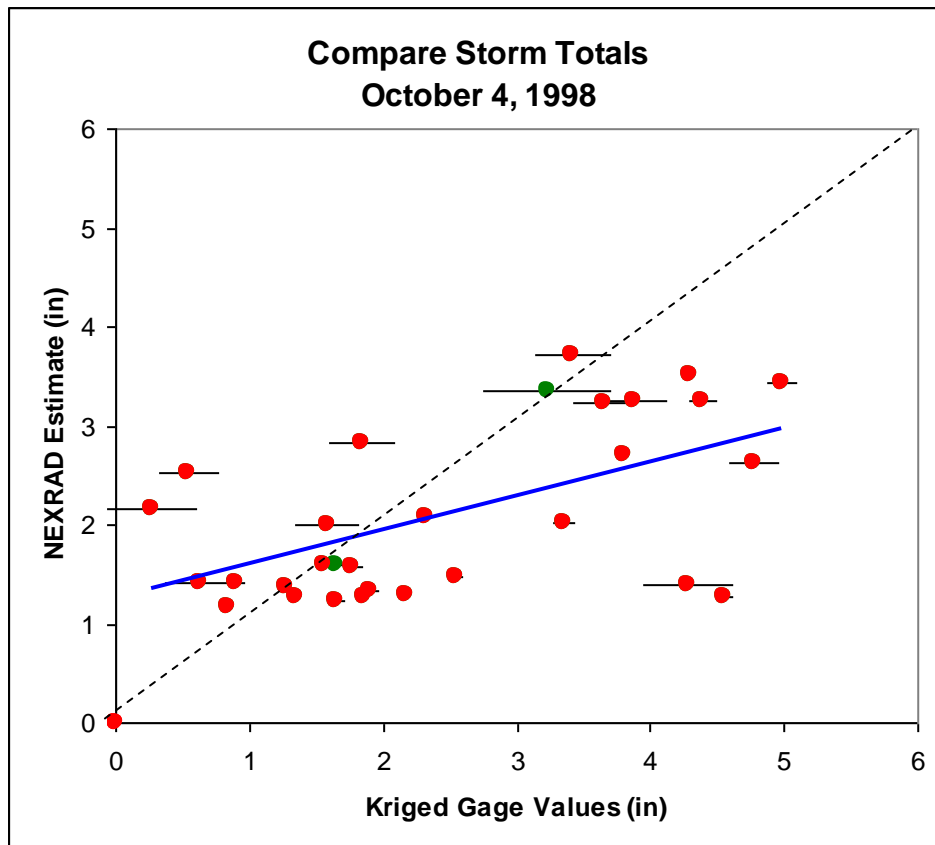
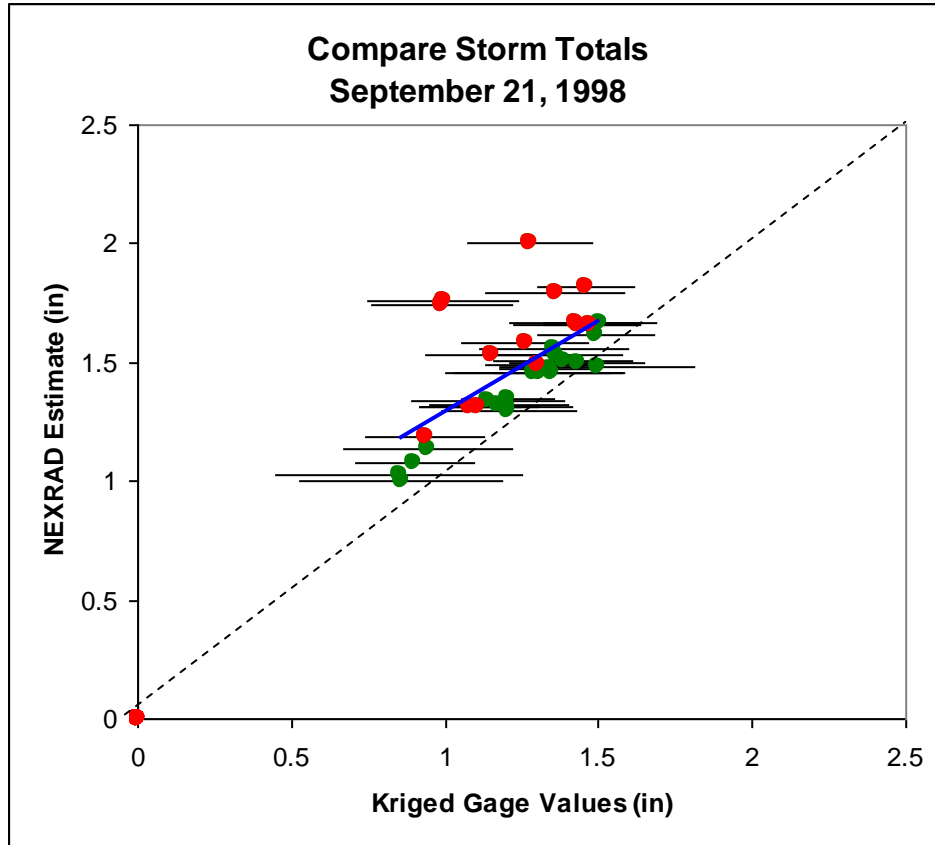
APPENDIX B

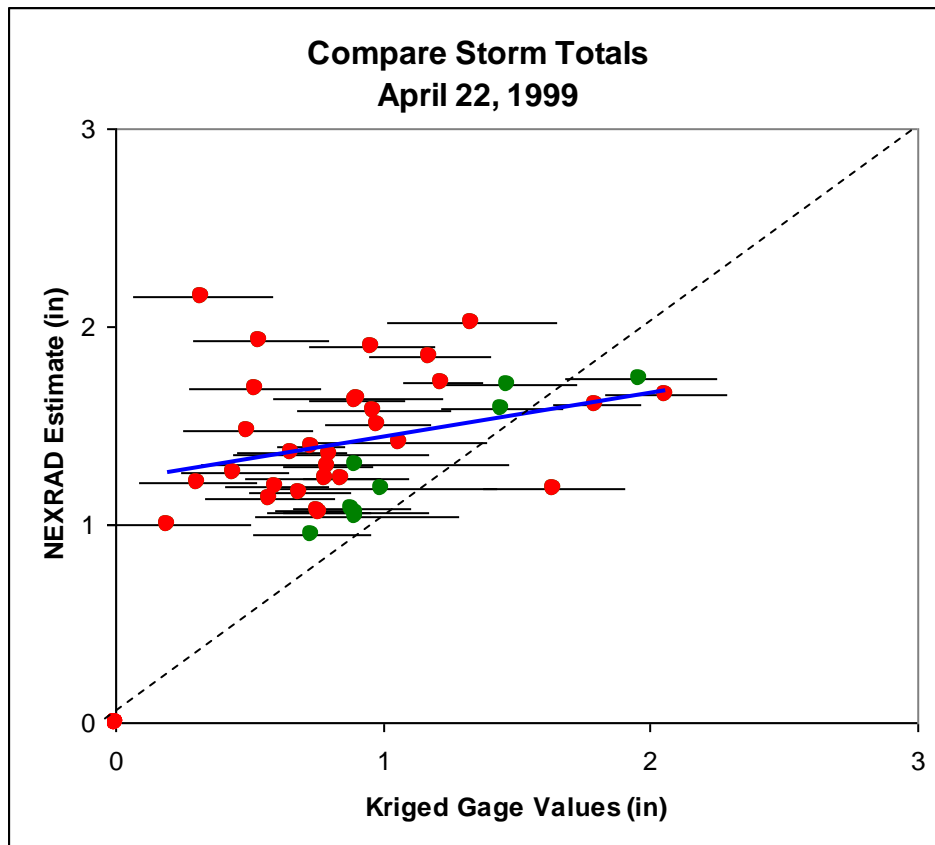
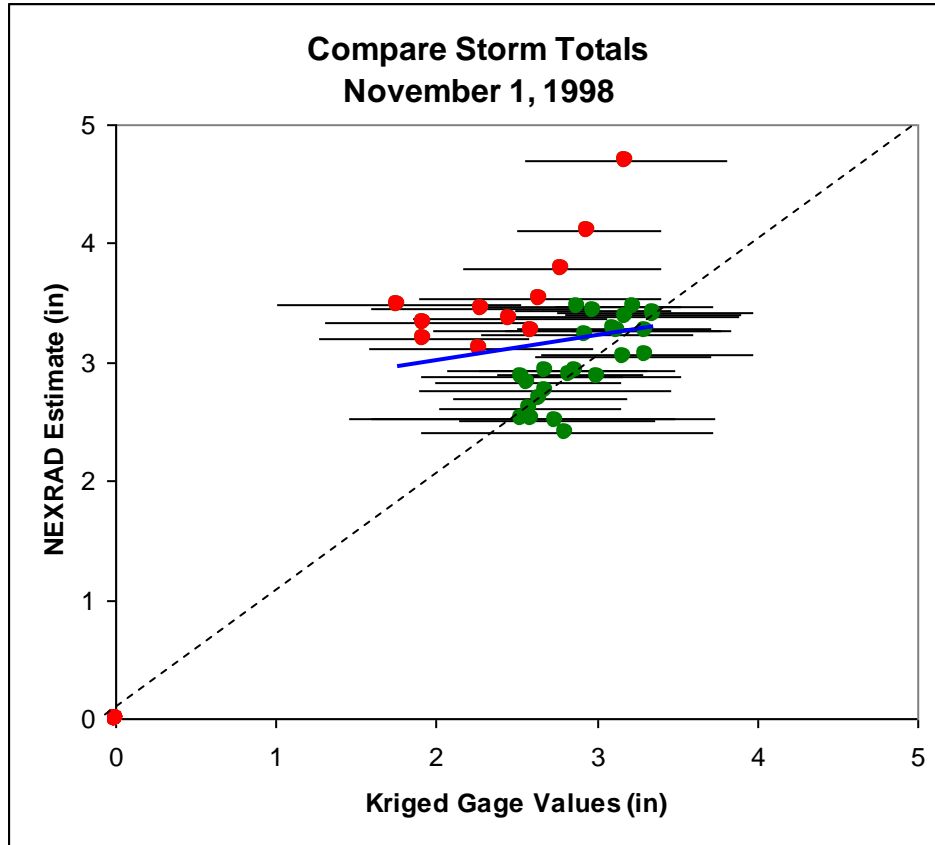
SCATTER PLOTS FOR STORM TOTAL ACCUMULATIONS

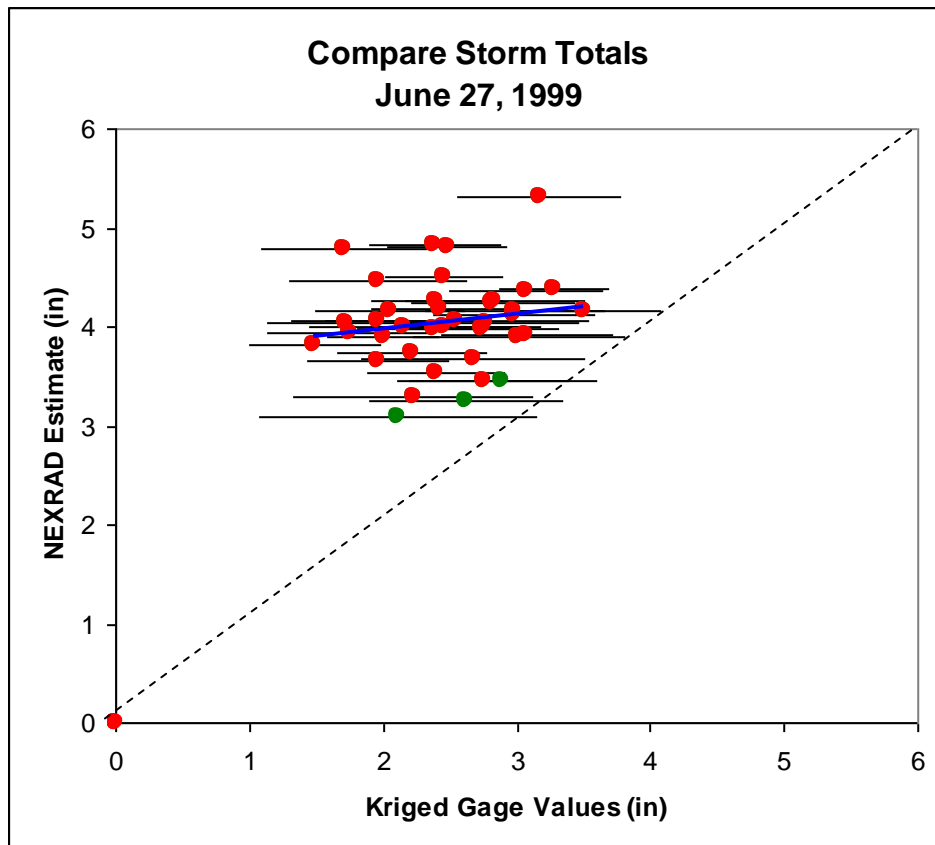
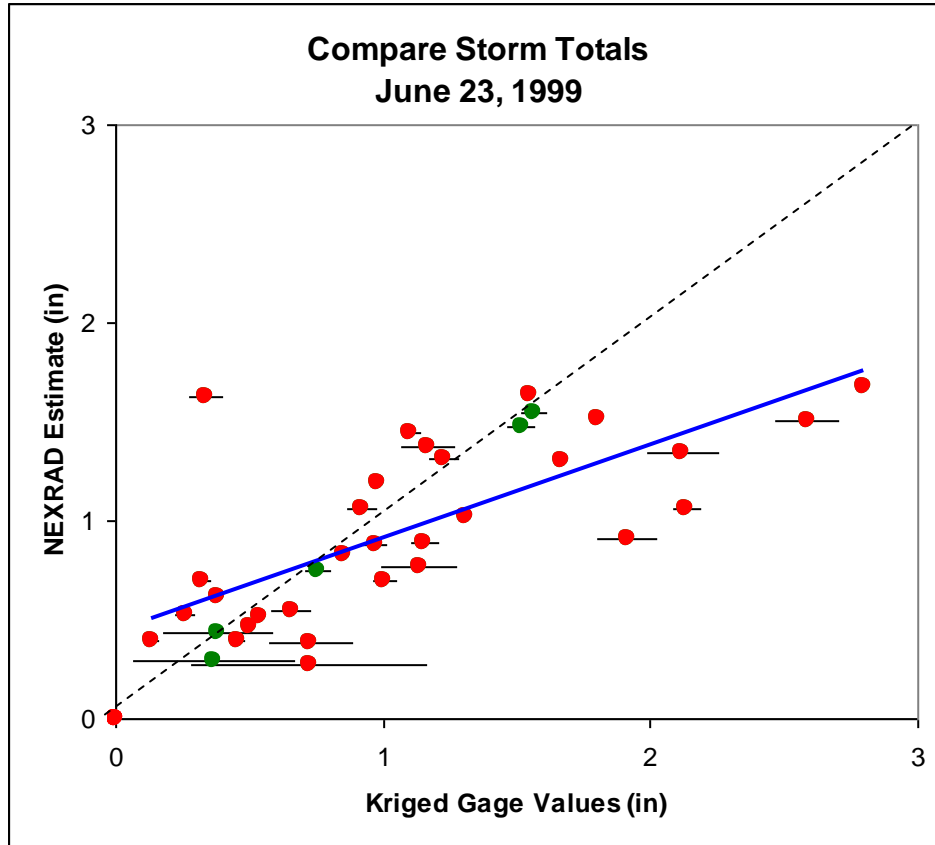


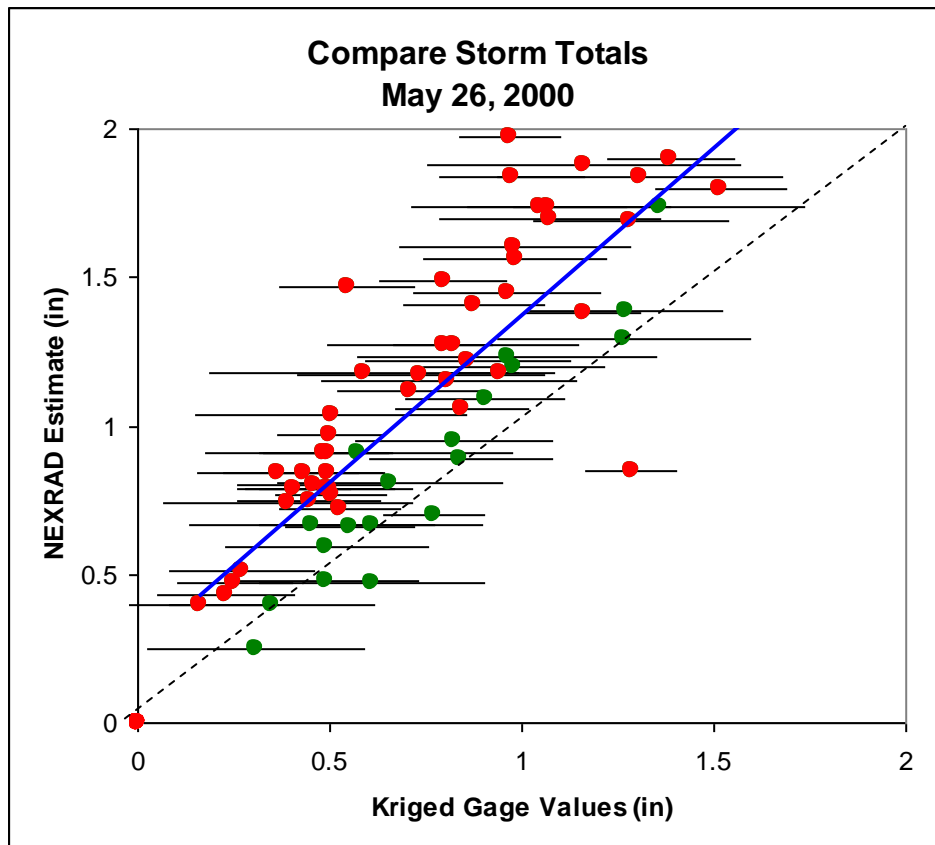
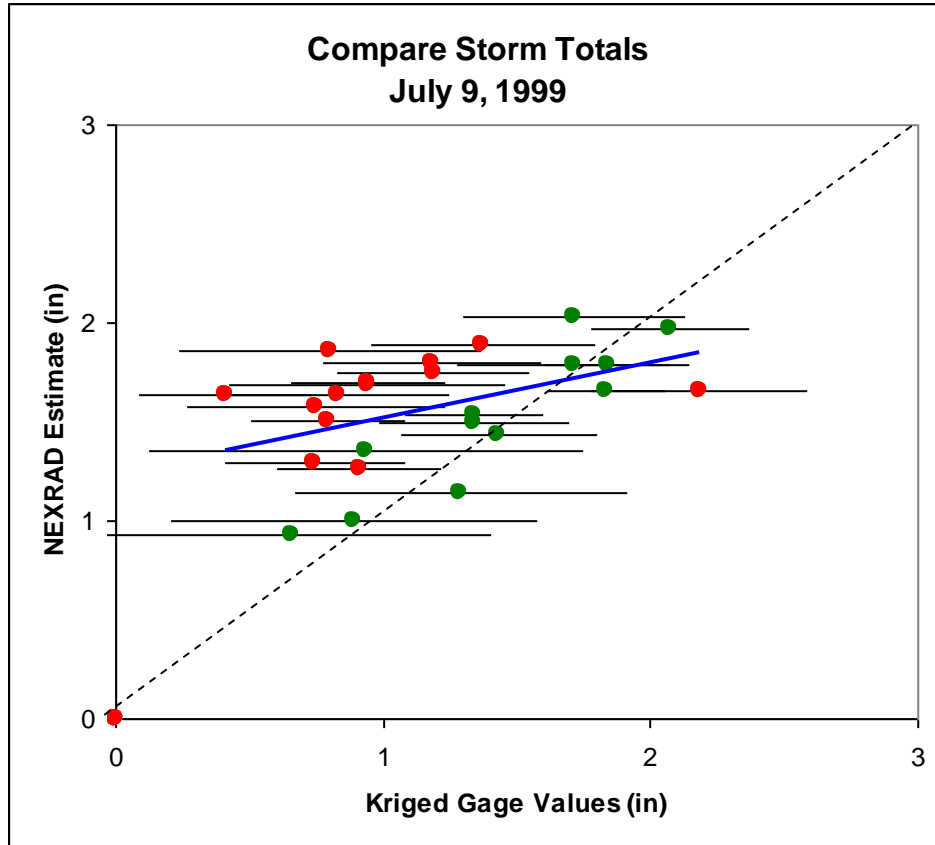


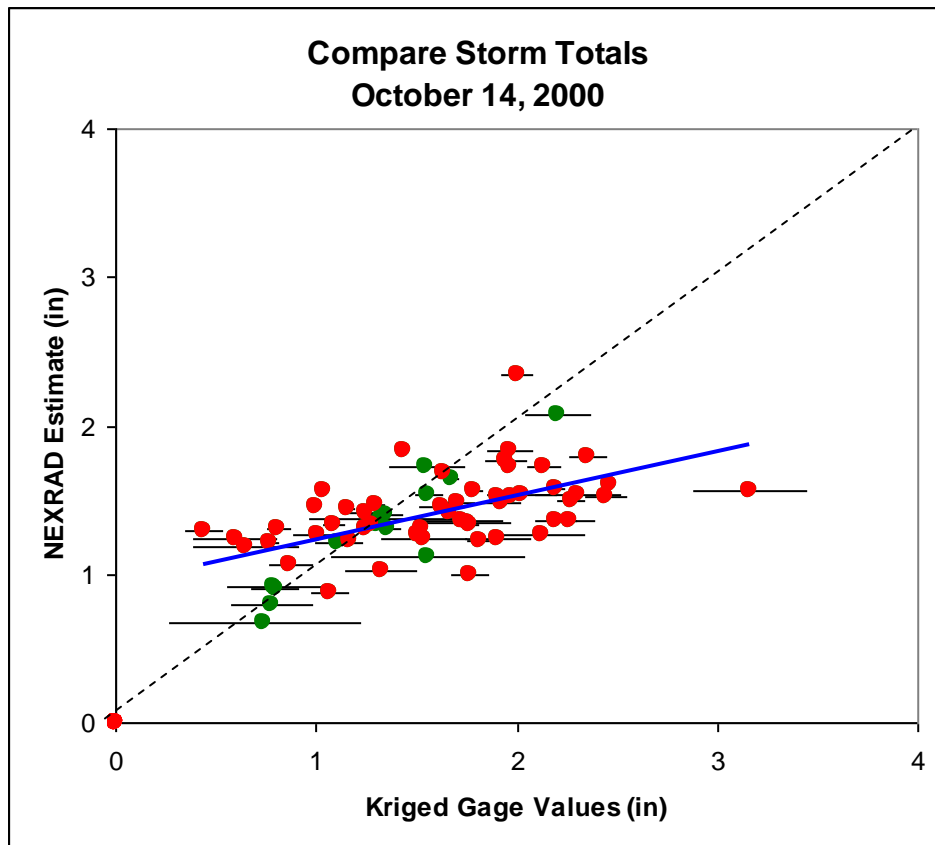
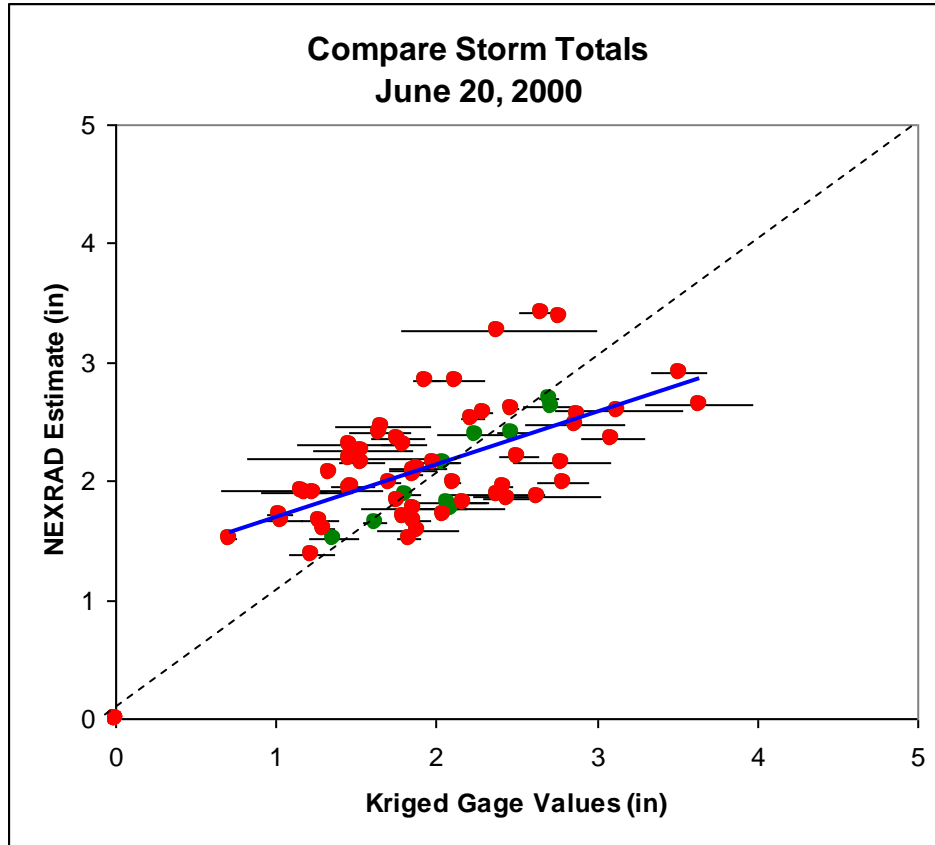


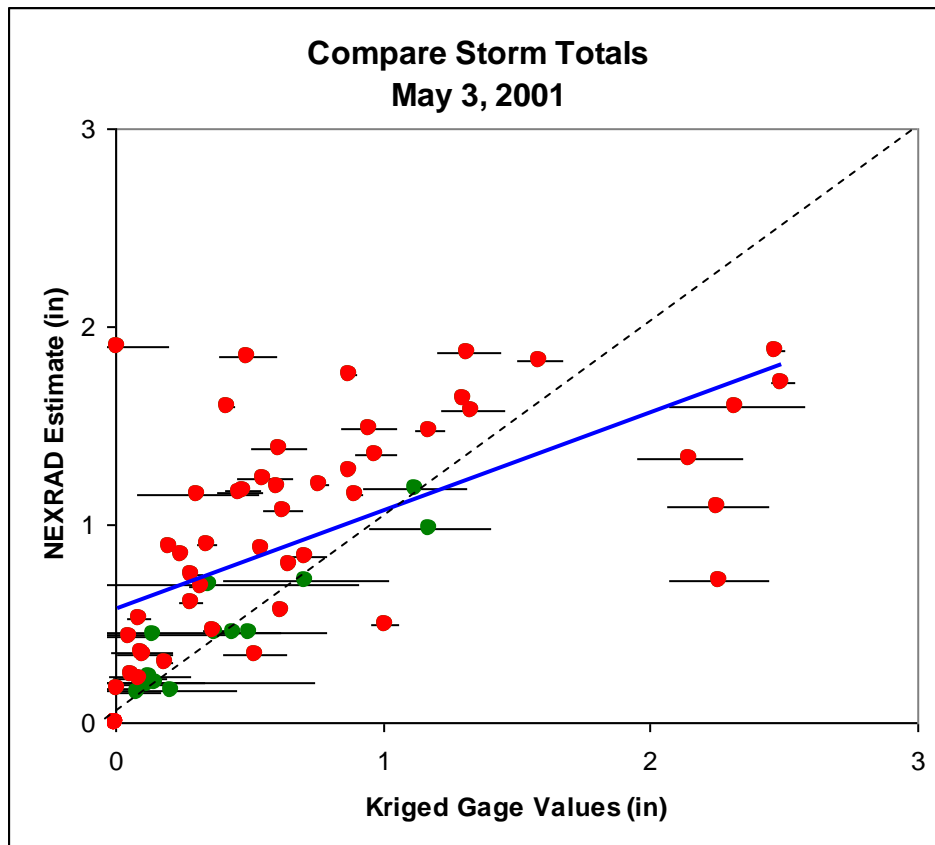
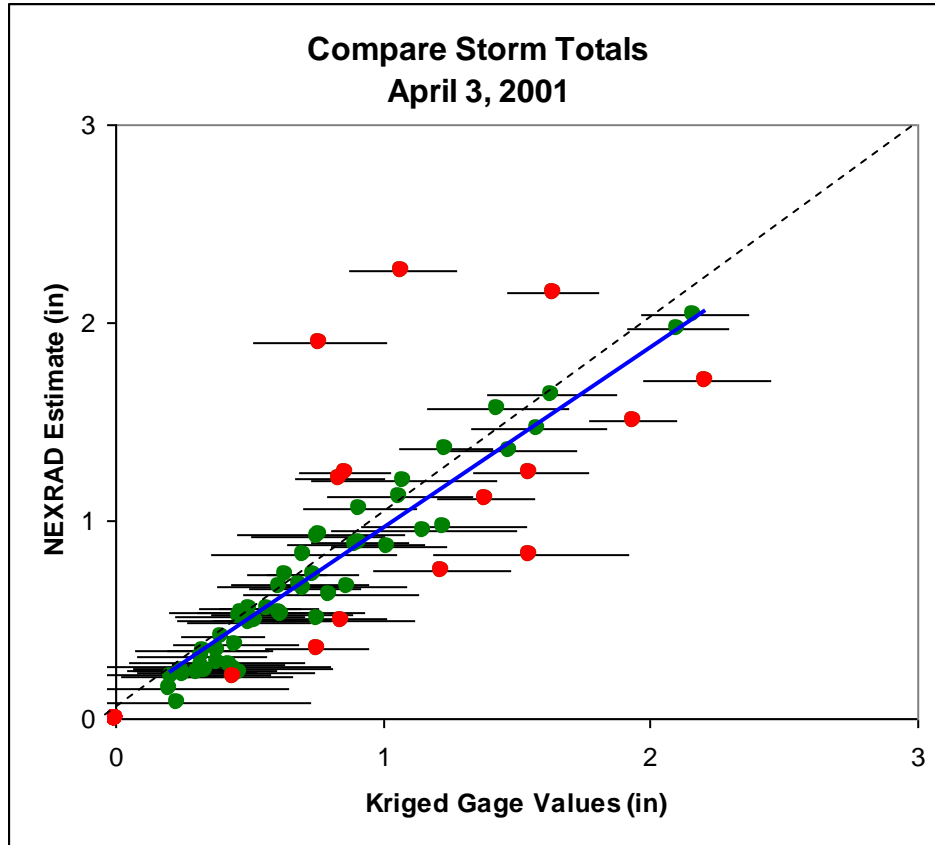


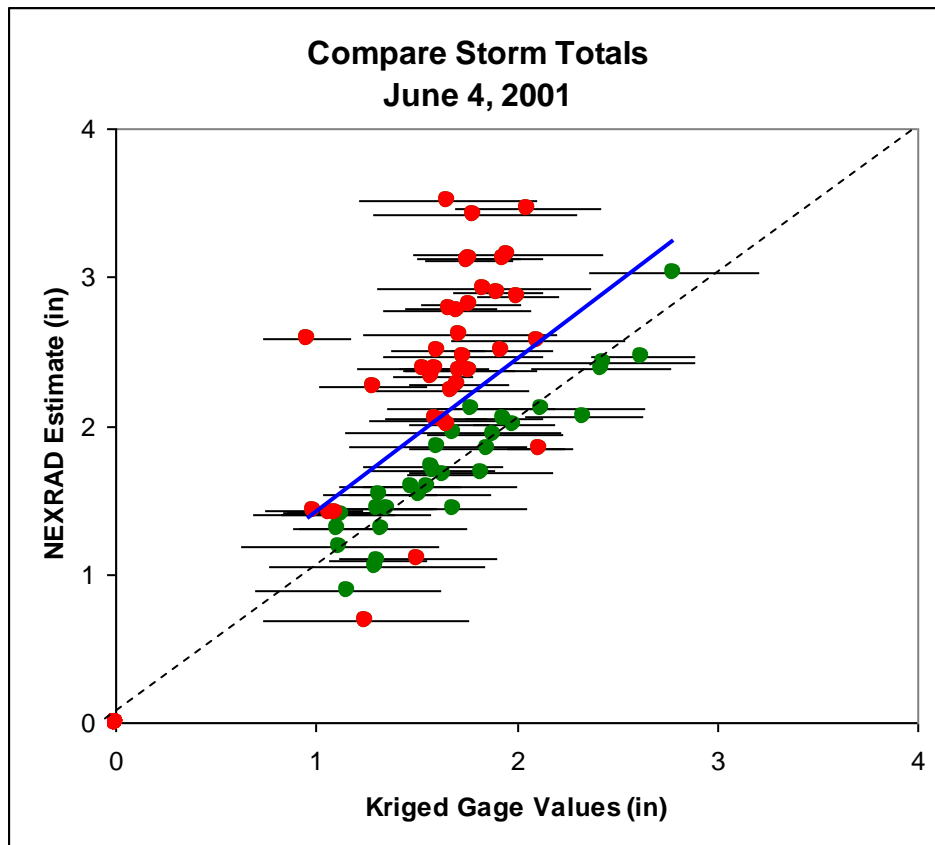
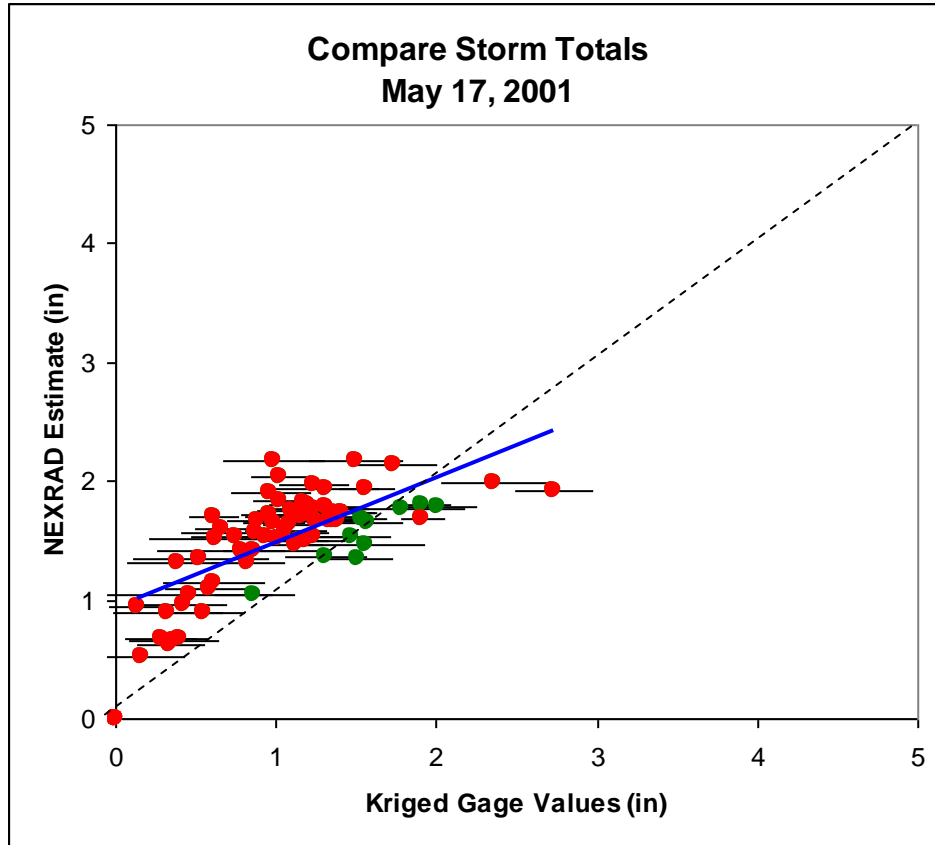


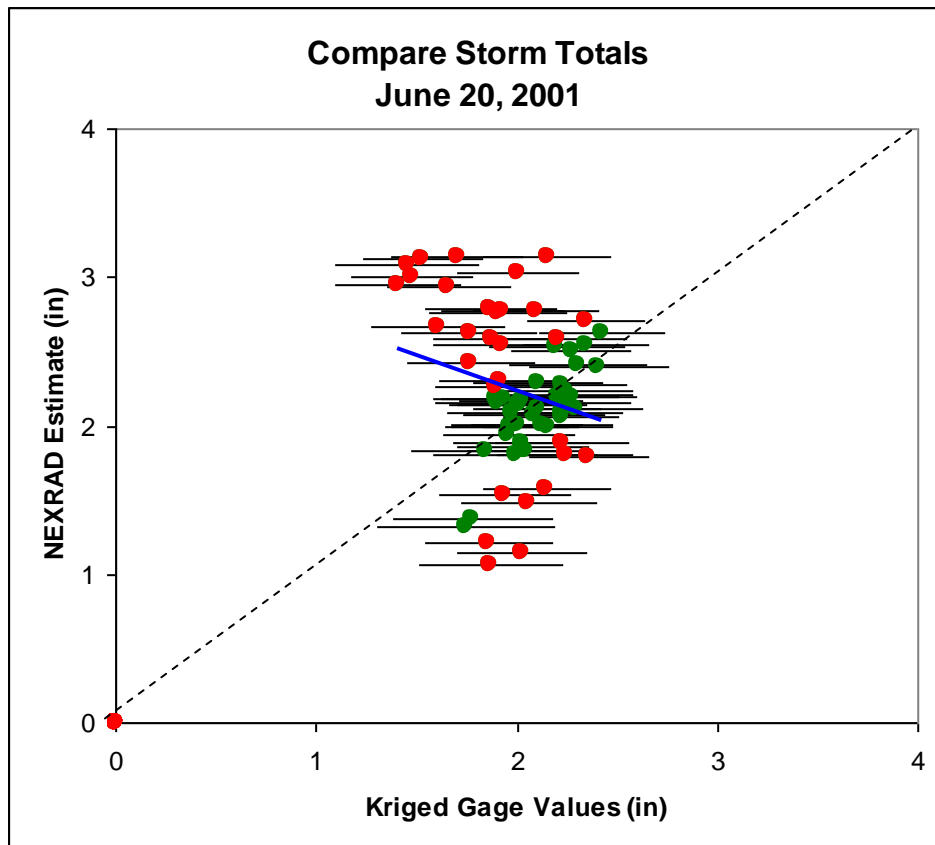
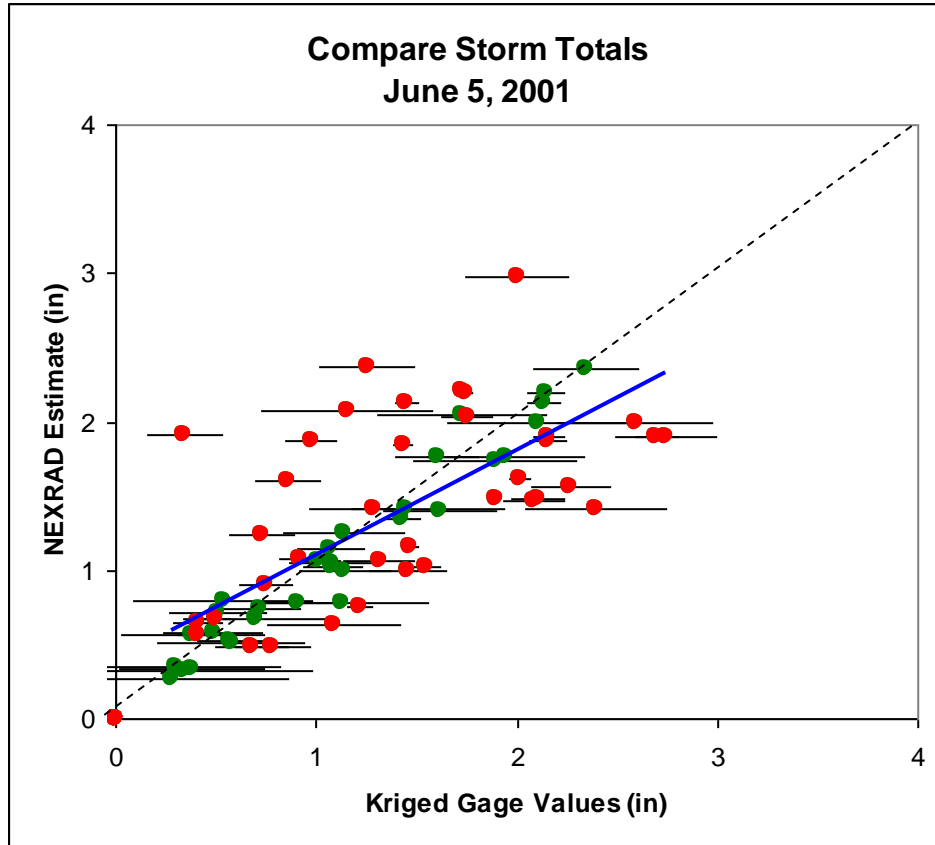


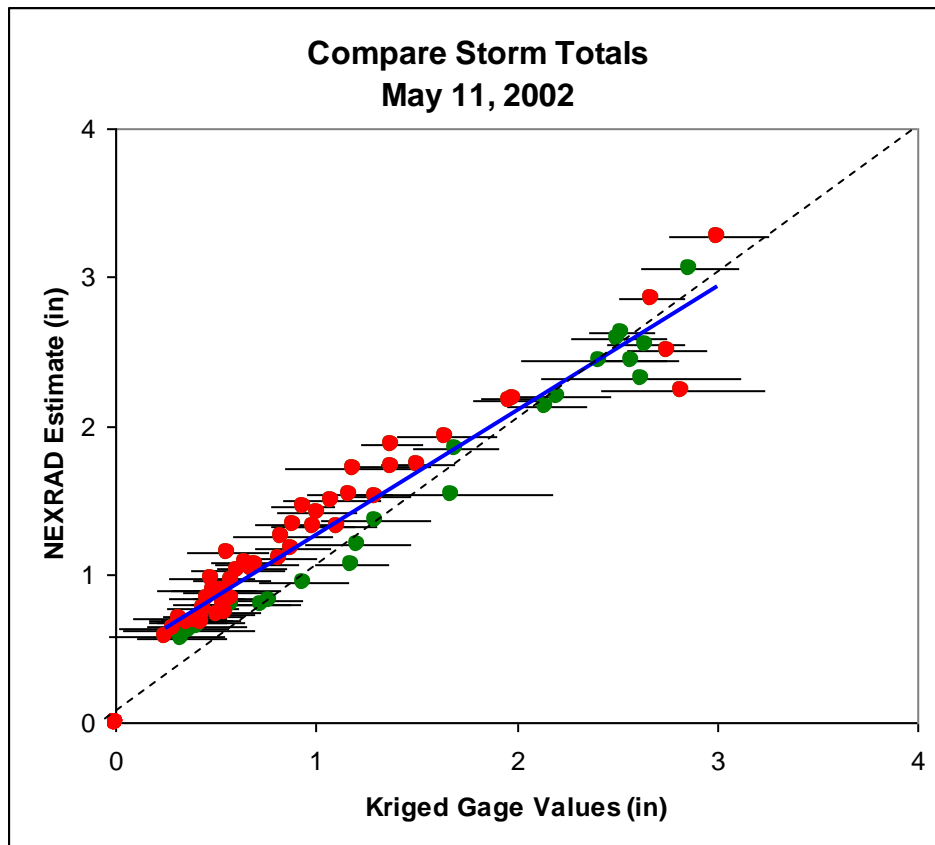
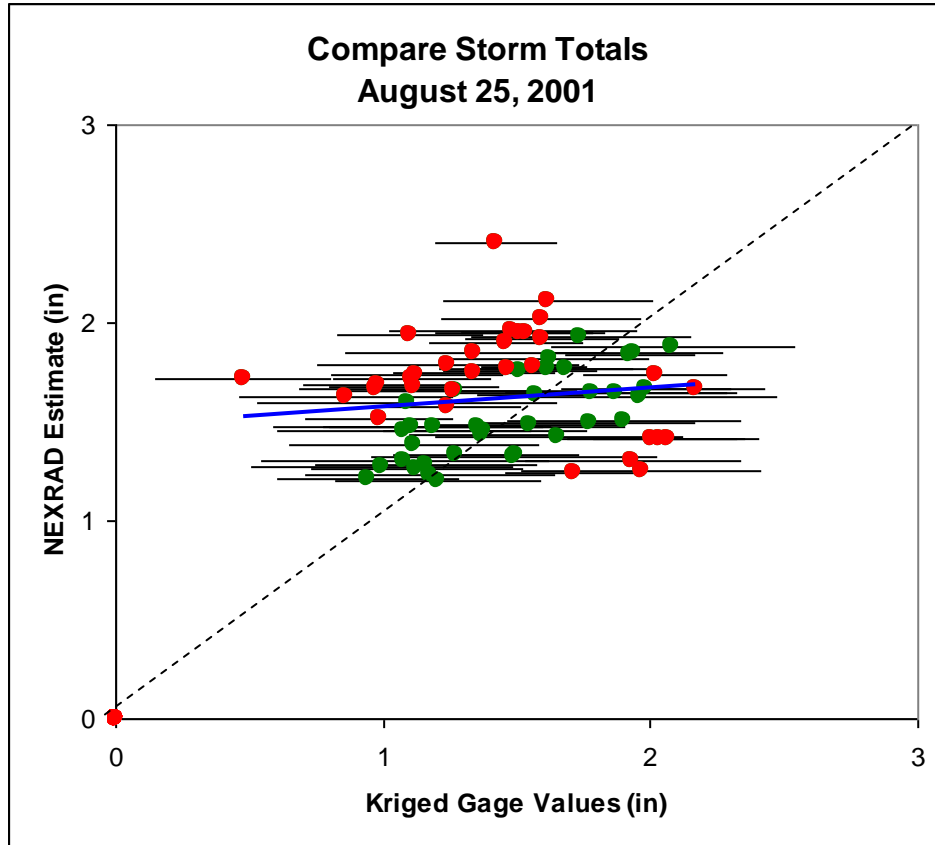


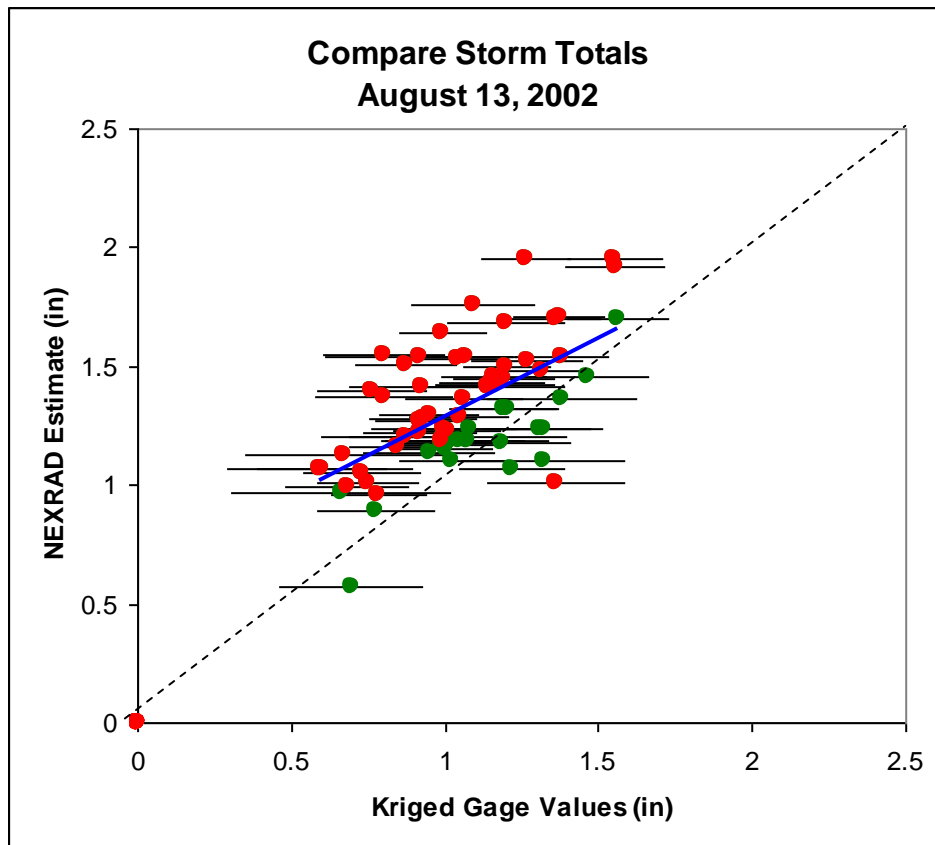
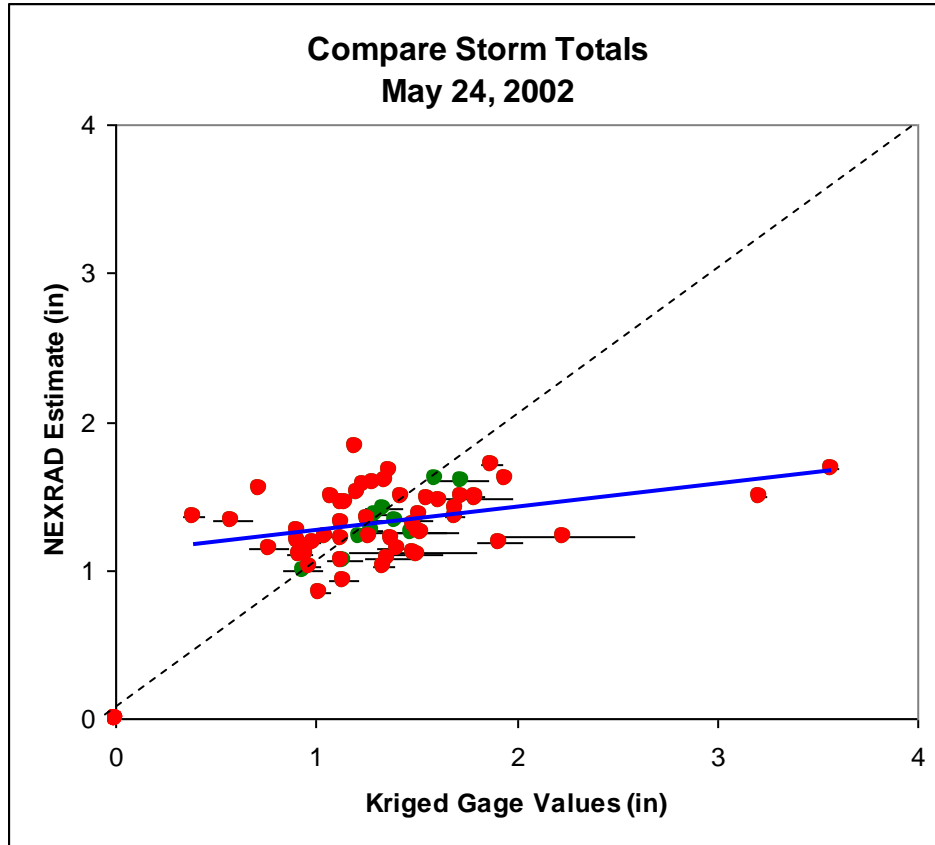


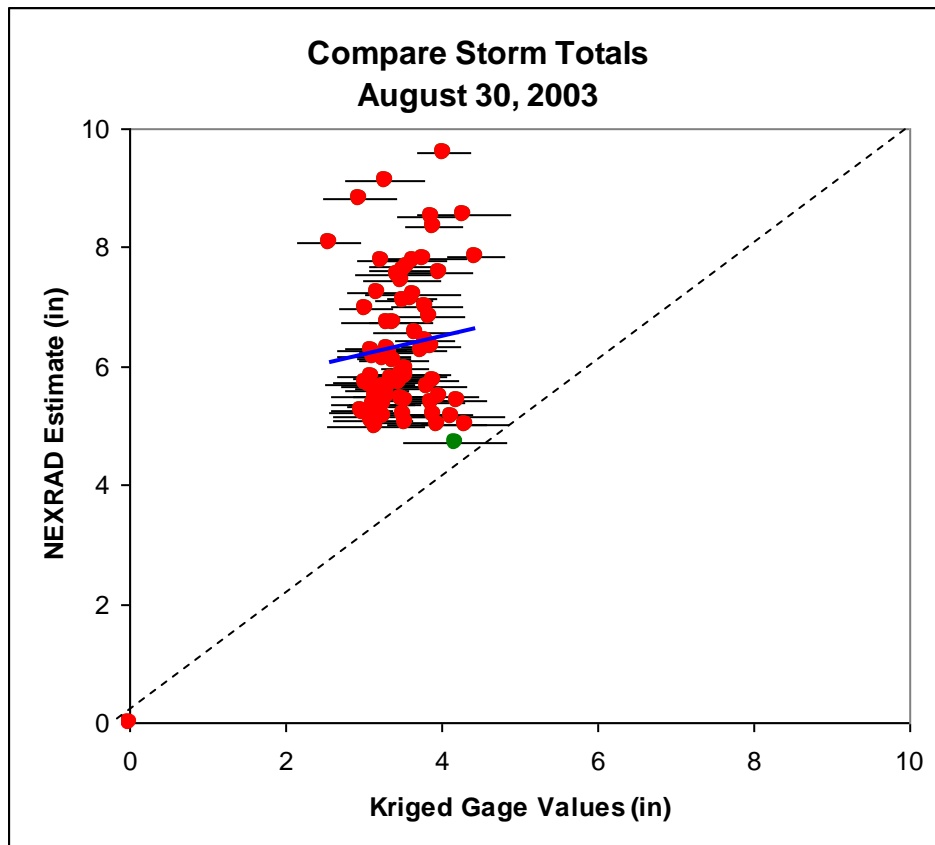
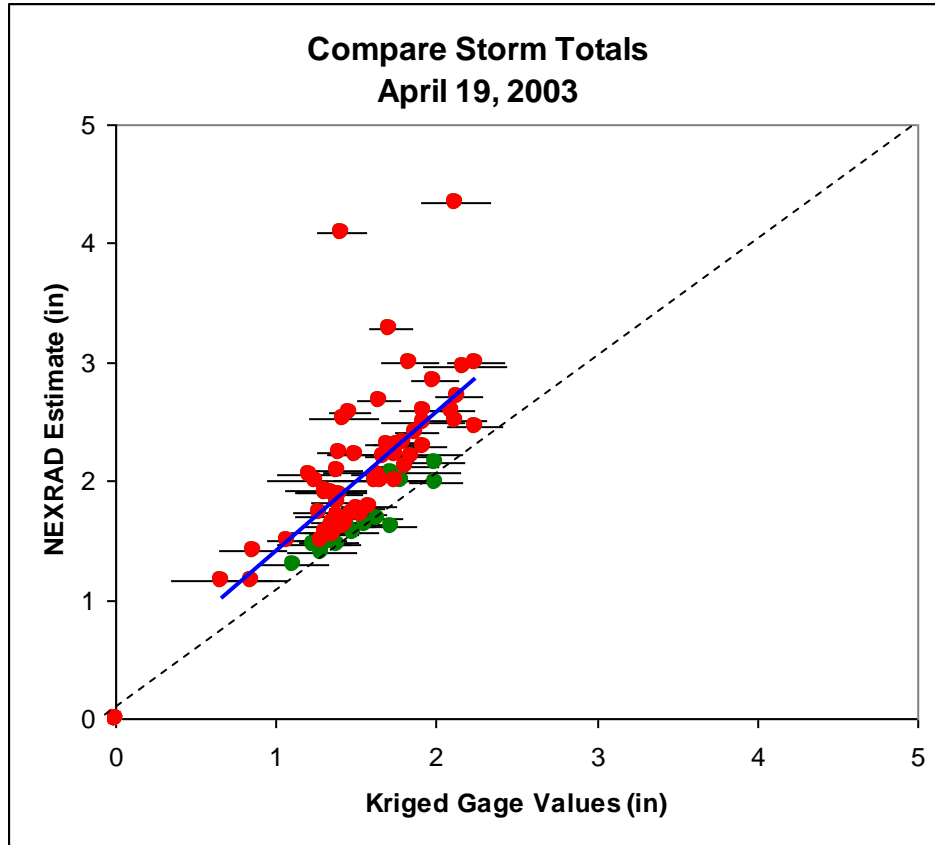


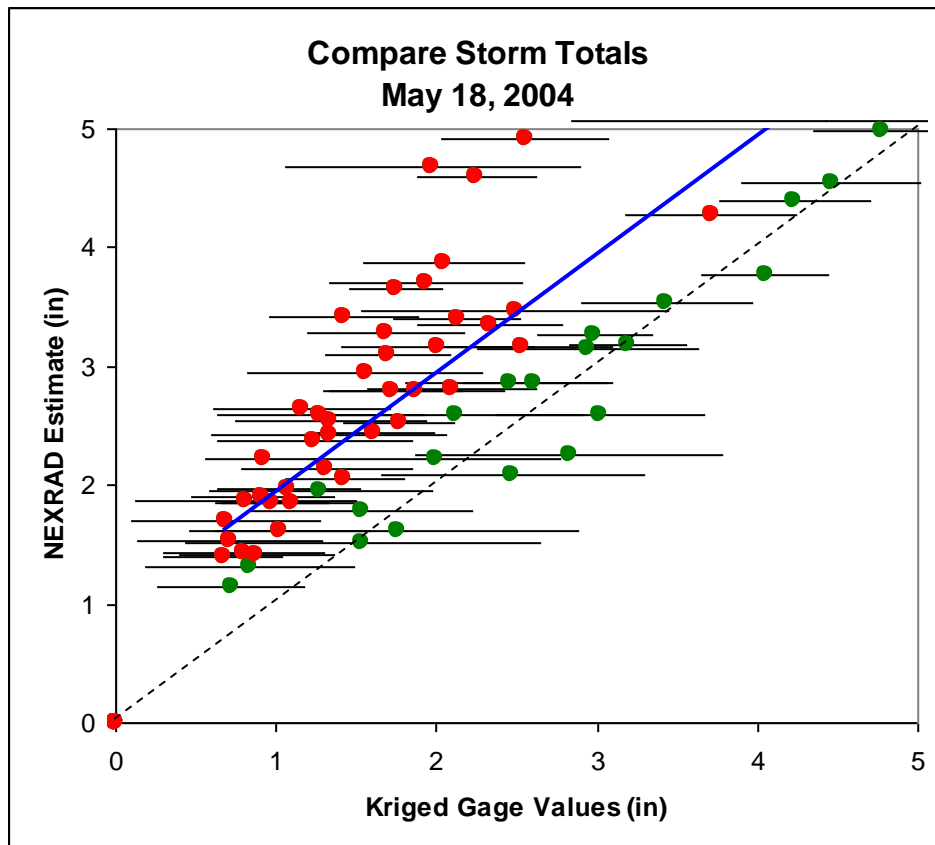
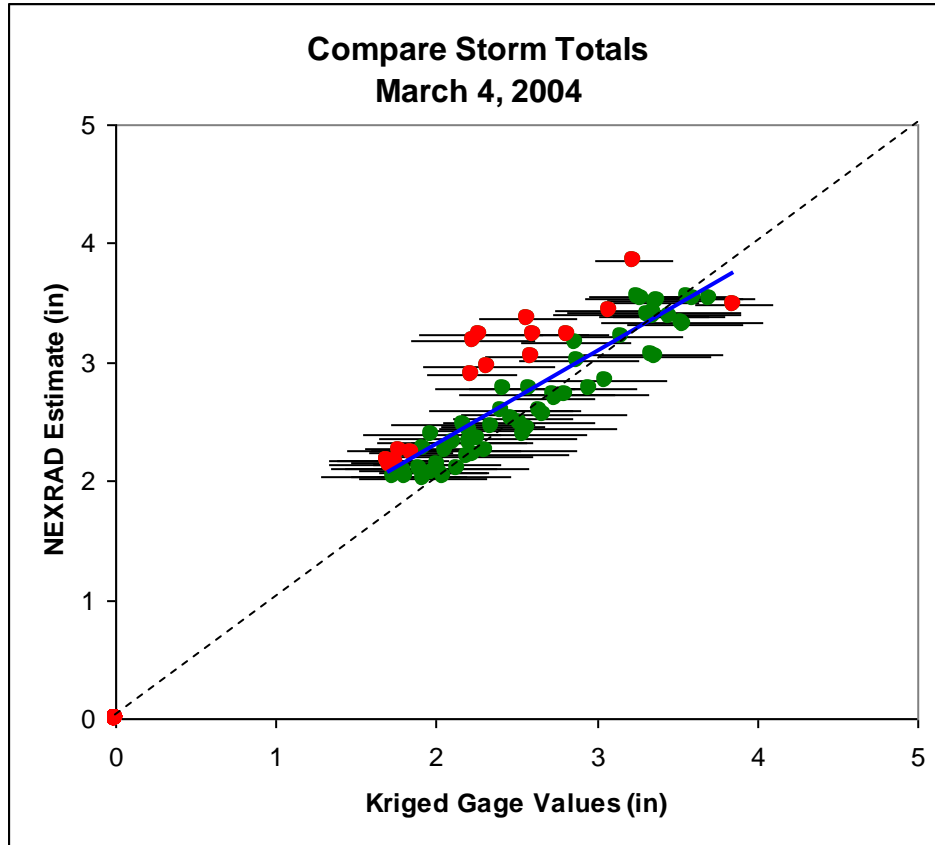


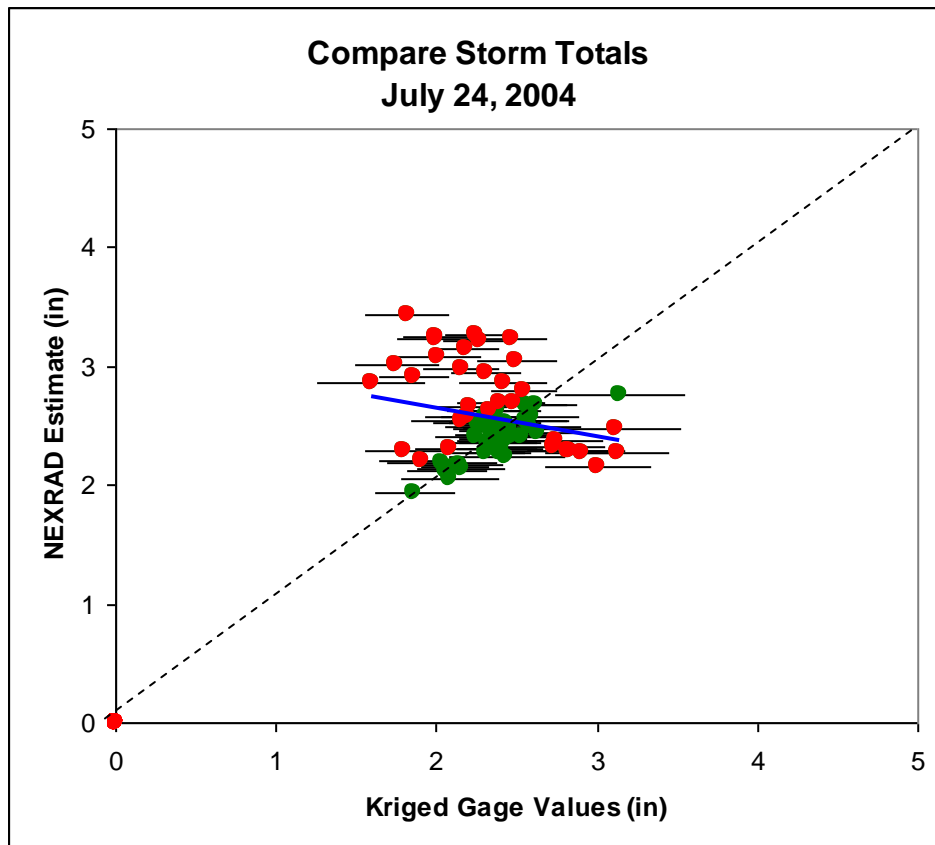
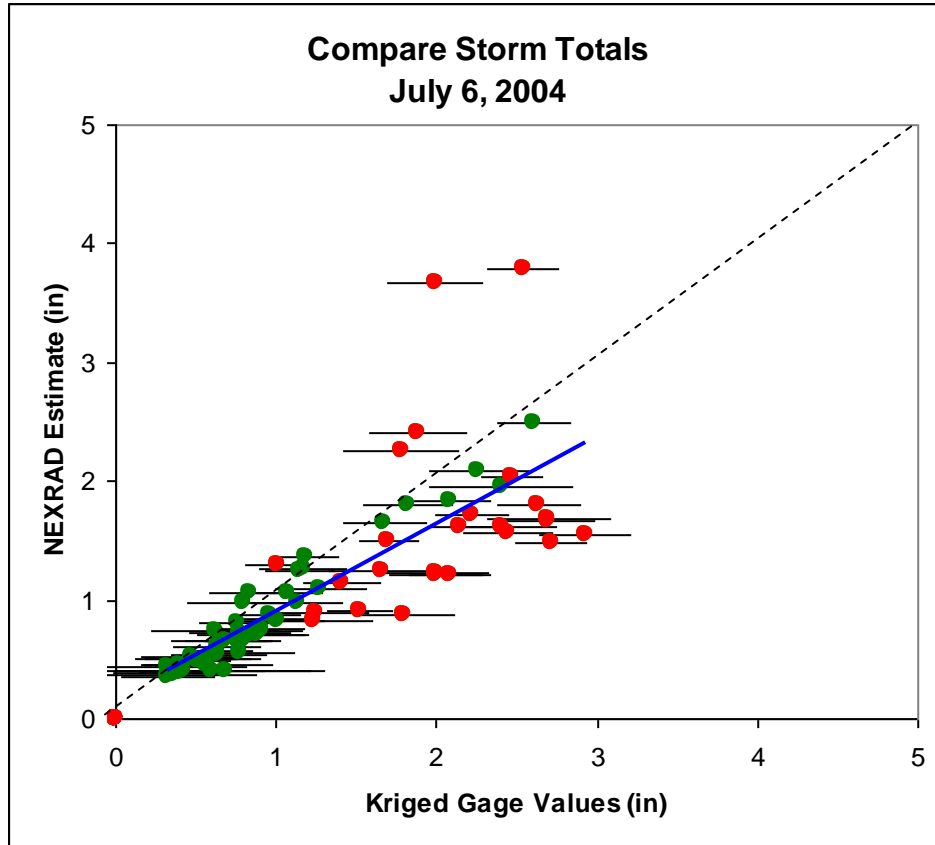


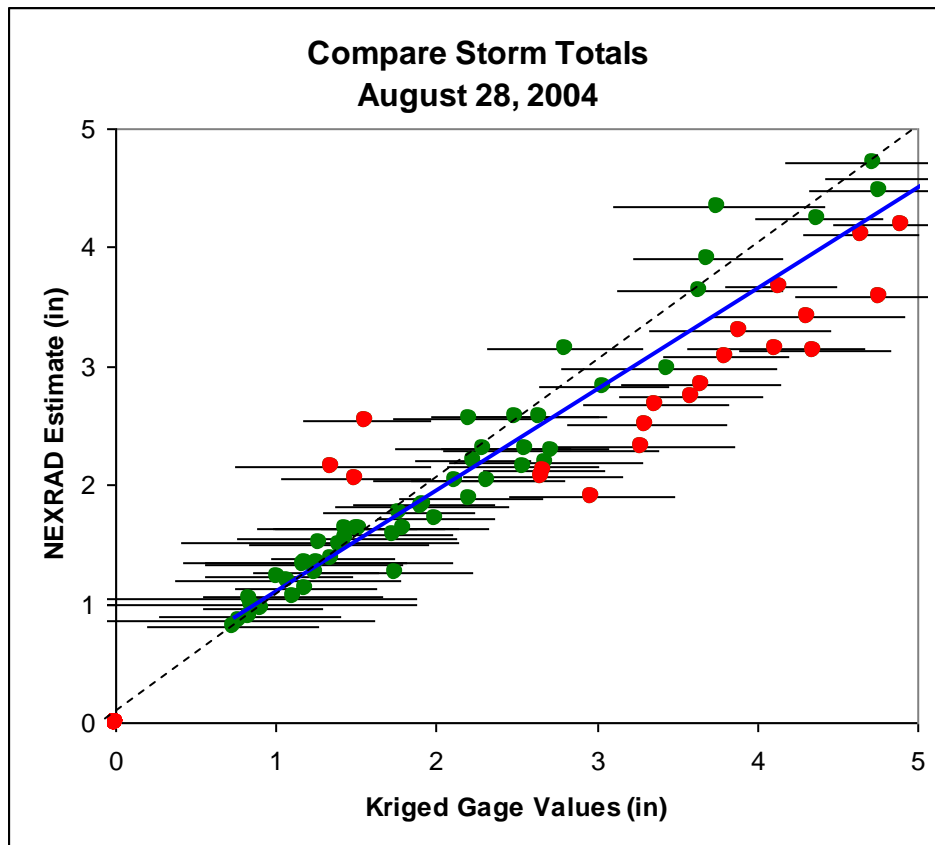
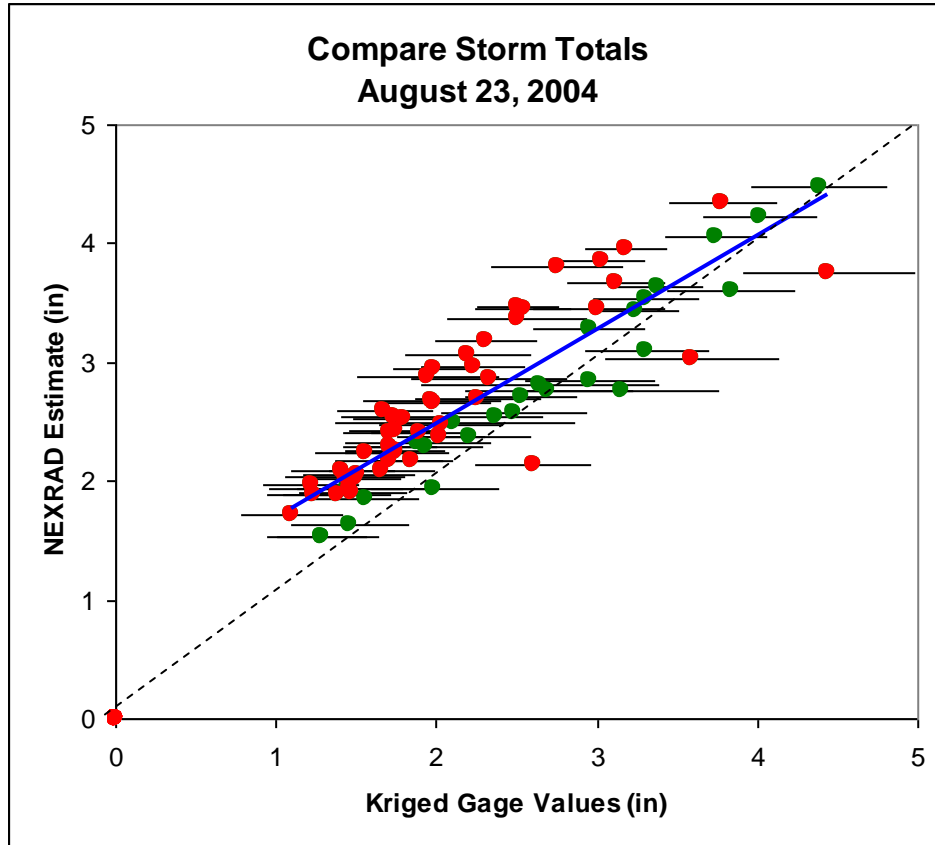












K - TRAN

KANSAS TRANSPORTATION RESEARCH
AND
NEW - DEVELOPMENTS PROGRAM



A COOPERATIVE TRANSPORTATION RESEARCH PROGRAM BETWEEN:

KANSAS DEPARTMENT OF TRANSPORTATION



THE UNIVERSITY OF KANSAS



KANSAS STATE UNIVERSITY

